University of Milan

PhD in Food Systems

PhD Project: Effective replacement in food packaging of oil based oxygen-barrier polymers (EVOH, PVDC), with bio-composites containing Cellulose Nanocrystals (CNCs) extracted from waste and biomasses

Supervisor: Prof. Luciano Piergiovanni   **PhD student**: Ghislain Fotie

Mat. Number: R11616

Table of content

Riassunto

Con l'inquinamento crescente e il riscaldamento globale dell'ambiente, è emerso un ampio spettro di tecnologie ingegneristiche per sviluppare imballaggi innovativi con meno rilascio di anidride carbonica ed emissioni di gas serra. Un imballaggio alimentare ideale deve soddisfare tutti i requisiti di sicurezza alimentare e conformarsi in concomitanza alle preoccupazioni ambientali. Una delle strategie per implementare un imballaggio che comprenda tutte le esigenze del consumatore è quella di ricorrere a laminati ecologici che combinano diversi strati di materiali con diverse funzioni in termine di barriera gas / olio / acqua e proprietà meccaniche. La ricerca di dottorato mirava a sostituire dei laminati barriera sintetica ai gas come il copolimero di etil vinil alcool (EVOH) attualmente usato, con dei laminati a barriera biologica contenenti i nanocristalli di cellulosa (CNCs) per l'estensione della shelf-life dei prodotti sensibili all'ossidazione. Dal punto di vista chimico-fisico, la cellulosa è una struttura microfibrillata composta da milioni di β1-4 glucosio legati da legami glicosidici; la sua organizzazione gerarchica denota delle regioni cristalline e amorfe contenenti catene di glucosio saldamente unite da legami idrogeno. I CNCs sono generalmente ottenuti per idrolisi acida o ossidativa della parte amorfa della cellulosa e sono delle particelle piccolissime e biodegradabili in cui almeno una dimensione è inferiore o uguale a 100 nm. I film plastici rivestiti con CNCs presentano proprietà barriera straordinarie ai gas. Tuttavia, poiché la maggior parte dei materiali biodegradabili sono di natura idrofila, i CNCs tendono ad assorbire umidità dall'ambiente circostante, che consente ai gas di diffondere molto velocemente attraverso i film plastici rivestiti. Quel fenomeno di sensibilità all'acqua dei CNCs è stato approfondito durante la prima fase della ricerca e due soluzioni sono state ritenute plausibili per alleviare questo inconveniente, ricorrendo alla modifica chimica dei CNCs per renderli più idrofobici o/e alla laminazione di rivestimenti di CNCs tra due film plastici idrorepellenti per proteggerli dall'umidità. CNCs standard (non modificati) ed esterificati

(modificati) sono stati prodotti e caratterizzati per valutare i loro gruppi funzionali, indice di cristallinità, dimensioni e comportamento idrofilo. Successivamente, i film plastici rivestiti dei CNCs sono stati caratterizzati mediante l'angolo di contatto, il potenziale Z e la permeabilità agli aeriformi (vapore acqueo, O_2, CO_2). I film plastici di CNCs rivestiti sono stati quindi laminati con adesivo poliuretanico e caratterizzati da test di delaminazione e permeabilità ai gas al 50% e all'80% di UR per valutare l'efficacia della laminazione. Dopo la laminazione, è stato ottenuto un miglioramento tra il 90% e il 1200% della barriera ai gas anche in condizioni umide. La modifica chimica dei CNCs combinata con la laminazione si è rivelata la migliore strategia per superare la sensibilità all'acqua dei CNCs in ambienti umidi. Infine, è stata eseguita con successo una valutazione comparativa della shelf-life utilizzando sia laminati sintetici (EVOH) che bio-laminati (CNCs) su formaggi grattugiati e caffè macinato. I risultati ottenuti hanno confermato con certezza che l'implementazione dei CNCs in sostituzione della barriera sintetica ai gas è efficace e che contribuirà allo sviluppo di imballaggi alimentari più avanzati e sostenibili in grado di ridurre la dipendenza dai polimeri sintetici promuovendo un'economia circolare.

Abstract

With increasing pollution and global warming of the environment, a wide spectrum of engineering technologies has emerged in food packaging to develop innovative materials with less carbon dioxide release and Green House emissions. Nowadays, an ideal food packaging must meet all the requirements of food safety and comply with environmental concerns concomitantly. One of the strategies to implement a food package that encompasses all consumer needs is to resort to eco-friendly laminates that combine several layers of materials with different functions in terms of gas/oil/water barrier and mechanical properties. The PhD research was focused on the replacement of currently used EVOH conventional gas barrier laminates with bio-based laminates containing cellulose nanocrystals (CNCs) for shelf-life extension of sensitive-oxidation foods products. Chemico-physically, cellulose is a microfibrillated structure, the most abundant biopolymer, made of millions of beta 1-4 glucose linked by glycosidic bonds; its hierarchical organization denotes from the crystalline and amorphous regions containing chains of glucose firmly hold together side-by-side by hydrogen bonds providing high tensile strength. CNCs are generally obtained by a chemical process called "top-down" either by acidic or oxidative hydrolysis of the amorphous part of cellulose. CNCs are biodegradable tiny particles whose at least one dimension is smaller than or equal to 100 nm. Actually, CNCs-coated polymers exhibit unique and extraordinary barrier properties to gases. However, since most biodegradable materials are hydrophilic by nature, CNCs tend to integrate water in wet environment which then allows the gases to pass through the coated polymers even abruptly. That phenomenon of water sensibility of CNCs was investigated in-depth during the first stage of the research and two solutions were considered plausible to alleviate that drawback, that of chemically modifying the CNCs surface for making them more hydrophobic or/and that of laminating the CNCs between two water-repellent plastic films to protect them from the humid

surrounding. Standard (unmodified) and esterified (modified) CNCs were produced and characterized to assess their functional groups, crystallinity index, apparent hydrodynamic diameter and size and hydrophilic behavior. Subsequently, plastic films were coated with standard and modified CNCs and characterized by the contact angle, Z-potential, gases permeability (Water vapor, O_2, CO_2). Coated-CNCs plastic films were then laminated with solvent-based polyurethanic adhesive and characterized by delamination test and gas permeability at 50% and 80% RH to evaluate the effectiveness of the lamination in the protection of CNCs coatings from the wet environment. Between 90% and 1200% improvement of gas barrier was achieved after the lamination. More importantly, the chemical modification of cellulose nanocrystals combined with the lamination resulted to be the best strategy to overcome the water sensitivity of CNCs in wet environment. Finally, a comparative food shelf-life assessment by using both synthetic (EVOH) and bio-based (CNCs) barriers laminates were successfully performed on grated cheese and ground coffee. The results obtained confirmed with certainty that CNCs implementation as a replacement of petroleum-based gas barrier is effective and that will contribute to develop more advanced and sustainable food packaging able to reduce the dependency on synthetic polymers and promoting a circular economy.

General Introduction

For more than eighty years, synthetic plastic polymers such as polyethylene (PE), polypropylene (PP), polystyrene (PS), polyvinylchloride (PVDC), polyethylene terephtalate (PET), Ethyl-vinyl-alcohol (EVOH) have been used for the packaging of food for their unique properties like stiffness, high gas barrier and optical properties (Mark, 2007; Urbanski et al., 1977).The vast majority of packaging products are based on fossil hydrocarbons; therefore, they are not biodegradable nor renewable, but toxic and unfriendly for our environment. In fact, those materials accumulate as debris in ocean and landfills rather than degrade and decompose (Thompson et al. 2009). In this decade, the growing consciousness about environmental and healthy damage caused by oil resins has encouraged manufacturers, researchers and scientists to seek alternatives such as bio-based materials to these synthetic resources. The world has taken the issue of environmental pollution very seriously and Europeans in particular have shown great interest in it. According to European bioplastics, a plastic material is defined as a bioplastic if it is bio-based, biodegradable, or both. The term bio-based means that the material is (partly) obtained from biomass such as corn, sugarcane, or cellulose whereas the term biodegradable is intended as the biodegradation of materials into water, CO_2 and compost by the microorganisms available in the environment through a chemical process without adding any artificial additives (Wool and Sun, 2011). A material biodegradation is rather linked to its chemical structure than its resource basis. In a nutshell, 100% bio-based plastics may be non-biodegradable and 100% petroleum based plastics can be biodegradable in environmental conditions (figure 1). Bioplastics are materials characterized by energy consumption saving during the production and lower carbon-dioxide gas during degradation. Not only are the bioplastics and biopolymers bio-based materials but they also exhibit higher functionalities and similar mechanical properties such as stiffness and tensile strength compared to synthetic counterparts. Increasing awareness of

developing and developed countries regarding the environmental concern and compelling laws/measures have contributed to increase the demand of bio-based packaging such as biopolymers and bioplastics, which has promoted the regeneration and provided the potential of carbon neutrality significantly.According to German nova-Institute (2018), the total production polymers is estimated to reach 400 million tonnes in 2020, with the bio-based share increasing from 1.5% to 3% in the same period of time, meaning that bio-based production rate will be faster than overall production.
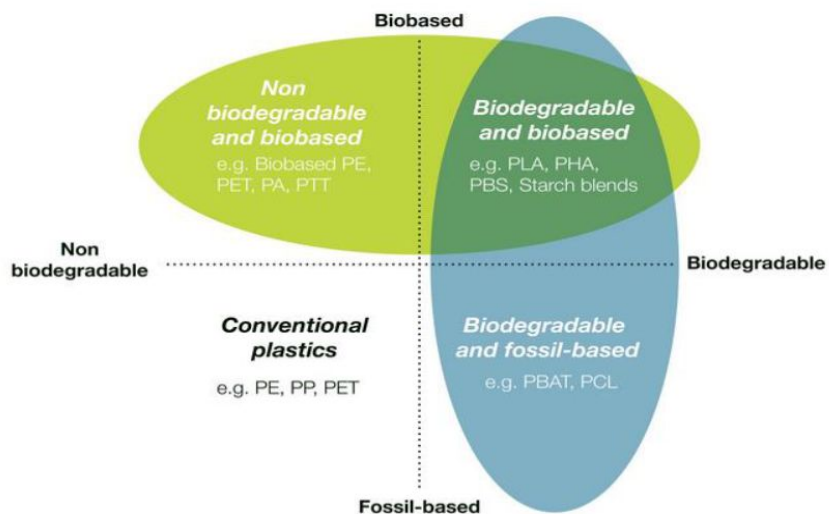

Figure1. Definitions and similarities of biobased, fossil-based, and biodegradable and biodegradable bioplastics.

From the graphs below, packaging sector will remain the most consumers with 56.8% of overall bio-based polymers in 2018 (1.2 million tons of the total bioplastics) (figure 2). Bioplastics materials have been used for years in many other sectors such as textiles, consumer goods and applications in the automotive and transport sector as well as the agriculture and horticulture sector. It is expected that, global bioplastics production capacity will increase from around 2.1 million in 2018 to 2.6 million tons in 2023 with the driving force

the growth of polylactic acid) and PHAs (polyhydroxyalkanoates). In addition, the largest plastics market is actually the packaging.
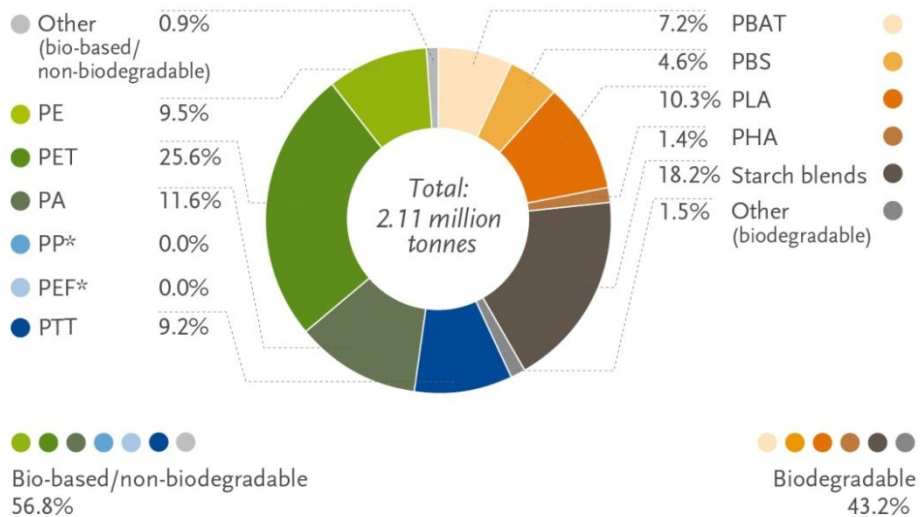

Figure 2. Global production capacities of bioplastics 2018 (by material type)

All this progress and improvements have been made in order to reduce the dependency of synthetic polymers in packaging with a subsequent decrease in human-caused greenhouse gases and CO_2 emissions. Notwithstanding all the advantages and assets of bio-based materials, it is still a challenge, that to use them as a mono-layer because they display poor mechanical and gas barrier properties. Actually, the combination of biopolymers with nanocellulose might contribute to obtain complex nanomaterials that meet relevant requirements of a food packaging. Nanocellulose (CN) represents a branch of the cellulose nanomaterials. As a rule of thumb, nanocellulose represent particles whose at least one size is smaller than or equal to 100 nm. CN can be subdivided into two categories: cellulose nanocrystals and cellulose nanofibrils. Cellulose nanocrystals (CNCs) are nanoparticles obtained by the chemical process through the acid hydrolysis or oxidation of the cellulose and the cellulose nanofribrils (CNFs), being obtained by the mechanical process where the cellulose is defibrillated to a nanoscale.CNCs

are biodegradable nano-spindles derived from the cellulose "top-down" which exhibit high performance properties capable of filling the gaps of both bio-based and synthetic polymers in terms of lack of gas barrier (Dufresne, 2013). The most captivating benefit is that CNCs can be used in synergy with biopolymers to implement a fully compostable food packaging with improved gas barrier properties for food shelf-life extension. The cellulose nanocrystals feature outstanding gas barrier properties and improved tensile strength; they can be incorporated into packaging for food shelf-life extension. Figure 3 and 4 indicate the main producers of cellulose nanofribrils and cellulose nanocrystals in 2018. It bears noting that **USA** and **Canada** are the leading producers of nanocellulose**.**

CNF Capacity 2018
(tonnes per year, dry basis)

Producer	Process	Capacity
Nippon Paper, Japan	TEMPO, carboxylated	560
University of Maine, U.S.	Mechanical	260
American Process, U.S.	SO_2 fractionation	130
CelluComp, UK	chemical pretreatment	100
Chuetsu Pulp and Paper, Japan	aqueous counter collision	100
Oji Paper, Japan	phosphate esterification	40
Sugino Machine, Japan	oblique collision	26
Seiko PMC, Japan	modified hydrophobic	24
SAPPI, Netherlands	Chemical	5
VTT, Finland	chemical, enzymatic	5
Tianjin Haojia Cellulose Co., Ltd, China	TEMPO, carboxylated	3
Dai-ichi Kyogo (DKS), Japan	TEMPO	1
U.S. Forest Products Lab, U.S.	TEMPO, mechanical	<1

Source: *Nanocellulose: Producers, Products, and Applications, A Guide for End Users,* TAPPI, 2017. Updated, Biobased Markets, Sept. 2018.

Figure 3. World production of cellulose nanofibrils, 2018 (per producer)

CNC Capacity 2018
(tonnes per year, dry basis)

Producer	Process	Capacity
CelluForce, Canada	sulfuric acid hydrolysis	260
American Process, USA	SO_2 fractionation	130
Melodea, Sweden	sulfuric acid hydrolysis	35
Alberta Innovates, Canada	acid hydrolysis	5
U.S. Forest Products Lab, USA	sulfuric acid hydrolysis	3
Blue Goose Biorefineries, Canada	catalytic conversion	2
FPInnovations, Canada	sulfuric acid hydrolysis	Pilot
Hangzhou Yeuha Technology Co., China	Proprietary	Pilot
Sweetwater Energy, USA	Reactive extrusion	Pilot
Tianjin Haojia Cellulose Co., Ltd., China	Modified and unmodified	Pilot

Figure 4. World production of cellulose nanocrystals, 2018 (per producer)

Nanocellulose Market Forecasts

	Tonnes (000)	Year
Vireo Advisors, high	56,481	potential
USDA	34,000	~2045
RISI, potential	23,551	potential
Vireo Advisors, low	18,283	potential
RISI, forecast	450	2025
Arbora Nano	145	NA
CelluForce	15	2017
Future Markets	0.8	2017

Figure 5. Nanocellulose market forecasts

From the 2015 TAPPI report, the nanocellulose market was around $250 million in 2014, with projected growth (CAGR) of 19% to 2019. The figure 5 reports the nanocellulose market forecasts for the next years. The cellulose nanocrystals (CNCs) feature outstanding gas barrier properties and improved tensile strength; they can be incorporated into packaging for food shelf-life extension. It can be observed in the figure 6 below that, the nanocellulose displays the highest oxygen barrier properties than synthetic polymers and biopolymers.
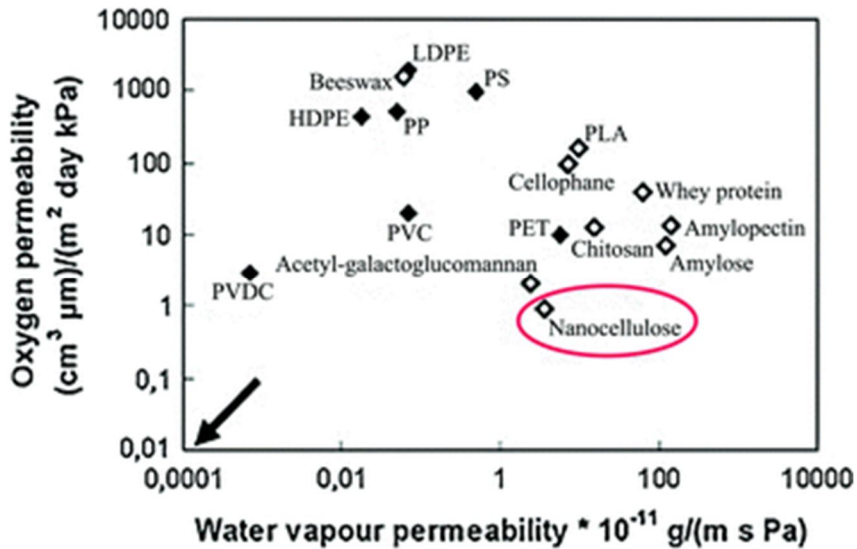
Figure 6. Oxygen and water vapour permeability of the nanocellulose in comparison with synthetic, bioplastics and bio-based structures (Nelson et al. 2016).

From that discovery, a new door was opened, that of using the CNCs to replace the synthetic gas barrier currently used in food packaging for a further contribution in the reduction of packaging dependency on synthetic polymers. Depending on the type of the extraction process adopted and the raw materials used, various functional groups present on the CNCs surface dictate their dispersibility in water or solvent to open a wide spectrum of their use in various fields of potential commercial applications (Nelson et al. 2016). In addition to material performance like rheological (the shear thinning) and gas barrier properties (oxygen, carbon dioxide…); exceptionally mechanical properties (high strength and stiffness); and optical properties (lightweight), cellulose nanocrystals gain a strong sustainability profile. Being obtained from biomass, it is renewable, biodegradable, compostable, and designed for making the environment friendly with a sustainable life cycle carbon footprint.

References

Dufresne, A., 2013. Nanocellulose: a new ageless bionanomaterial*Materials today, 16*(6), pp.220-227.

Mark, J. E. (Ed.), 2007. *Physical properties of polymers handbook* (Vol. 1076, p. 825). New York: Springer.

Nelson, K., Retsina, T., Lakovlev, M., van Heiningen, A., Deng, Y., Shatkin, J.A. and Mulyadi, A., 2016. American process: production of low cost nanocellulose for renewable, advanced materials applications. In *Materials research for manufacturing* (pp. 267-302). Springer, Cham.

Thompson, R.C., Moore, C.J., Vom Saal, F.S. and Swan, S.H., 2009. Plastics, the environment and human health: current consensus and future trends. *Philosophical Transactions of the Royal Society B: Biological Sciences, 364*(1526), pp.2153-2166.Wool, R. and Sun, X.S., 2011. *Bio-based polymers and composites*. Elsevier.

Urbanski, J., Czerwinski, W., Janicka, K., Majewska, F., & Zowall, H., 1977. *Handbook of analysis of synthetic polymers and plastics* (pp. 179-179). Chichester, England: Ellis Horwood.

Wool, R., & Sun, X. S., 2011. *Bio-based polymers and composites*. Elsevier.

Chapter 1

Literature Review

Chapter 1. Literature Review

1. Nanotechnology: current trends, capabilities and applications.

Nanotechnology is the art and science of manipulating matter at the nanoscale to create new and unique materials (Paul and Robeson, 2008). That term was first coined by Richard Feyman in 1959 and afterwards, it was then spread in the world of scientists who showed a high interest in the possibility of developing more advanced and engineering materials at the nanoscale (Maynard, 2006). During 2000 to 2015, the number of nano-articles has increased from 19754 to 141663. In 2015, more than 110 countries in the world took part in publishing of nano-articles, and the two countries United States and China ranked first and second with a huge distance with other countries (Statnano, 2017).Nanotechnology, an emerging area which shows how atoms, molecules and supramolecules can be organized differently to regain high performance properties with evolutionary advances for the development of cutting-edge and peak performance packaging, machinery and computation. From 1996 and 2018, as it is indicated in figure 1, the nanotechnology has definitely sprung up with its implementation in a bewildering array of applications such as medicine, energy, agriculture automotive, food packaging, composites (Barreto et al., 2011; Baruah and Dutta, 2009; Duncan, 2011; Srinivas et al., 2009; Wilkinson, 2003). Nanoparticles are ultrafine particles whose at least one dimension is equal to or less than 100 nanometers. Nanomaterials are generally characterized by their their tiny size, high surface area per unit, lightweight, strength which feature new properties and functions (Guozhong, 2004).
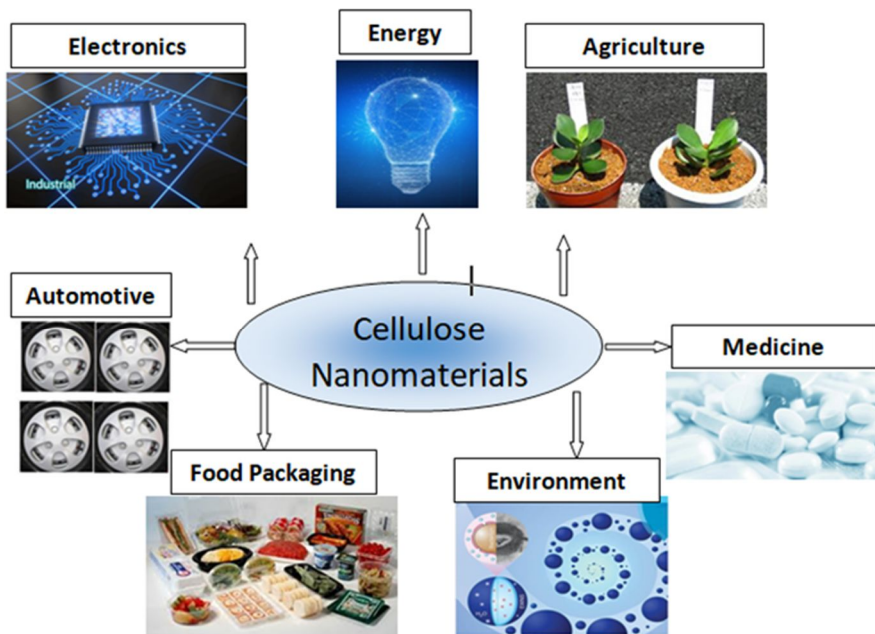
Figure 1. Applications of cellulose nanomaterials

The nanotechnology is a very promising field for promoting disruptive food packaging which concomitantly guarantees unique mechanical properties and gas barrier properties for food shelf-life extension meeting the environmental requirements. The potential of the nanotechnology can be very beneficial to the food packaging and the non-exhaustive list of recent trends is:

i. Improvement of adsorption and nutrients delivery

ii. Active packaging development referred to antimicrobials and oxygen scavengers

iii. Nanosensors and nanodevices applications to detect freshness, contaminants or packaging structure modification.

iv. Sensorial improvement (such as texture, colour and flavor modifications

v. Nanoparticles incorporation for developing intelligent and active materials

vi. Nanocoatings and nanoemulsions in combination with polymer matrix for conferring gas barriers and mechanical properties to the materials.

vii. Biodegradable nanocomposites and nanoparticles fillers.

Nanocomposites term was first published by Komarneni in 1983 while describing the nano-heteregenous sol-gel matrix. Nanocomposite is referred to a material composed of more than one solid phase (Koo, 2006). Polymer nanocompites are obtained by the combination of polymer and solid phase such nanoparticles and are characterized by their high surface area unit, very low density, high stiffness and tensile strength, flexibility (Paul and Robeson, 2008). In the past years, nanoparticles from magnesium oxide and zinc oxide have been successfullytested for food shelf-life extension due to their antimicrobial properties (Rekha et al., 2010; Xie et al., 2011); in addition, silica and nano-sized montmorillonite have been used for packaging durability increase. However, the inorganic character of these nanoparticles does not guarantee consumers safety and food/ medicine security. The research of organic nanoparticles becomes a necessity and the cellulose nanomaterials comply with all the requirements of biodegradability and therefore, because they are isolated from the cellulose, consumers would be inclined to accept them.

2. Branches and aspects of cellulose nanomaterials

Cellulose nanomaterials (CNMs) are a new family of innovative materials that has sprung up over the last 30 years. CNMs include bewildering array of technologically advanced applications such as membranes, transparent-flexible electronics, flexible shoes, papers money, high resistant shoes, templates for electronic components, food and polymers coatings, antimicrobial films, optical and biomedical, adhesives reinforcers, cements, inks, polymer reinforcement, nanocomposites, transparent films, layer-by-layer films, paper products, cosmetics (Moon et al., 2011). Generally, CNMs

are materials that encompass cellulose of various sizes, shapes and functional surface in their structure, opens a new gate for offering biodegradable, biocompatible and multifunctional innovative-materials (Sacui et al., 2014). CNMs can be used in combination with polymers to reduce the dependency on petroleum-based polymers and contribute to make the environment friendly for humans and animals. The implementation of such amalgamation is possible due to the unique and extraordinary gas barrier and mechanical properties that the CNMs exhibit, and that favors their blending with polymers structures in various ways such as CNMs-coating, CNMs-laminating, CNMs-layer-by-layer, CNMs-fillers (Shatkin et al., 2014). In CNMs act as a nucleating agent increasing the polymer crystallization rate and reinforcing structures, and the main mechanical properties are the tensile strength, Young's modulus and the storage modulus (Kargarzadeh et al., 2018). CNMs can include 4 groups: nanocellulose (NC) derived from the plants and wood(Dufresne, 2011; Thakur et al., 2014); algal cellulose (AC) obtained from the frequently studied species of algae such as*Micrasterias denticulata, Micrasterias rotate, Valonia, Caldophora,* and *Boergesenia*(Hua et al., 2014; Klemm et al., 2011); bacterial cellulose (BC)obtained from the one of the most studied species called*Gluconacetobacter xylinus* (reclassified from *Acetobacter xylinum*) (Gatenholm and Klemm, 2010) and finally, the tunicate cellulose (TC) derived from the most studied species like *Halocynthia roretzi, Halocynthiapapillosa* and *Metandroxarpa uedai* (Zhao et al., 2015).

The nanocellulose that will be the focus in the next discussion, can be subdivided into two categories: cellulose nanocrystals and cellulose nanofibrils. Cellulose nanocrystals (CNCs) are nanoparticles obtained by the chemical process through the acid hydrolysis or oxidation of the cellulose and the cellulose nanofribrils (CNFs) being obtained by the mechanical process where the cellulose is defibrillated. Prior to implementing the "top-down" process (chemical or mechanical shear) which can be assisted by the microwave (De Melo et al., 2017), the raw materials containing cellulose are

pre-treated first with enzymes, alkali and acid to facilitate the disintegration of fibers and make consistent and efficient the subsequent treatments with a much higher CN yield (Phanthong et al., 2018). Water immersion, heating and sonication can also contribute to make the extraction easier mostly from recalcitrant sources such as materials with high lignin content (Cui et al., 2016). CN is characterized by its size, morphology aspect and shape, cellulose I polymorph surface charges, rheological properties, tensile strength and stiffness, the degree of crystallinity which all depend not only on the type of process acquired but also on the raw material sources (plant) used for the production.

Throughout the years, the nomenclature of the CNCs has changed from being called whiskers, needles to rod-like, crystallites while CNFs have been referred to as nanofribrillated cellulose, cellulose microfibrils; however, the ISO standard terms "cellulosenanocrystals" (CNCs) and "cellulose nanofibrils" (CNFs) have been adopted by TAPPI (Technical Association of Pulp and Paper Industry) as acronyms to be used to avoid confusion.

2.1. General features of the cellulose

Cellulose is one of the most abundant biopolymer on the earth. It is generally synthesized by plants, but it is also found in some bacteria (*Acetobacter xylinum…*) (Andrade et al., 2010*).* From the table 1, it can be observed that the highest cellulose content was found in cotton with about 82-95% cellulose, compared to wood that has about 40–50% cellulose content and other sources (Oliveira de Castro et al., 2015) or bast fibers such as flax, hemp, or ramie, which have about 70–80% cellulose content (Abdul et al., 2012; Fernandes et al., 2013) while the maize straw and rice husk contain about 35-40% of cellulose. (Marin et al., 2015; Nunes et al., 2013; Rehman et al., 2014)

Fiber Source	Origin	% Cellulose
Banana	Leaf	60,0 – 65,0
Coir	Fruit	32,0 – 43,0
Cork bark	Leaf	12,0 – 25,0
Corn cob	Stalk	33,7 – 41,2
Cotton	Seed	82,7 – 95,0
Curaua	Leaf	63,4 – 73,6
Flax	Stem	64,0 – 84,0
Hardwood	Stem	39,0 – 50,0
Hemp	Stem	67,0 – 78,0
Jute	Bast	51,0 – 78,0
Kenaf	Bast	44,0 – 72,0
Maize Straw	Straw	28,0 – 44,0
Nettle	Bast	53,0 – 86,0
Ramie	Bast	67,0 – 99,0
Rice Husk	Straw	25,0 – 35,0
Softwood	Stem	42,0 – 50,0
Sugar cane bagasse	Stem	32,9 – 50,0
Sisal	Leaf	60,0 – 73,0
Wheat Straw	Stalk	30,0 – 35,0

Table 1. List of cellulosic sources and percentage in cellulose content.

D-glucopyranose molecules contribute to the building blocks of cellulose polymer chains. Cellulose contains 44.44% carbon, 6.17% hydrogen, and 49.39% oxygen. The chemical formula ofcellulose is $(C_6H_{10}O_5)n$ where n is the degree of polymerization and represents the number of glucose groups. Cellulose chains form anhydroglucose units when linked by 1-4 glucosidic bonds and form anhydrocellobiose when they form two units of anhydroglucose. The figure shows the β1-4 glicosidic bonds formed between two and millions of units of glucose to give the cellobiose and cellulose structures respectively.
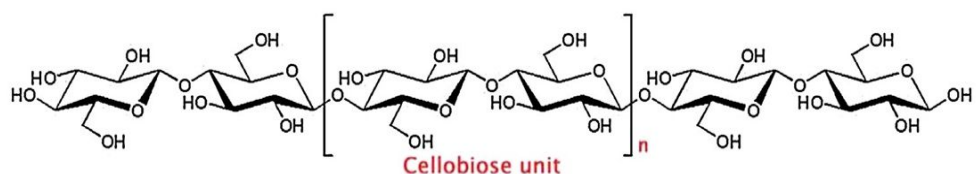

Figure 2. Cellobiose and glucose units

The cellulose degree of polymerization (DP) is generally expressed in terms of anhydroglucose with each unit having 6 carbon atoms and 3 hydroxyl

groups at the position C2, C3 and C6 atoms. The accessibility of hydroxyl groups to reaction depends on swelling effects and degree of crystallinity of the fibrous structure (Turbak et al., 1983). Cellulose is a hydrophilic, biodegradable and chiral structure due to their hydrogen bonds, hydroxyl groups and molecular structure. Cellulose chains are a tough, fibrous, and water-insoluble structure arranged in microfibrils with high strength and other superior mechanical properties (Zimmermann et al., 2004). The intramolecular bonds provide stiffness to the polymer chain, while the intermolecular bonds provide sheet structures. Cellulose fibers are insoluble in water and most conventional organic solvents because of their high crystallinity and many hydrogen bonds present in their structure. In nature, cellulose is in the form cellulose I and can be converted to other crystalline forms. Cellulose II is formed by treating cellulose I with NaOH (mercerization), with alkali/salt or by removing the functional groups from cellulose, derivatives (regenerated cellulose). Cellulose II is the most thermodynamically stable form of cellulose. Cellulose II is antiparallel probably due to its precipitation from solution as it occurs with many synthetic polymers. Cellulose III is formed by soaking cellulose in cold (about − 80 °C) liquid anhydrous ammonia followed by its subsequent evaporation. Cellulose I and cellulose II are transformed into cellulose III1 and cellulose III2 respectively (Hearle, 2001). When rehydrated, cellulose III returns to its original form. Finally, Cellulose IV is formed by soaking cellulose in hot (about 200 °C) glycerol followed by its subsequent removal with 2-propanol and water. Cellulose I is transformed into cellulose IV1 and cellulose II is transformed into cellulose IV2 (Wickholm et al., 2001). The hydroxyl groups of mercerized cotton cellulose II has a lower degree of crystallinity than natural cotton cellulose I but are more covalently reactive. Generally, due to the hydroxyl groups, cellulose fibers interact more with water than solvents. Methanol interacts to a greater degree with cellulose I than with cellulose II but, this phenomenon can be reversed if the methanol

is mixed with water. Native cellulose (Figure 3) contains crystalline regions interspersed with amorphous regions (Atalla and Vanderhart, 1984).
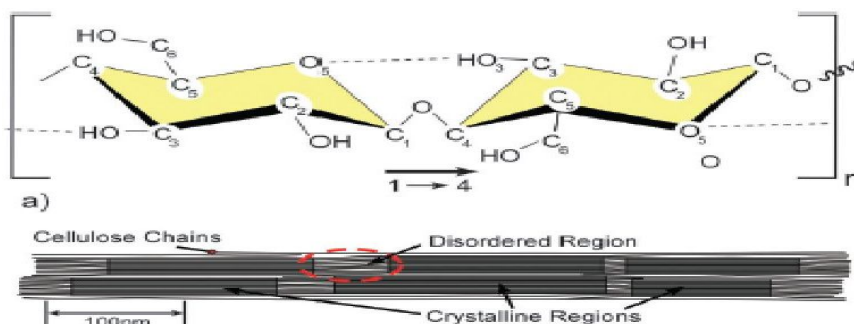

Figure 3. Schematics of (a) repeating single cellulose chain unit with the directionality of the 1-4 linkage and intra chain hydrogen bonding (dotted line), (b) idealized cellulose microfibril illustrating a suggested configuration of the crystalline and amorphous regions.

The amorphous regions are more porous than the crystalline regions, allowing water or dyes to be absorbed increasing the reactivity to acid or enzymatic hydrolysis. When purified cellulose fibers are subjected to dilute acid hydrolysis, the amorphous regions selectively hydrolyze because they are lower packed and the crystalline regions are released unaffected

2.2. Cellulose nanofribrils (CNFs)

CNFs as a new cellulosic material was first coined by Turbak et al. (1983) and Herrick et al. (1983) who produced cellulose with lateral dimensions in nanometer range by passing a softwood pulp aqueous suspension several times through a high-pressure homogenizer. Even nowadays, CNFs are nanoparticles still obtained mechanically from the cellulosic materials. The mechanical isolation of the CNFs can be combined with a chemical or enzymatic treatment not only to further facilitate the disintegration (high shearing forces) of the cellulose fibers with a yield increase but also, the functionalization of the CNFs can be obtained during the production (Arvidsson et al., 2015). Residual charges can be found on the surface of the CNFs because combinations such as tempo-mediated oxidation and mechanical treatment, carboxymethylation and mechanical treatment,

phosphorylation and mechanical disintegration have been used recently to develop diverse functional charges (Nechyporchuk et al., 2016; Saito et al., 2007). CNFs and CNCs are both nanoscale materials but they are different from their shape, size and surface chemistry. CNFs are known to be more flexible and less crystalline than the CNCs due to the presence of both amorphous and crystalline domains in their structure; however, they bear better mechanical properties. CNFs possess high aspect ratio and form gels in water with shear-thinning and thixotropic behavior. CNFs has a morphology with length >1μm, width 25-100 nm and aspect ratios 10-100. The figure illustrates the steps which comprise the cellulose nanofribrils isolation from the cellulose pulp.
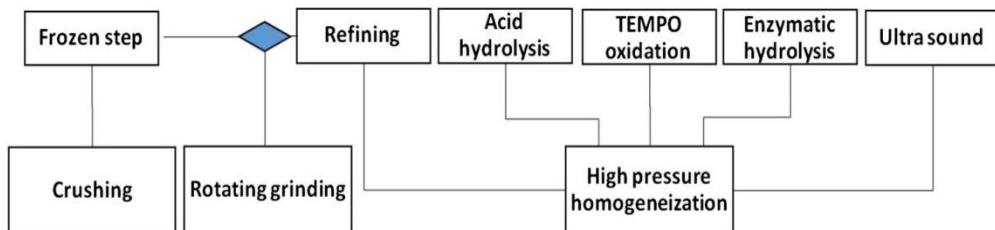

Figure 4. Mechanical, chemical and enzymatic steps for CNFs production

These features included the surface chemistry and degree of branching are dependent on many factors such as the type of the mechanical shear process, the raw materials used or the utilization of an eventual pretreatment. Experts of the nanotechnology field suggest to use CNFs as a mechanical properties reinforcer and CNCs as a gas barrier enhancer in complex and composite structures (Khalil et al., 1012, 2014).

2.3. Cellulose nanocrystals (CNCs)

It is worth noting that the first CNCs production was introduced by Ranby, (1951), When cellulosic materials are subjected to a combination of mechanical, chemical and enzymatic treatments, amorphous regions of the cellulose are hydrolyzed letting unblemished the crystalline regions (figure 5)

which can be isolated easily. CNCs are stiff and ordered nano-spindles which exhibit high surface area, higher specific strength and higher crystalline compared to the bulk cellulose (George and Sabapathi, 2015). Generally, the chemical hydrolysis is the most efficient way to extract the CNCs. However, the high-pressure homogenization, micro-fluidization, high-intense ultrasonic (Tang et al., 2014) and chemical pretreatments (acidic and basic) have been utilized in combination with the chemical hydrolysis to obtain a higher yield of the CNCs production (Lu and Hsieh, 2010). Microcrystalline cellulose production follows the same steps of process but the hydrolysis occurs in a more diluted acid followed by the sonication. Traditionally, CNCs are isolated by acid hydrolysis with the grafting of functional groups such as sulfate half esters or phosphate half esters if they are extracted with sulfuric or phosphoric acid respectively (Camarero et al., 2013). CNCs can be also oxidized with the formation of aldehyde and carboxyl groups on their surface due to the use of periodic acid, ammonium persulfate (APS).
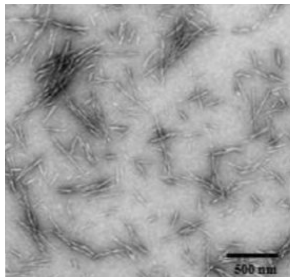

Figure 5. Cellulose nanocrystals (CNCs) by TEM.

Common ways to extract the CNCs by removing the amorphous regions from cellulose fibers by acid or oxidative hydrolysis. The crystals obtained from both methods are pure with different yield, morphology, surface chemistry, morphology, rheology properties and crystallinity.

2.3.1. Cellulose nanocrystals isolation by acid hydrolysis

The production of CNCs by acid hydrolysis typically involves the following steps:

✓ Hydrolysis of cellulose under controlled conditions (acid concentration, temperature, time, agitation, acid and water to cellulose ratio);

✓ Stop and cool of the reaction by addition of water under stirring (this step dilutes the solubilized products), followed by successive purification and centrifugation to eliminate the amorphous parts hydrolyzed;

✓ Extensive dialysis to eliminate residual acids;

✓ Mechanical treatment by sonication for dispersion of the particles;

✓ Filtration, ultrafiltration and soxhlet-extraction to remove the remaining residues of amorphous solid and to obtain the final stable colloidal suspension

✓ Concentration of the nanoparticles and, when needed, freeze-drying and spray-drying to obtain solid CNCs.

Acid hydrolysis is traditionally adopted to isolate high crystalline materials called cellulose nanocrystals (CNCs) from the cellulosic sources (Bondeson et al., 2006). The tightly-packed nature of the cellulose makes the crystalline regions less accessible to acid attack but preferably accessible to amorphous regions which are less organized. The raw materials can be cotton linters, wood fibers, microcrystalline cellulose (MCC), soy husks, rice hulls and other natural resources (Bondeson et al., 2006). Various acids such as sulfuric acid, hydrochloride acid, periodic acid and phosphoric acid have been successfully employed for the extraction of CNCs. Although CNCs obtained by HCl do not contain charges on their surface (Boujemaoui et al., 2015), CNCs obtained by other acids contain residual charges derived from the acid used for its isolation (George and Sabapathi, 2015). As a result of the reaction, a wide spectrum of residual charges has been found on the CNCs surface, providing great benefits for their functionalization (Habibi et al., 2010). Native cellulose

contains amorphous and crystalline regions. After the disintegration of the amorphous regions which hydrolyze easily, the solution is purified through centrifugation, dialysis and filtration.
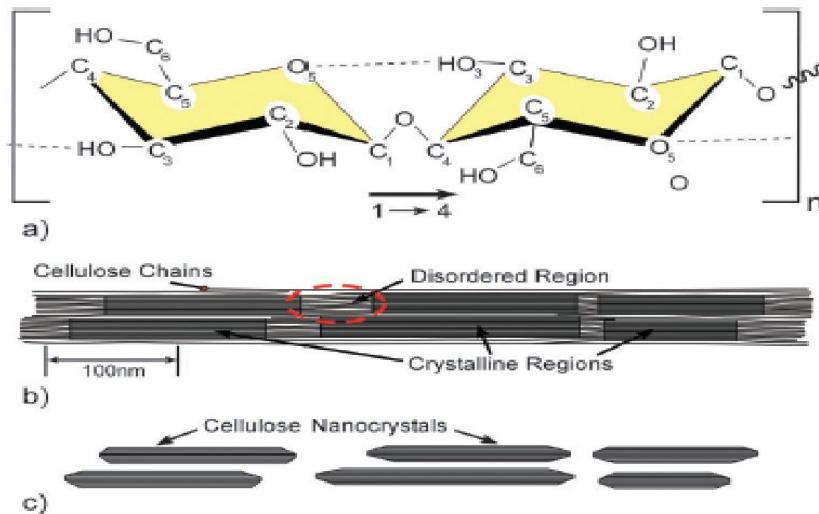

Figure 6. Schematics of (a) repeating single cellulose chain unit with the directionality of the 1-4 linkage and intra chain hydrogen bonding (dotted line), (b) idealized cellulose microfibril illustrating a suggested configuration of the crystalline and amorphous regions, and (c) cellulose nanocrystals with disordered regions removed.

The final colloidal suspensionnow contains only crystals, also called nanowhiskers or cellulose nanocrystals. The table 2 clearly indicates that the geometrical features (length, width, aspect ratio, morphology) of the CNCs depend strongly on the botanic origin of the raw materials. The size and morphology of the CNCs are also influenced by the time/temperature of the reaction, the concentration of the acid used for the hydrolysis.

Source	Preparation method	Length (nm)	Width (nm)	Aspect ratio (L/D)
Wood	H_2SO_4 hydrolysis	100–300	3–5	20–100
Cotton	HCl hydrolysis	100–150	5–10	10–30
Ramie	H_2SO_4 hydrolysis	70–200	5–15	~12
Sisal	H_2SO_4 hydrolysis	100–300	3–5	~60
Valonia	H_2SO_4 hydrolysis	1,000–2,000	10–20	50–200
Tunicates	H_2SO_4 hydrolysis	>1,000	10–20	~100
Bacteria	H_2SO_4 hydrolysis	100–1,000	10–50	2–100
Bacteria	HCl hydrolysis	160–420	15–25	7–23

Table 2. Dimensions of cellulose nanocrystals (by type of preparation) adopted by **George and Sabapathi, (2015)**

2.3.2. Cellulose nanocrystals isolation by oxidative hydrolysis

Generally, a simultaneous hydrolysis and oxidation of the celluloseis possible when a strong oxidizing agent like the 2,2,6,6-tetramethylpiperidine-1-oxyl (Tempo) is used for the CNCs production (Saito and Isogai, 2004). Tempo is used for the oxidation of hydroxyl groups present on the CNCs surface following the acid hydrolysis with the hydrochloride acid (HCl) producing uncharged CNCs. Very recently, Leung et al. (2011) has developed a valid alternative to isolate the cellulose nanocrystalsfrom the cellulosic raw materials. More importantly, the use of the APS allows the bleaching of the raw materials, hydrolyze the amorphous parts of the cellulose and oxidize the hydroxyl groups simultaneously during the reaction in one-step production, therefore; APS-assisted oxidation can be performed directly on the cellulosic materials to obtain oxidized CNCs. Both APS and TEMPO allow the production of CNCs with residues of carboxylic acid on their surface and that, opens a wide spectrum of functionalizations of the CNCs surface (esterification, amidation…).

3. Properties and drawbacks of cellulose nanocrystals

After the production, the cellulose nanocrystals are characterized by their size, morphology, charges density, crystallinity and other relevant parameters useful for a better understanding of the properties of the CNCs.

CNCs size and morphology

The apparent and actual size of the cellulose nanomaterials can be assessed by the means of dynamic light scattering (DLS) and transmission electron microscopy (TEM). By DLS, Stokes–Einstein equation relates the radius of the particles, while they are subjected to fluctuations in scattered light under the assumption, that the particles have a constant diffusion during the fluctuations over time (Kholodenko and Douglas, 1995). It is worth mentioning that DLS has been developed only for spherical particles and polymers but which was further used for obtaining "the apparent particles size" of rodlike or nanowhiskers while the actualsize (length, thickness and width) to be determined by TEM and the morphology by the atomic force microscopy (AFM). Apparent diameter cannot be correlated because nanowhiskers have different translationaldiffusion constants, which depend on the orientation of the particles (parallel, orthogonal…). Critical parameters to consider while using the DLS to obtain the apparent size of a colloidal dispersion of CNCs, are the temperature, sample concentration, the absence of impurities and the pH. The stability of the colloidal suspension is dictated by the negative charges present on the CNCs surface which create the electrostatic repulsion. Noting that accurate TEM imaging is obtained when the pH of the never-dried or redispersed CNCs is adjusted at pH between 4 and 5 to provide more acidic forms (negatively protonated) prior to setting on carbon-coated TEM grids.

Microscopy techniques readily used for imaging the CNCs are AFM and TEM because they have the nanometer scale resolution capabilities. Real dimensions (i.e., length and width) of the CNCs can be observed and identified by TEM. Morphology, surface topography, mechanical properties can be studied and obtained by means of the AFM. Both AFM and TEM might be used in combination to provide a deeper description of the nanoparticles morphology. Another technique called photon correlation spectroscopy (PCS) has also been used to obtain the particle size of the nanoparticles. PCS was

applied on CNCs added of electrolyte screens to prevent the CNCs not to undergo agglomeration (Dong and Gray, 1997).

Charges density and colloidal stability of CNCs

Charges density and colloidal stability of dispersed CNCs have been evaluated by Z potential measured through electrophoretic light scattering (ELS) where the mobility of particles occurs in an applied electric field according to the Henry equation with Huckel and Smoluchowski considerations. Conductometric titration has been used to assess the charges density (strong and weak charges) of the charged CNCs but not the CNCs obtained by HCl which are uncharged, common Z potential values are between -20 and -50 mV dependent upon the degree of oxidation (Abitbol et al., 2013). Reliable zeta potential values are obtained at 0.25 wt% of suspended CNCs with or without 5-10mM of NaCl. The most important parameter, which strongly affects the Z potential, is the pH because it causes the protonation and deprotonation of negative charges generating a different electrostatic interaction. Generally, CNCs obtained by oxidative hydrolysis strongly depend on the pH and have values of Z potential higher than CNCs obtained by acid hydrolysis (Romdhane et al., 2015).

Optical properties of the cellulose nanocrystals

Scientists have extensively studied optical properties of the cellulose nanocrystals in recent years. CNCs suspension can be stable as a result of the repulsion of electrostatic negative charges. It is worth noting that CNCs can spontaneously auto-assemble into a chiral nematic phase above a critical value of CNCs concentration. Further information on the organization and dispersion as well as on the pitch of the chiral nematic and anisotropic-isotropic ration can be obtained via a polarized light (Mariano et al., 2014). The anisotropic (birefringent) behavior of the CNCs depends on the concentration of the dispersed CNCs which can show a switch between lower chiral nematic liquid crystalline phase and an upper isotropic phase above a

certain concentration (>2 wt%). Bright light patterns diffraction appears when dispersed CNCs are stirred and this is related to the parallel alignment of individual CNCs. Poor and well dispersed CNCs provide visible monochromatic and polychromatic domains respectively. The critical parameters which dictate the crystalline behavior of the CNCs, are the size of the crystals, the concentration of the dispersed CNCs and necessary time to obtain the crystalline equilibrium and the chiral nematic and birefringent behavior (Foster et al., 2018). Numerical Control can be used to observe a bluish color due to the chiral nematic classification and the length of the pitch spacing (p). Therefore, CNCs films of different colors can be seen if the films are thin enough because CNCs are able to absorb visible light and, depending on the different wavelengths are absorbed and the reflected light emits different colors (Revol et al., 1992).
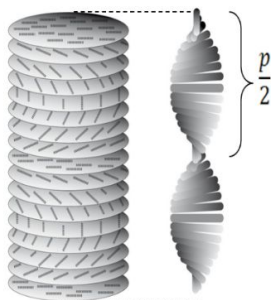

Figure 7. At certain concentrations, the nanocrystals self-organize into a chiral nematic ordering where the length of the pitch gap (p) in the helical structure can absorb different wavelengths and emit wavelengths with different colors (Revol et al., 1992).

Cellulose nanocrystal crystallinity index

The study of the crystallinity provides insights on the purity of the crystalline network / lattice of the cellulose nanocrystals isolated from the cellulose. High crystallinity index translates the purity of the raw materials used and the efficiency of the extraction process. According to Bragg law, $n\lambda=2d\sin\theta$ the cleavage faces of crystals appear to reflect X-ray beams at certain angles of

30

incidence (theta, θ). The variable distance between atomic layers in a crystal, and the variable lambda λis the wavelengthof the incident X-ray beam; n is an integer. This observation is an example of X-ray wave interference when it leaves the crystals measuring their average spacings between layers or rows of atoms correlated to the size, size and internal stress of particles. The crystallinity of the cellulose nanocrystals depends on various factors such as the origin of the native cellulosic fibers used, the type of the extraction process, the time and the temperature applied during the extraction and the concentration of the acids used for the extraction (Dong and et al., 1998). As a matter of facts, the degree of polymerization decreases as the acid hydrolysis proceeds since the non-crystalline regions in the microfibril will be removed. Due to the loss of amorphous regions, the crystallinity will increase and also the insolubility in water because the crystalline regions are less accessible (Hamad and Hu, 2010; Leung et al., 2011).
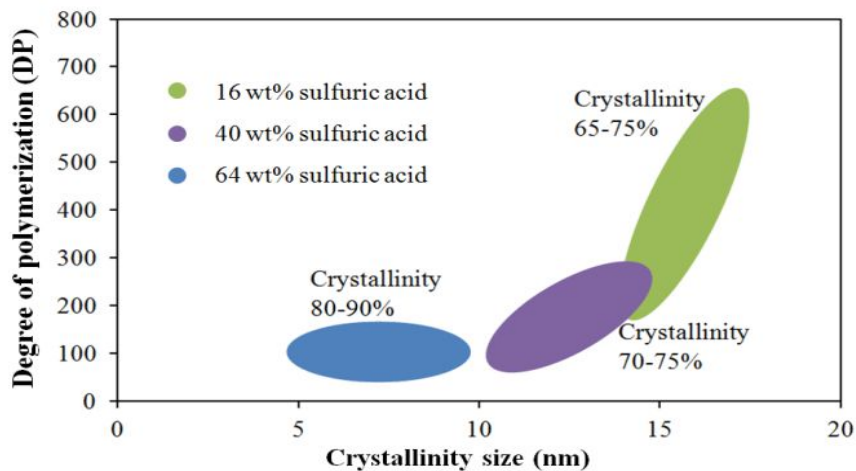

Figure 8. Crystallinity size in relation to the DP. During acid hydrolysis, the DP will decrease and the cellulose crystallinity will increase, due to loss of non-crystalline regions and, as a result, smaller crystal size will be obtained.

Mechanical properties of the cellulose nanocrystals

Mechanical properties are strongly affected by the source and type of the cellulose. The entanglement of the fibers plays a vital role in the structure as the hydrogen bondings. Cellulose I with intramolecular and intermolecular bonding has a young's modulus of approximately 137 GPA and 92 GPA respectively. Regenerated cellulose also called cellulose II has a young's modulus close to 113 GPA. CNCs whose density is about 1.5-1.6 g/cm^3 which do not contain the amorphous regions have a young's modulus of 60-125 GPA similar to that of Kevlar (density is approximately 1.45 g/cm^3) but higher to that of glass fibers, which has a young's modulus of 70 Gpa and a density of 2.6 g/cm^3(Mariano et al., 2014). The specific Young's modulus of cellulose crystals was found to be greater than that of the stainless steel. In addition, Nanocomposites like polymer-CNCs blendings could allow to improve physical properties such as robustness, flexibility, durability, weight and transparency of various high-performance structural applications (Boufi et al., 2014). CNCs have been blended in many matrices, such as polyacrylonitrile, with a consequent increase in tensile modulus and strength from 14.5 to 19.6 GPA and from 624 GPA to 709 MPA respectively. Moreover, the Young's modulus and tensile strength of the resulting composite increased from 0.51 to 344 MPA and 4.27 to 14.86 MPA, respectively in presence of water-based polyurethane (Khan et al., 2012).

Thermal properties of cellulose nanocrystals

The acid hydrolysis of the cellulose by sulfuric acid provides more stable colloidal suspension of cellulose nanocrystals in water because of the repulsion of the negatives charges (sulfate half esters) present on their surface (Kargarzadeh et al., 2012). The hydrolysis breaks down the amorphous regions of the cellulose allowing the isolation of crystalline parts with a consequent decrease of degree of polymerization and thermal stability compared to cellulose fibers. That drawback represents a major pitfall for their

incorporation into nanocomposites generally processed at a temperature of over 200°C; therefore, it can be justified the lack of nanocellulose employment in polymer matrix. Thermal stability improvements of structures containing CNCs and waterbone epoxy composites (Xu et al., 2013), bacterial polyester and CNCs were obtained (Yu et al., 2012)**; moreover**, according to the recent findings, PLA thermal properties were improved after they were blent with the nanocellulose (Arrieta et al., 2014; Siqueira et al., 2013).

3.1. Reactivity of the cellulose nanocrystals

Due to their hydrophilic nature, scientists have been involved in search of strategies to confer hydrophobic nature to cellulose nanocrystals in order to promote their incorporation into hydrophobic nanocomposites.

Reactive and chemical charges such as carboxyl and hydroxyl groups present on the surface of the cellulose nanocrystals have been studied to better understand their ratio, specific surface area reactivity and availability for functionalization. The specific surface area has been considered as one of the most important parameters to assess in order to study the availability of the CNCs. Based on the cellulose source, the specific surface area of the CNCs varies between 150 and 150 m2/g (Chazeau et al., 1999; Terech et al., 1999), while that of the MCC and MFC is much lower, 1.8 m^2/g and 7-20 m^2/g respectively (Lu et al., 2008; Portugal et al., 2010). Therefore, the functionalization of the CNCs provide various properties useful for being embedded and incorporated into many organic matrices. Tegge et al. (1981) demonstrated that the primary hydroxyl groups of the cellulose reacted tentimes faster than the secondary ones in position 2 and 3 during the esterification at the processing conditions. Subsequently, steric effects due to the supramolecular structure of the cellulose (Lenz, 1994) will govern the reaction of the hydroxyl groups of the cellulose nanocrystals surface, under heteregenous conditions. A single cellulose chain with a 1g mass has one exposed C1 hydroxyl and one exposed C4 hydroxyl. The study of the

availability revealed that only 1/3 of the hydroxyl groups could participate in chemical modifications of the cellulose and the cellulose nanocrystals since some of the hydroxyl groups are oriented geometrically to the internal part of the crystal (Siqueira et al., 2010). Therefore, it is worth emphasizing that the reactivity of the CNCs is not based on the number of the total number of hydroxyl groups but rather on their availability to react with other surrounding compounds during the functionalization. In addition, operative conditions such as pH, temperature, time and other critical parameters have to be controlled during the chemical modification (Cetin et al., 2009). Lin et al. 2012 developed mathematic equations to calculate the content of hydroxyl groups (nOH) on the CNCs surface.

$$nOH = 3 \left(\frac{w}{\rho \text{cell} * \text{Vcnc}} \right) \left(\frac{Scnc}{S'} \right) \left(\frac{1}{NA} \right) \quad (1)$$

$$Vcnc = \Pi \left(\frac{d}{2} \right)^2 * L \quad (2)$$

$$Scnc = \Pi dL - \Pi \left(\frac{d}{2} \right)^2 S' = d'L' \quad (3)$$

Where *w* is the weight of CNC sample (1g in this case), NA is the Avogadro number (6.02 x10^{23} mol^{-1}), *Vcnc* is the volume and *Scnc* is the surface area of an individual nanocrystal calculated with the width(d) and the length (L) measured by microscopic techniques (AFM, TEM…) and *S'* is the surface area of two units of glucose. For 1 g of CNCs, the computerized surface of hydroxyl roups has to be found to be between 2-4mmol/g depending on the crystal dimensions and the active hydroxyl amount deduced was 0.4 and 0.8 mmol/g. Therefore, the resulting product of the modifications can be linked either by covalent or non- covalent bonds. Covalent bonds derive from the chemical interaction with CNCs surface through esterification, amidation, etherification, etc. Surfactants and CNCs can form non-convalent interaction through hydrogen bonding, electrostatic interaction and van der walls forces to improve their dispersibility in the solvents.

3.2. Drawbacks of the cellulose nanocrystals

The CNCs bear several useful capabilities in terms of gas barrier, rheological and mechanical properties and more importantly, they have high surface area with functional chemical groups which opens up a wide spectrum array of applications in food packaging, pharmaceutical applications, automobile, electronics…; however, the high propensity of the cellulose nanocrystals to swell in presence of the water is detrimental to their extraordinary features. The water sensitivity of the cellulose nanocrystals and cellulosehas been extensively studied to identify the type of chemical relationships and interactions that exist between the water and the cellulose-based materials when they are in contact. Fotie et al. (2017) have explored the impact of the water on the CNCs-coated polymers in terms of the gas barrier performance (oxygen, carbon dioxide). The gas permeation performed on the coated PET films was found to be quite null in the absence of the water, while a dramatic and abrupt increase of the gas permeation was observed with the increase in the relative humidity. This behavior was attributed to the water, which occupies the free volume, therefore,progressively acts as a plasticizer and disrupts the crystalline lattice to facilitate the gas to diffuse with minor obstacle.For the reasons cited above, notwithstanding the relevant properties and potential of the cellulose nanocrystals, their application in food packaging will be effective only if there are made more hydrophobic via the functionalization of their surface (esterification, amidation, sylation…) and/or via the lamination of the CNCs- coatings layers to isolate them from the external surroundings.

3.3. Biodegradability and Toxicology assessment of cellulose nanocrystals

Several scientific works have proved the biodegradability of the cellulose nanocrystals. The first study of the biodegradability of the nanocellulose used as a reinforcer in the polymers was performed by Coma et al. (1994) and

according to their findings, the complex matrix was biodegradable. Although the nanoparticles are very tiny and small, their biodegradability is not compromised (Kummerer et al., 2011). In fact, they reprted reported that the nanoparticles from cellulose and starh were even rapidly than their macrocospic counterparts. It is a strong proof that the nanocellulose into the packaging will be recycled readily.

Nanomaterials have recently drawn the attention of the scientific community about their possible adverse effects on health and safety have extensively been evaluated. Cytotoxicity, genotoxicity and ecotoxicity potential of the nanomaterials have been evaluated by researchers of the field. Nanometerials properties differ from their parent bulk materials because of their smaller size, different morphology and larger surface area resulting in their ability to cross natural barriers including electronic and plasmonic effects. Pure cellulose cellulose-based foods additives such as carboxylmethyl cellulose, microcrystalline cellulose, etc are generally known as a safe and non toxic food substance. Recently, a Canadian research group CNCs assessed the potential environmental risks of the carboxymethyl cellulose and cellulose nanoparticles and according to their findings, the toxicity potential and environmental risk of both cellulose-based materials are negligible (Kovacs et al., 2010). Ni et al. (2012) found a low cytotoxicity of the nanomaterials to L929 cells and MTT assay; in addition, Moreira and co-workers tested the potential genotoxicity of bacterial cellulose on fibrous nanoparticles and through vitro analysis and other techniques, they did not find any genotoxic effect. Vartiainen found no imflammatory effects or cytotoxic on mouse and human macrophages after being exposed for 6 and 24 h to nanocellulose. Furthermore, the health effects of the modified nanocellulose (oxidized and carboxilated) obtained from various biomass sources, were studied by exposing the cells (Spodoptera frugiperda insect cells, Sf9) to the nanocellulose. After they evaluated by electric cell by their spreading and viability according to the findings, none of the nanocellulosic materials

produced significant cytotoxic effects based on 50 % inhibition concentration (Lam et al., 2012). It was assessed by using standard ecotoxicological and mammalian test protocols and have, to date, been shown to be practically nontoxic in each of the individual tests. In addition, CNCs have recently obtained regulatory approval under Canada's New Substances Notification Regulations (NSNR) for unrestricted use in Canada and is the first organic nanomaterial to be added to Canada's domestic substance list.

4. Chemical functionalization of cellulose nanocrystals

Modifications of the cellulose nanocrystals can be grouped into 3 different categories:

i) Interaction between surface hydroxyl groups with small molecules to provide carboxyl, esters, amides, urea, and silyl groups on the cellulose nanocrystals surface

ii) Polymer surface modification by the "grafting onto" with coupling agents.

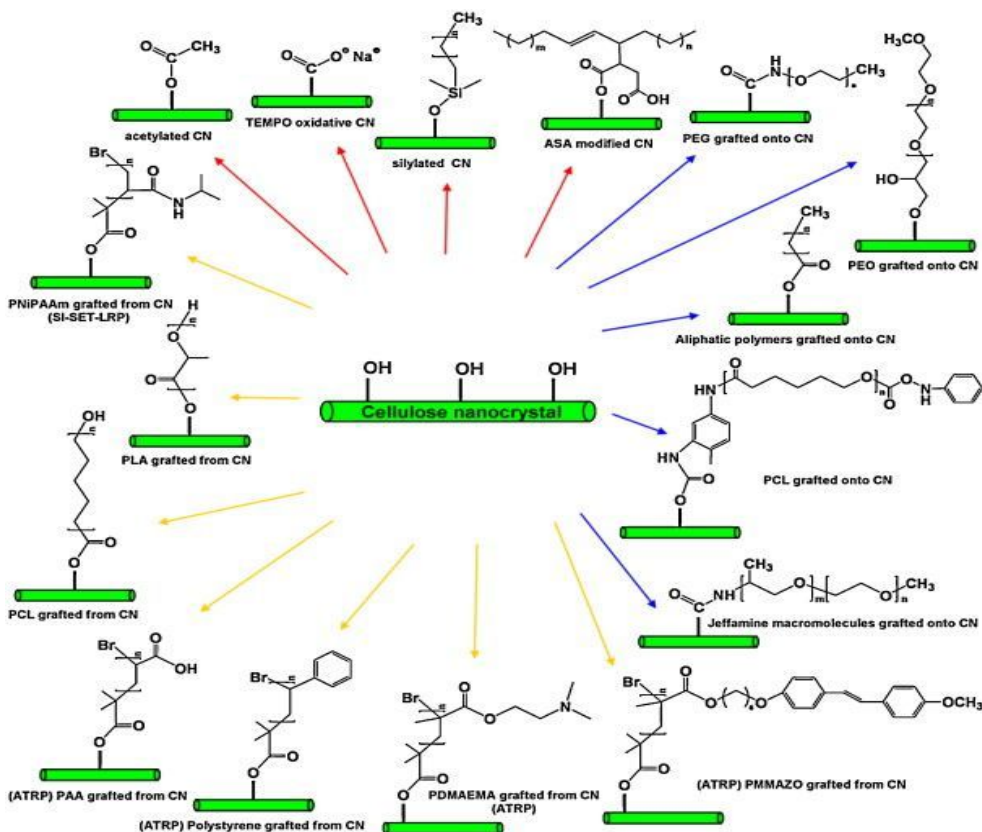iii) Polymer surface modification by the "grafting from" with radical polymerization.

Figure 9. Grafting agents used for physical and chemical functionalization of cellulose nanocrystals (Dufresne, 2013)

4.1. Functionalization by adsorption

Cellulose nanocrystals can be modified by adsorption of surfactants or cationic agents on the cellulose nanocrystals through electrostatic phenomena to improve their dispersion in organic media. Negative charges of the cellulose nanocrystals such as carboxylate or sulfate half esters can interact with cationic agents through an electrostatic mechanism. The most important advantage is the preservation of the crystalline core of the CNCs. Recently, quaternary ammonium salts (c18 alkyl, phenyl, glycidyl and allyl) was successfully adsorbed onto the tempo-oxidized CNCs surface (Salajkova et al. 2012) keeping the birefringence properties intact. The performance of

the CNCs as filler in composite based on polylactide (PLA) was improved after the exchange of the counterions between the cetyltrimethylammonium bromide (CTAB) and the sulfate half ester groups (Abitbol et al. 2014). The main drawback of the adsorption is the possibility of adsorbed molecules to leach out during dilution, processing (coating, extrusion, laminating) or storage.

4.2. Functionalization by covalent linkage

It can be allowed to CNCs to react with single molecules or polymers chain. Molecules such as isocyanates, epoxides, acid anhydride, carboxylic acid, amines interact with the hydroxyl groups or carboxylic groups present on the CNCs surfaces.

4.2.1. Reaction with single molecules

Esterification & Acetylation

The esterification of the cellulose nanocrystals has been extensively discussed. The ester compounds are formed when the carboxylic acid or acyl halides react with the alcohol. When CNCs are subjected to oxidation by APS o Tempo, carboxylated cellulose nanocrystals (CNCs-COOH) are obtained. CNCs-COOH groups interact with a hydroxyl group (–OH) to form the ester groups. Parameters to take under control in order to provide high degree of substitution during the esterification are the temperature, the pH, the concentration of the reagents and the duration of the reaction (Eyley and Thielemans, 2014). Braun and Dorgan, (2008) implemented the first esterification of the CNCs in situ during the hydrolysis by applying the 12 principles of the green chemistry. Although a very high degree of conversion can be detrimental to the crystallinity of the modified CNCs due to the unavailability of the hydrogen because most reactive hydroxyl groups at C2 and C6 are involved in the interchain hydrogen bonds. Converted ester groups can be revealed and quantified through FTIR spectra at a wavelength between

1735 and 1746 cm^{-1}. The efficiency of the graftingcan be also monitored by the evaluation of the increase in C-C/C-O peak in XPS analysis, to obtain high dispersibility of esterified CNCs in acetone and ethanol compared with the unmodified CNCs.The single-step was developed by the presence of mixed acids such as acetic and butyric acid (90 wt%) in HCl hydrolysis; about half of hydroxyl was converted into esters and the dispersion in organic solvents was improved (Huang et al., 2015). Sulfation and phosphorylation are examples of esterification reactions but the only examples of in-situ functionalization which occurs during the hydrolysis is the acetylation and the butyration of the CNCs by one-step acid-catalyzed Fischer esterification in presence of the hydrochloric acid. Acetylated cellulose nanocrystals can also be performed by the use of acetic anhydride in pyridine (reactive solvent); in addition, Sassi and Chanzy, (1995) perfomed the acetylation of cellulose using mixture of acetic acid and acetic anhydride in toluene to stop swelling and dissolution of acetylated nanocrystals which have reduced diameter but unchanged length (Peng et al., 2011; Sassi and Chanzy, 2015).Recently, Jasmani et al.(2013) used p-toluenesulfonyl chloride to form mixed anhydrides with 4-(1-bromomethyl)benzoic acid *in situ* for a one step reaction (esterification and nucleophilic substitution) with pyridine to produce high level of modified CNCs (cationic cellulose nanocrystals) with the crystallinity unmodified. Transesterification is one of the recent reactions which has been used to modify the nanocrystals in the so-called "grafting from" approach to modify the cellulose nanocrystals with poly(ε-caprolactone) or poly(lactide) by ring-opening polymerization (Eyley and Thielemans, 2014; Habibi et al., 2008; Labet and Thielemans, 2011).
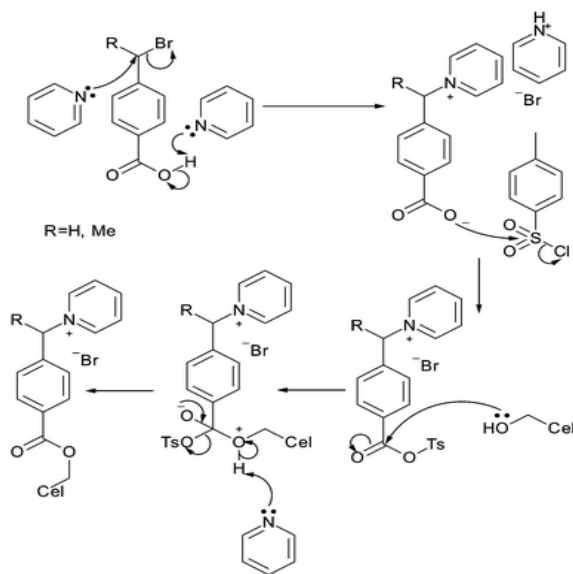
Figure 10. One pot esterification cationization of cellulose nanocrystals as performed by Jasmani *et al.* (2013)

Oxidation of cellulose nanocrystals

Substitution of hydroxyl groups with carboxylic acid or aldehyde functionalitiesoccurs when uncharged CNCs obtained by hydrochloric acid (HCl) hydrolysis are treated with the Ammonium persulfate(APS) or 2,2,6,6-Tetramethylpiperidinyloxyl radical (TEMPO) and the nitric acid (Xiong et al., 2012). Generally, oxidation is performed with a catalytic amount of TEMPO with a secondary oxidant such as sodium hypochlorite or sodium chlorite to recycle TEMPO (Saito et al., 2007). Sodium bromide is quite often used to increase the degree of substitution, during the oxidation process, through the formation of sodium hypobromite in situ.At pH <8 the reaction proceeds slowly and the selectivity between primary and secondary alcohols is not as relevant as at 9 <pH <11 where the reaction shows a good selectivity for primary alcohols due to hindered transition state in alkaline conditions(Eyley and Thielemans, 2014) as the figure below shows (Bailey et al., 2007).After the oxidation, negative charges are imparted to the surface of cellulose nanocrystals that then increase the stability of aqueous suspensions. The

APS isanother strong oxidizing agent thatis used directly on the cellulosic raw materials even on those containing aromatic rings. In fact, the APS provide carboxilated CNCs from a simultaneous hydrolysis and oxidation of the cellulose (Castro-Guerrero and Gray, 2014). In addition, Periodate oxidation was implemented by a selective cleavage of vicinal diols, in the case of cellulose, the 2,3-diol breaking the glucopyranose ring and forming two aldehyde functionalities (Lin et al., 2009).
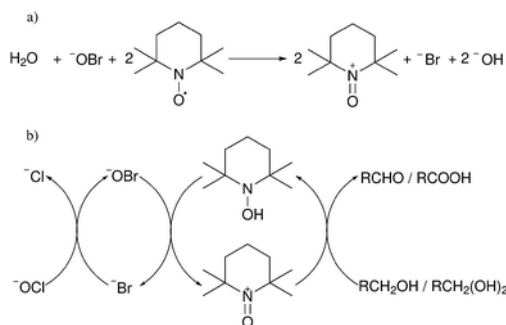

Figure 11. (a) Oxidant formation from Tempo radicals and (b) Catalytic cycle of TEMPO oxidation using sodium hypochlorite and sodium bromide as stoichiometric oxidant.
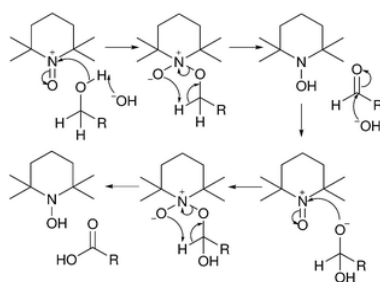

Figure 12. Mechanism of periodate oxidation of cyclic 2,3-diols

Amidation

One of the most common modifications consists of the use of coupling agents with Tempo or APS oxidized cellulose nanocrystals as a starting structure with the goal of implementing the amidation of the CNCs.The mechanism of amidation is formedby the involvement of the carboxylic acid reacting with a

primary amine. Araki et al. (2001) were the first to apply the technique of amidation of the CNCs by usingof a combination of 1-ethyl-3-(3-dimethylaminopropyl) carbodiimide (EDC) and *N*-hydroxysuccinimide (NHS), therefore, carboxyl groups were partly substituted by amides carried out specifically at the C6 position of the cellulose.

Etherification

Etherification of the cellulose nanocrystals is one of the most ubiquitous approach actually performed by many workers. The common way of etherification of CNCs is the application of Glycidyltrimethylammonium chloride (GTMAC) or derivatives to cationize the CNCs surface. The GTMAC is added to suspended CNCs in 1.75 M NaOH solution and heated at 60°Cfor several hoursto favor the modification and the modified cotton derived CNCs have DS=0.02 and DS=0.04 for modified wood derived CNCs. By using NMR, O3 and O6 positions appeared to be the most substituted compared to O3 position during the etherification process of the CNCs. Due to the hydrolysis of Dimethyl GTMAC which has a negative effect on the etherification, CNCs were first suspended in a mixture of Dimethyl sulfoxide (DMSO) and water prior to enacting the reaction with GTMAC (Hasani et al., 2008). The same method was adopted withone epoxide reagent to modify the cellulose nanocrystals with epichlorohydrin. The very first modification to attach the fluorophores to CNCs for bioimaging with this approach was successfully carried out and reported by Dong and Roman, (2007). Epichlorohydrin was also usedrecently for the attachment of β-cyclodextrin to the surface of cellulose nanocrystals (Tang et al., 2017). Before the addition of the desired amount of epichlorohydrin, nanocrystals were first suspended in 2.5 M NaOH with β-cyclodextrin. The surface chemical modification of the CNCs was demonstrated by 1D and 2D NMR spectroscopy; moreover, z potential analysis was used for assessing the colloidal stability modified by the cationization of the CNCs during the etherification. The pitch of the grafting was assessed by gravimetric analysis and photometric titration as 16.9%

weight which corresponds to DSsurf = 0.13–0.25 (considering cross-section of 10–20 nm) (Dong and Roman, 2017).

Carbamination

The carbaminationhas been implemented by the reaction of isocyanates with the hydroxyl groups of the cellulose nanocrystals providing them a hydrophobic behavior. Theoluene-2,4-diisocyanate (TDI) was used to attach polymers and molecules while non-polar isocyanates were used to modify the nanocrystals properties. The first modification with the grafting of polycaprolactone (PCL) to cellulose nanocrystals using TDI. The reaction was performed in toluene with triethylamine as a catalyst and reacting for 7 days at 90 °C, a method previously employed on starch nanocrystals. The PCL was first endcapped with phenyl isocyanate at one end, then reacted in 1:1 stoichiometry with TDI to form a monoisocyanate which was subsequently reacted with cellulose to avoid cross-linking of the nanocrystals. The CNCs modification was proved by the means of the spectroscopy techniques (IR, ^{13}C NMR and XPS). It was reported by Siqiera *et al.*2008 the reaction of sisal cellulose nanocrystals with n-octadecyl isocyanate without any catalysts, the authors noted that only 3.7% of accessible hydroxyl groups reacted with DS=0.7 (Siqueira et al., 2008). It was also reported the hydrophobization of the cellulose nanocrystals by using isocyanates and grafting with phenylisocyanates through TDI and trimethylamine in catalyzed conditions (Abushammala, 2019). The level of modification was found to be 21% mass determined by elemental analysis of the change in carbon content of the modified structure leading to an increase of hydrophobicity from 45° to 9° in water contact angle measurements. Another covalent bond CNCs networking interaction was performed by Rueda et al. in 2011 using 1,6-hexamethylene diisocyanate (HDI). The grafting occurred in dry DMF at 80°C with various molar ratios of HDI in accordance with the number of hydroxyl groups present

in a given mass of CNCs (1:1 and 1:5). The ^{13}C NMR and IR spectroscopy was used to characterize the modified CNCs and their incorporation in polyurethane matrix allows to assess their reinforcing character (Rueda et al., 2011).

4.2.2. Modification by polymer chain

In this type of functionalization, the polymerization can be distinguished in two main categories: "the grafting" onto which derives from the direct interaction between the end functional preformed and characterized polymer and the functional group of the CNCs surface. On the other hand, the "grafting from" approach is based on the growth of the polymer chains, which takes place from the activation or initiation of the functional groups of the CNCs obtaining the grafting before the polymerization with a huge advantage of achieving a higher grating percentage, due to the easy accessibility of active groups of the CNCs, which is characterized only at the end of the modification. Polymerization and ring opening polymerization are examples of grafting from routes actually used (Habibi et al., 2008).

"Grafting onto" mechanism

One of the first grafting occurred by the development of the malted polypropylene grafted cellulose nanocrystals. After the grafting, it resulted a significant reinforcement of the atactic polypropylene while the layer of the grafted CNCs showed a significant decrease of mechanical properties (Ljungberg et al., 2005). Another modified structure was built up polycaprolactone diol (PCLD) polymerization with carboxylic groups along the polymeric chain to make it waterbone and isocyanate as end groups for further reaction with the hydroxyl groups present on the CNCs surface. Subsequently, the diisocyanate was added after the reaction between the PCLD and the dimethyllol propionic acid in order produce the waterborne polyurethane by the neutralization with the trimethyl amine. (Krouit et al., 2008). The polymerized structure was finally grafted onto the cellulose nanocrystals

surface. The modification of the CNCs was confirmed by the high increase of the C1 signal in XPS scans and the grafted chains were found crystalline on the CNCs allowing the crystallization of the polymer matrix (Cao et al., 2009).

"Grafting from" mechanism

It can be divided in the graft polymerization, the ring opening and the radical polymerization.

Ring-opening polymerization (ROP) is a chemical route to open cyclic monomers such as lactones, dilactones, lactams, cyclic carbonates, cyclic ethers, and oxazolines to produce long chain of polymers (Coulembier et al., 2009; Dechy-Cabaretet al., 2009; Yu et al., 2008). The ROP can be initiated by −OH groups for some monomers allowing their reaction with CNCs as they exhibit a density of -OH (Labet and Thielemans, 2011). When the cellulosic substrate acts as a macro-initiator, the polymerization process is referred to as SI-ROP (surface initiated); noting that the most important parameters are the initiator and the catalyst. For the preparation of SI-ROP from CNCs, the nanocrystals act as the initiator and the mechanism depends only on the catalyst; therefore, the water has to be completely removed from the dispersed CNCs before the reaction (Namazi and Dadkhah, 2008).
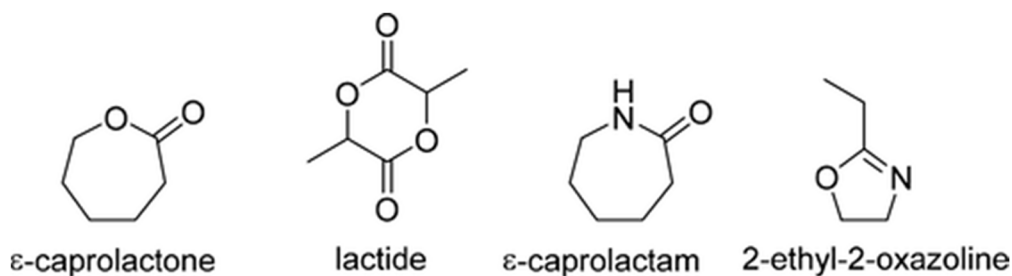

Figure 13. Chemical compounds for "grafting mechanism" of CNCs

The surface-initiated free radical polymerization (SI-FRP) represents one of the most common techniques for developing the grafting of vinyl polymers. The polymer was allowed to grow at the CNCs surface when the initiaror

species is activated first via hydrogen abstraction generating a reactive radical on the CNCs surface to be reacted with monomers to form polymers (Wohlhauser et al., 2018). Among initiators, potassium persulfate (KPS) is a thermal initiator widely used to graft CNCs surfaces with polymer chains, due to the stability of free radicals and compatibility with aqueous solutions. The radical formation occurs in the aqueous phase by the thermal homolytic dissociation of the KPS peroxide bond, at a temperature between 60 and 70 °C (Hebeish et al., 2014). An example performed is reported below. The monomer called acrylic acid (AA) was used and grafted poly(acrylic acid) (PAA) chains offered CNC-based hydrogels excellent water retention properties with a swelling ratio of 323 g/g in distilled water versus 33 g/g in sodium chloride (NaCl) solution (Liu et al., 2018; Yang et al., 2012).
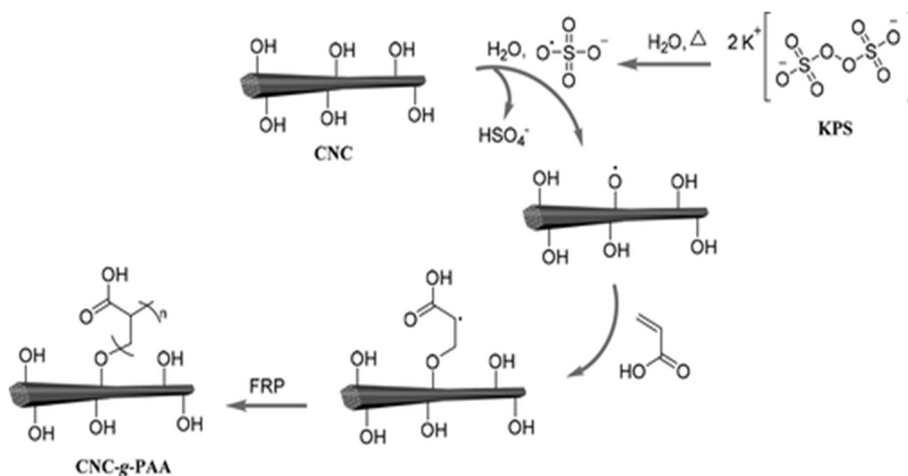

Figure 14. Surface-initiated free radical polymerization using potassium persulfate for grafting polymers from CNCs (Wohlhauser et al., 2018).

5. Cellulose nanocrystals applications in Food packaging

5.1. Forms of cellulose nanocrystals

Cellulose nanocrystals can be used in various forms. After the preparation, the aqueous dispersed CNCS is obtained forming a stable colloidal suspension. CNCs can be wet or dried:

CNCs colloidal suspension

Freeze-dried CNCs

Spray-dried CNCs

Oven-Dried CNCs

Supercritically dried CNCs
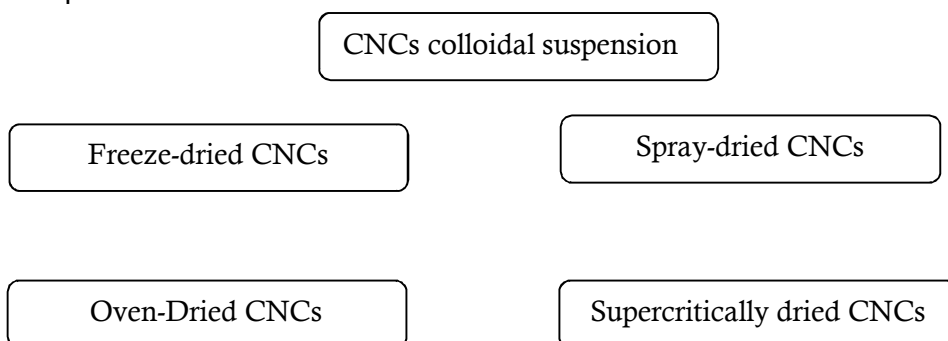
The forms of the CNCs have an important relevance for the organization, morphology, conformation and crystallinity. CNCs powder or whiskers should be stored under lower temperature and humidity while wet CNCs in the refrigerator (4°C). For instance, Multi-scale crystalline network is obtained from the freeze-drying and supercritical-drying, while industrially spray-drying technique is more employed at the industrial level (Beck et al., 2012). It is important to note that after the drying process, residue of water and counter ion remain on the cellulose nanocrystals surface which ultimately play a very important role in the redispersibility and the stability of the colloidal suspension. Well-dispersed sodium-salt nanocellulose is fully dispersible in water (Missoum et al., 2012) and freeze-dried CNCs can be stored and incorporated into other materials. CNCs obtained from HCl resulted not to be redispersible even with intense sonication because of van der walls interactions and hydrogen bonding present. Freeze-dried CNCs are flake-like and iridescent appearance particles which stem from the liquid crystal before the drying and that makes more difficult the redispersibility of the CNCs.

Spray-dried CNCs are redispersed in water by adding a small amount under vigorous agitation.

5.2. Coating of cellulose nanocrystals

There are many intrinsic and extrinsic factors which influence the efficiency of cellulose nanocrystals coating onto paper or plastic films. After the coating of the cellulose nanocrystals, the gas barrier properties are significantly improved. Howeverany lack of the accuracy is critical on the performance of gas barrier of coated materials.
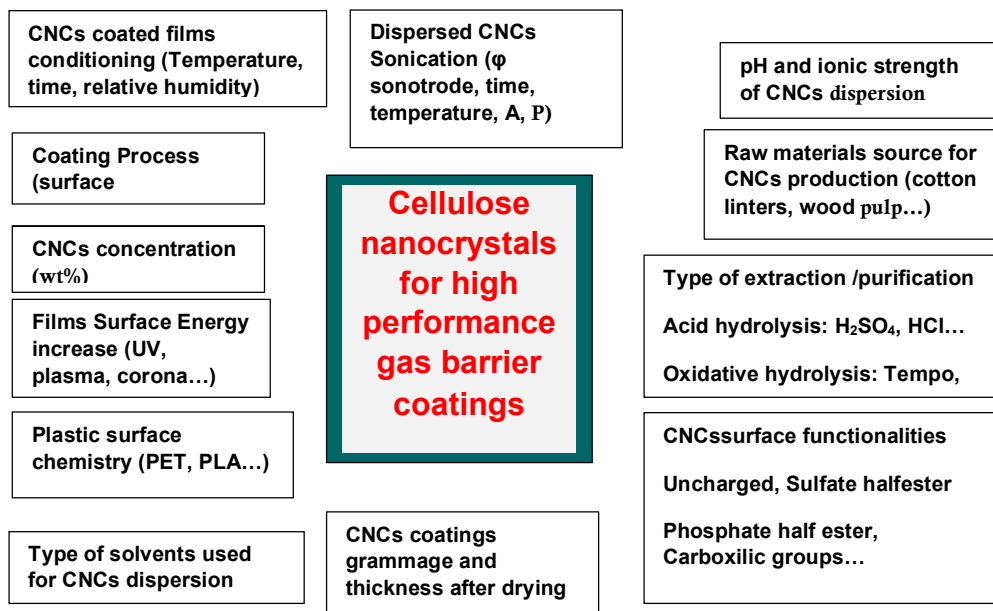
CNCs coated films conditioning (Temperature, time, relative humidity)	Dispersed CNCs Sonication (φ sonotrode, time, temperature, A, P)		pH and ionic strength of CNCs dispersion
Coating Process (surface			Raw materials source for CNCs production (cotton linters, wood pulp…)
CNCs concentration (wt%)	**Cellulose nanocrystals for high performance gas barrier coatings**		Type of extraction /purification Acid hydrolysis: H_2SO_4, HCl… Oxidative hydrolysis: Tempo,
Films Surface Energy increase (UV, plasma, corona…)			
Plastic surface chemistry (PET, PLA…)			CNCssurface functionalities Uncharged, Sulfate halfester Phosphate half ester, Carboxilic groups…
Type of solvents used for CNCs dispersion	CNCs coatings grammage and thickness after drying		

Figure 15. Extrinsic and intrinsicfactors for high performance gas barrier coatings.

When the plastic films and papersare coated with cellulose nanocrystals, the gas barrier is significantly improved. However, the preparation of the cellulose nanocrystals dispersion and the process of their coating on the polymers are very critical operations, because any lack of accuracy results in an abrupt increase in the permeation of the gases. CNCs are obtained chemically either by hydrolysis acid (HCl, H_2SO_4, H_3PO4…) or oxidative hydrolysis (Tempo, APS). Generally, CNCs have hydroxyl groups located on their surfacewhile some are polymerized into carboxylic groups (-COOH) for CNCs obtained

from APS and Tempo while CNCs, by using sulfuric and phosphoric acids, CNCs obtained contain sulfate and phosphate half ester groups on their surface respectively. CNCs might be at various formats such as wet, freeze-dried, spray-dried. Therefore, prior to proceeding with the coating step, it may be necessary to re-disperse the CNCs in water. When redispersed sprayed-dried CNCs in water, it is strongly recommended to put them gradually (small amount added little by little) and maybe in presence of sodium chlorite under vigorous stirring and let it sit down for at least 1h till all the aggregates are dispersed followed by the sonication. CNCs-APS dispersion must be brought to pH> 7 and CNCs-H_2SO_4 to pH> 4.3 to allow a complete re-suspension of CNCs in water as a result of deprotonation of-COOH and -HSO_3 groups respectively, which contributes to obtain a stable and uniform colloidal suspension. The suspension concentration of the cellulose nanocrystals for the coating shall be between 6% and 10wt%. A lower concentration requires several layers of dispersed CNCs for a complete coverage of the plastic films and a higher concentration relative up to the critical level causes the brittleness of the dried substrate of CNCs (a plasticizer such as sorbitol can be required). Due to the hydrophilic character of the CNCs, Plastic polymers to be completely covered during the coating must be subjected to corona, plasma, UV treatment for increasing their surface energy and adhesion with the aqueous CNCs suspension. The intensity of the treatment (power and time) to set depends on the initial hydrophobicity of the substrate and the type of the polymers. After the coating, the coated plastic films are suspended and dried under lower humidity and temperature conditions (30 ° C to 40 ° C) for about 48 hours.

5.3. Layer-by-layer (LbL) assembly

LdL assembly has been long employed for the deposition of a very thin layer of functional substances onto surfaces. Dispersions of cellulose nanocrystals are coated several timeson solid substrates (several layers) till the thickness reached is sufficient to provide gas barrier properties and wet-strength

required (Ankerfors et al., 2016; Aulin et al., 2013). Layers of muticomponents films can be coated on polymers or papers to form a complex mosaic of multi-structures useful to preserve properties that are important in food packaging. It worth mentioning that the electrostatic interaction between polyanion and polycation or hydrogen bonds formed between layers can be exploited to obtain denser and ultra-thin layers in some cases (Jean et al., 2009). Other researchers and co-authors have implemented LbL by alternating the nanocellulose with the chitosan (Li et al., 2015) or poly-(etheneimine) (Aulin et al., 2013), cationic starch, cationic polyelectrolytes such as poly-(ethyleneimine), poly (allylamine hydrochloride and poly-(diallyldimethylammonium chloride) (Marais et al., 2013) or polyamido-amine wet-strength resin (Ankerfors et al., 2016). The combination of multiple layers showshigh versatility as the coating of containers, trays, bottles and objects is possible and easy, high density and strength between layers due to good affinity and gas barrier improvements.

5.4. Nanocomposite extrusion

Extrusion is a very simple process of transforming solid materials into a liquid state at a desired thickness. However, the incorporation of nanocellulose into plastic polymers is a challenge due to the lack of compatibility between both materialsMiao and Hamad (2013). Recently, nanocellulose was used as nanofiller reinforce of adhesives and polymers such as PLA taking advantage of the very high aspect ratio and specific surface area of the nanocellulose (Li et al., 2015).

5.5. Electrospinning

Electrospinning (ES) is a technology that utilizes electrical forces for electrostatic fiber formation to produce polymers fibers with diameters ranging from 2 nm to macrometric scale (Bhardwaj and Kundu, 2010). The viscous flow of the natural and synthetic polymers makes possible the alignment of individual polymer chains (Park et al., 2017). That type of process helps to

overcome problems of compatibility of the nanocellulose and polymers. ES technique was successfully used to incorporate microfibrils into poly (ethylene oxide) improving the thermal and mechanical properties through crystallinity change and nanocellulose alignment along the fiber length (Fortunat et al., 2012). Peresin et al., (2010) achieved electrospun poly(vinylalcohol) with CNCs providing reinforced nanofibers (Peresin et al., 2010).

5.6. Casting and evaporation

Redispersing the nanocellulose into aqueous and non-aqueous media is challenging. Subsequently, this technique is used to control the nanocellulose concentration at moderate temperatures (Lu et al., 2014; Li et al., 2015). Not really common in packaging, casting process was used by the combination between nanocellulose and amylopectin-glycerol. More recently, cellulose nanocrystals were dispersed from an aqueous solution containing chitosan (Svagan et al., 2007, 2009).

For example, etherification reaction can be promoted with hydroxyl groups while ester groups are the resulting reaction between carboxyl and hydroxyl groups. Amidation mechanism is also possible with the reaction between amines and carboxyl groups. Adsorption of chemical compounds onto the cellulose nanocrystals surface can be either by "affinity" or by "electrostatic interaction" with surfactants or positive charges.

6. Conclusions and approach of the thesis

From the findings of many scientists, it is clear that cellulose nanocrystals have a bright future and the many huge assets of these crystals will be soon exploited in several fields of applications. Cellulose nanocrystals can find application in many sectors packaging, electronics, Medecine, etc. In particular, cellulose nanocrystals can be used in food packaging as coatings to set up more advanced gas barrier packaging. The oxidation of foods remains one of the major problems actually faced by scientists and manufacturers. In the same context, environmental concerns are stimulating

the world to seek alternative resources to synthetic polymers which are not safe for the living being. Cellulose nanocrystals display extraordinary capabilities such gas gas barrier and mechanical properties required in food packaging. Furthermore, cellulose nanocrystals are obtained from the cellulose, which is the most abundant biopolymer on Earth. However, the water sensitivity of the coatings-based cellulose nanocrystals is a major obstacle for their implementation in food packaging. It was found out that, gas barrier properties of cellulose nanocrystals are destroyed in conditions of high humidity. Therefore, my thesis will be divided into 3 sections:

A- Investigation on water sensitivity of coatings-based cellulose nanocrystals in relation with barrier to oxygen and carbon dioxide

B- Research and implementation of solutions to overcome the drawback

C- Effective application of cellulose nanocrystals in food packaging and food shelf-life assessment.

References

Khalil, H. A., Bhat, A. H.,Yusra, A. I., 2012. Green composites from sustainable cellulose nanofibrils: A review. *Carbohydrate polymers*, *87*(2), 963-979.

Abitbol, T., Kloser, E., Gray, D.G., 2013. Estimation of the surface sulfur content of cellulose nanocrystals prepared by sulfuric acid hydrolysis. *Cellulose*, *20*(2), pp.785-794.

Abitbol, T., Marway, H., Cranston, E.D., 2014. Surface modification of cellulose nanocrystals with cetyltrimethylammonium bromide. *Nordic Pulp & Paper Research Journal*, *29*(1), pp.46-57.

Abushammala, H., 2019. A Simple Method for the Quantification of Free Isocyanates on the Surface of Cellulose Nanocrystals upon Carbamation using Toluene Diisocyanate. *Surfaces*, *2*(2), pp.444-454.

Andrade, F., Pertile, R., Dourado, F., Gama, F.M., 2010. Bacterial cellulose: properties, production and applications.

Araki, J., Wada, M., Kuga, S., 2001. Steric stabilization of a cellulose microcrystal suspension by poly (ethylene glycol) grafting. *Langmuir*, *17*(1), pp.21-27.

Arrieta, M.P., Fortunati, E., Dominici, F., Rayón, E., López, J. and Kenny, J.M., 2014. Multifunctional PLA–PHB/cellulose nanocrystal films: Processing, structural and thermal properties. *Carbohydrate polymers*, *107*, pp.16-24.

Arvidsson, R., Nguyen, D., Svanström, M., 2015. Life cycle assessment of cellulose nanofibrils production by mechanical treatment and two different pretreatment processes. *Environmental science & technology*, *49*(11), pp.6881-6890.

Atalla, R.H., Vanderhart, D.L., 1984. Native cellulose: a composite of two distinct crystalline forms. *Science*, *223*(4633), pp.283-285.

54

Bailey, W.F., Bobbitt, J.M., Wiberg, K.B., 2007. Mechanism of the oxidation of alcohols by oxoammonium cations. *The Journal of organic chemistry*, *72*(12), pp.4504-4509.

Barreto, J.A., O'Malley, W., Kubeil, M., Graham, B., Stephan, H., Spiccia, L., 2011. Nanomaterials: applications in cancer imaging and therapy. *Advanced materials*, *23*(12), pp.H18-H40.

Baruah, S., Dutta, J., 2009. Nanotechnology applications in pollution sensing and degradation in agriculture: a review. *Environmental Chemistry Letters*, *7*(3), pp.191-204.

Beck, S., Bouchard, J., Berry, R., 2012. Dispersibility in water of dried nanocrystalline cellulose. *Biomacromolecules*, *13*(5), pp.1486-1494.

Bondeson, D., Mathew, A., Oksman, K., 2006. Optimization of the isolation of nanocrystals from microcrystalline cellulose by acid hydrolysis. *Cellulose*, *13*(2), p.171.

Boufi, S., Kaddami, H., Dufresne, A., 2014. Mechanical performance and transparency of nanocellulose reinforced polymer nanocomposites. *Macromolecular Materials and Engineering*, *299*(5), pp. 560-568.

Boujemaoui, A., Mongkhontreerat, S., Malmström, E., Carlmark, A., 2015. Preparation and characterization of functionalized cellulose nanocrystals. *Carbohydrate polymers*, *115*, pp.457-464.

Camarero Espinosa, S., Kuhnt, T., Foster, E.J., Weder, C., 2013. Isolation of thermally stable cellulose nanocrystals by phosphoric acid hydrolysis. *Biomacromolecules*, *14*(4), pp.1223-1230.

Cao, X., Habibi, Y., Lucia, L.A., 2009. One-pot polymerization, surface grafting, and processing of waterborne polyurethane-cellulose nanocrystal nanocomposites. *Journal of Materials Chemistry*, *19*(38), pp.7137-7145.

Chang, P. R., Ai, F., Chen, Y., Dufresne, A., Huang, J., 2009. "Effects of starch nanocrystal-graft-porycaprolactone on mechanical properties of waterborne polyurethane-based nanocomposites," Journal of Applied Polymer Science, vol. 111, no. 2, pp. 619–627.

Chazeau, L., Cavaille, J. Y., Canova, G., Dendievel, R., Boutherin, B., 1999. Viscoelastic properties of plasticized PVC reinforced with cellulose whiskers. *Journal of Applied Polymer Science*, *71*(11), 1797-1808.

Coma, R., Gili, J.M., Zabala, M., Riera, T., 1994. Feeding and prey capture cycles in the aposymbiontic gorgonian Paramuricea clavata. *Marine Ecology Progress Series*, pp.257-270.

Coulembier, O. and Dubois, P., 2009. Polyesters from β-lactones. *Handbook of Ring-Opening Polymerization*, pp.227-254.

Cui, S., Zhang, S., Ge, S., Xiong, L., Sun, Q., 2016. Green preparation and characterization of size-controlled nanocrystalline cellulose via ultrasonic-assisted enzymatic hydrolysis. *Industrial Crops and Products*, *83*, pp.346-352.

De Melo, E.M., Clark, J.H., Matharu, A.S., 2017. The Hy-MASS concept: hydrothermal microwave assisted selective scissoring of cellulose for in situ production of (meso) porous nanocellulose fibrils and crystals. *Green Chemistry*, *19*(14), pp.3408-3417.

Dechy-Cabaret, O., Martin-Vaca, B., Bourissou, D., 2009. Polyesters from dilactones. *Handbook of Ring-Opening Polymerization*, pp.255-286.

Dong, X.M., Gray, D.G., 1997. Effect of counterions on ordered phase formation in suspensions of charged rodlike cellulose crystallites. Langmuir, 13(8), pp.2404-2409.

Dong XM, Revol J-F, Gray DG., 1998. Effect of microcrystallite preparation conditions on the formation of colloid crystals of cellulose. Cellulose. 5:19–32

Dong, S., Roman, M., 2007. Fluorescently labeled cellulose nanocrystals for bioimaging applications. *Journal of the American Chemical Society*, *129*(45), pp.13810-13811.

Dufresne, A., 2013. Nanocellulose: a new ageless bionanomaterial. *Materials today*, *16*(6), pp.220-227.

Duncan, T.V., 2011. Applications of nanotechnology in food packaging and food safety: barrier materials, antimicrobials and sensors. *Journal of colloid and interface science*, *363*(1), pp.1-24.

Eyley, S., Thielemans, W., 2014. Surface modification of cellulose nanocrystals. *Nanoscale*, *6*(14), pp.7764-7779.

Fernandes, EM, Pires, RA, Mano, JF, Reis RL., 2013. Bionanocomposites from lignocellulosic resources: Properties, applications and future trends for their use in the biomedical field. Prog Polym Sci. Elsevier Ltd; 38(10-11): 1415–41

Foster, E.J., Moon, R.J., Agarwal, U.P., Bortner, M.J., Bras, J., Camarero-Espinosa, S., Chan, K.J., Clift, M.J., Cranston, E.D., Eichhorn, S.J. and Fox, D.M., 2018. Current characterization methods for cellulose nanomaterials. *Chemical Society Reviews*, *47*(8), pp.2609-2679.

Gatenholm, P., Klemm, D., 2010. Bacterial nanocellulose as a renewable material for biomedical applications. *MRS bulletin*, *35*(3), pp.208-213.

George, J., Sabapathi, S.N., 2015. Cellulose nanocrystals: synthesis, functional properties, and applications. *Nanotechnology, science and applications*, *8*, p.45.

George, J., Sabapathi, S.N., 2015. Cellulose nanocrystals: synthesis, functional properties, and applications. *Nanotechnology, science and applications*, *8*, p.45.

Guozhong, C., 2004. *Nanostructures and nanomaterials: synthesis, properties and applications*. World scientific.

Habibi, Y., Lucia, L.A., Rojas, O.J., 2010. Cellulose nanocrystals: chemistry, self-assembly, and applications. *Chemical reviews*, *110*(6), pp.3479-3500.

Hamad, W.Y., Hu, T.Q., 2010. Structure–process–yield interrelations in nanocrystalline cellulose extraction. *The Canadian Journal of Chemical Engineering*, *88*(3), pp.392-402.

Hasani, M., Cranston, E.D., Westman, G., Gray, D.G., 2008. Cationic surface functionalization of cellulose nanocrystals. *Soft Matter*, *4*(11), pp.2238-2244.

Hearle, J. W., Woodings, C. A. L. V. I. N., 2001. Fibers related to cellulose. *Regenerated Cellulose Fibers; Woodhead Publishing: Sawston, Cambridge, UK*, 156-173.

Hebeish, A., Farag, S., Sharaf, S., Shaheen, T.I., 2014. Thermal responsive hydrogels based on semi interpenetrating network of poly (NIPAm) and cellulose nanowhiskers. *Carbohydrate polymers*, *102*, pp.159-166.

Herrick, F.W., Casebier, R.L., Hamilton, J.K. and Sandberg, K.R., 1983, January. Microfibrillated cellulose: morphology and accessibility. In *J. Appl. Polym. Sci.: Appl. Polym. Symp; (United States)* (Vol. 37, No. CONF-8205234-Vol. 2). ITT Rayonier Inc., Shelton, WA.

Hua, K., Carlsson, D.O., Ålander, E., Lindström, T., Strømme, M., Mihranyan, A. and Ferraz, N., 2014. Translational study between structure and biological response of nanocellulose from wood and green algae. *Rsc Advances*, *4*(6), pp.2892-2903.

Kargarzadeh, H., Ahmad, I., Abdullah, I., Dufresne, A., Zainudin, S.Y. and Sheltami, R.M., 2012. Effects of hydrolysis conditions on the morphology, crystallinity, and thermal stability of cellulose nanocrystals extracted from kenaf bast fibers. *Cellulose*, *19* (3), pp.855-866.

Kargarzadeh, H., Mariano, M., Gopakumar, D., Ahmad, I., Thomas, S., Dufresne, A., Huang, J., Lin, N., 2018. Advances in cellulose nanomaterials. *Cellulose*, *25*(4), pp.2151-2189.

Khalil, H.A., Bhat, A.H., Yusra, A.I., 2012. Green composites from sustainable cellulose nanofibrils: A review. *Carbohydrate polymers*, *87*(2), pp.963-979.

Khalil, H.A., Davoudpour, Y., Islam, M.N., Mustapha, A., Sudesh, K., Dungani, R., Jawaid, M., 2014. Production and modification of nanofibrillated cellulose using various mechanical processes: a review. *Carbohydrate polymers*, *99*, pp.649-665.

Khan, A., Khan, R.A., Salmieri, S., Le Tien, C., Riedl, B., Bouchard, J., Chauve, G., Tan, V., Kamal, M.R. and Lacroix, M., 2012. Mechanical and barrier properties of nanocrystalline cellulose reinforced chitosan based nanocomposite films. *Carbohydrate polymers*, *90*(4), pp.1601-1608.

Kholodenko, A.L., Douglas, J.F., 1995. Generalized Stokes-Einstein equation for spherical particle suspensions. *Physical Review E*, *51*(2), p.1081.

Klemm, D., Kramer, F., Moritz, S., Lindström, T., Ankerfors, M., Gray, D., Dorris, A., 2011. Nanocelluloses: a new family of nature-based materials. *Angewandte Chemie International Edition*, *50*(24), pp.5438-5466.

Koo, J.H., 2006. *Polymer nanocomposites*. McGraw-Hill Professional Pub.

Kovacs, T., Naish, V., O'Connor, B., Blaise, C., Gagné, F., Hall, L., Trudeau, V., Martel, P., 2010. An ecotoxicological characterization of nanocrystalline cellulose (NCC). *Nanotoxicology*, *4*(3), pp.255-270.

Krouit, M., Bras, J., Belgacem, M.N., 2008. Cellulose surface grafting with polycaprolactone by heterogeneous click-chemistry. *European Polymer Journal*, *44*(12), pp.4074-4081.

Kümmerer, K., Menz, J., Schubert, T., Thielemans, W., 2011. Biodegradability of organic nanoparticles in the aqueous environment. *Chemosphere*, *82*(10), pp.1387-1392.

Labet, M., Thielemans, W., 2011. Improving the reproducibility of chemical reactions on the surface of cellulose nanocrystals: ROP of ε-caprolactone as a case study. *Cellulose*, *18*(3), pp.607-617.

Lam, E., Male, K.B., Chong, J.H., Leung, A.C., Luong, J.H., 2012. Applications of functionalized and nanoparticle-modified nanocrystalline cellulose. *Trends in biotechnology*, *30*(5), pp.283-290.

Leung, A.C., Hrapovic, S., Lam, E., Liu, Y., Male, K.B., Mahmoud, K.A., Luong, J.H., 2011. Characteristics and properties of carboxylated cellulose nanocrystals prepared from a novel one-step procedure. *Small*, *7*(3), pp.302-305.

Leung, A.C., Hrapovic, S., Lam, E., Liu, Y., Male, K.B., Mahmoud, K.A. and Luong, J.H., 2011. Characteristics and properties of carboxylated cellulose nanocrystals prepared from a novel one-step procedure. *Small*, *7*(3), pp.302-305.

Lin, N., Dufresne, A., 2014. Surface chemistry, morphological analysis and properties of cellulose nanocrystals with gradiented sulfation degrees. *Nanoscale*, *6*(10), pp.5384-539

Lin, N., Chen, G., Huang, J., Dufresne, A., Chang, P.R., 2009. Effects of polymer-grafted natural nanocrystals on the structure and mechanical properties of poly (lactic acid): A case of cellulose whisker-graft-polycaprolactone. *Journal of Applied Polymer Science*, *113*(5), pp.3417-3425.

Lin, N., Huang, J., Dufresne, A., 2012. Preparation, properties and applications of polysaccharide nanocrystals in advanced functional nanomaterials: a review. *Nanoscale*, *4*(11), pp.3274-3294.

Liu, X., Yang, R., Xu, M., Ma, C., Li, W., Yin, Y., Huang, Q., Wu, Y., Li, J. and Liu, S., 2018. Hydrothermal Synthesis of Cellulose Nanocrystal-Grafted-Acrylic Acid Aerogels with Superabsorbent Properties. *Polymers*, *10*(10), p.1168.

Ljungberg, N., Bonini, C., Bortolussi, F., Boisson, C., Heux, L. and Cavaillé, J.Y., 2005. New nanocomposite materials reinforced with cellulose whiskers

in atactic polypropylene: effect of surface and dispersion characteristics. *Biomacromolecules*, *6*(5), pp.2732-2739.

Lu, P., Hsieh, Y.L., 2010. Preparation and properties of cellulose nanocrystals: rods, spheres, and network. *Carbohydrate polymers*, *82*(2), pp.329-336.

Mariano, M., El Kissi, N. and Dufresne, A., 2014. Cellulose nanocrystals and related nanocomposites: review of some properties and challenges. *Journal of Polymer Science Part B: Polymer Physics*, *52*(12), pp.791-806.

Marin, DC., Vecchio, A., Ludueña, LN., Fasce, D., Alvarez, VA., Stefani, PM., 2015. Revalorization of rice husk waste as a source of cellulose and silica. Fibers Polym.16(2):285–93.

Maynard, A.D., Aitken, R.J., Butz, T., Colvin, V., Donaldson, K., Oberdörster, G., Philbert, M.A., Ryan, J., Seaton, A., Stone, V. and Tinkle, S.S., 2006. Safe handling of nanotechnology. *Nature*, *444*(7117), p.267.

Missoum, K., Bras, J., Belgacem, M.N., 2012. Water redispersible dried nanofibrillated cellulose by adding sodium chloride. *Biomacromolecules*, *13*(12), pp.4118-4125.

Moon, R.J., Martini, A., Nairn, J., Simonsen, J. and Youngblood, J., 2011. Cellulose nanomaterials review: structure, properties and nanocomposites. *Chemical Society Reviews*, *40*(7), pp.3941-3994.

Namazi, H., Dadkhah, A., 2008. "Surface modification of starch nanocrystals through ring-opening polymerization of ε-caprolactone and investigation of their microstructures," Journal of Applied Polymer Science, vol. 110, no. 4, pp. 2405– 2412.

Nechyporchuk, O., Belgacem, M.N. and Bras, J., 2016. Production of cellulose nanofibrils: A review of recent advances. *Industrial Crops and Products*, *93*, pp.2-25.

Ni, H., Zeng, S., Wu, J., Cheng, X., Luo, T., Wang, W., Zeng, W. and Chen, Y., 2012. Cellulose nanowhiskers: Preparation, characterization and

cytotoxicity evaluation. *Bio-medical materials and engineering*, *22*(1-3), pp.121-127.

Nunes, R. de M., Guarda EA., Carlos J, Serra V., 2013. Resíduos agroindustriais: potencial de produção do etanol de segunda geração no Brasil. Rev Lib.14(22):113–238.

Oliveira de Castro, D., Frollini, E., Ruvolo-Filho, A., Dufresne, A., 2015. "Green polyethylene" and Curauá Cellulose nanocrystal based nanocomposites: Effect of vegetable oils as coupling agent and processing technique. J Polym Sci Part B Polym Phys.n/a – n/a

Paul, D.R. and Robeson, L.M., 2008. Polymer nanotechnology: nanocomposites. *Polymer*, *49*(15), pp.3187-3204.

Phanthong, P., Reubroycharoen, P., Hao, X., Xu, G., Abudula, A. and Guan, G., 2018. Nanocellulose: Extraction and application. *Carbon Resources Conversion*, *1*(1), pp.32-43.

Rånby, B.G., 1949. Aqueous colloidal solutions of cellulose micelles. Acta Chem. Scand. 3, 649–650.

Rehman, N., de Miranda MIG., Rosa, SML., Pimentel, DM., Nachtigall, SMB., Bica CID., 2014. Cellulose and Nanocellulose from Maize Straw: An Insight on the Crystal Properties. J Polym Environ. 22(2):252–9.

Rekha, K., Nirmala, M., Nair, M.G. and Anukaliani, A., 2010. Structural, optical, photocatalytic and antibacterial activity of zinc oxide and manganese doped zinc oxide nanoparticles. *Physica B: Condensed Matter*, *405*(15), pp.3180-3185.

Revol, J-F, Bradford, H, Giasson, J., 1992. Marchessault RH, Gray DG. Helicoidal Self-Ordering of Cellulose Microfibrils in Aqueous Suspension. Int J Biol Macromol.14:170–172.

Romdhane, A., Aurousseau, M., Guillet, A. and Mauret, E., 2015. Effect of pH and ionic strength on the electrical charge and particle size distribution of starch nanocrystal suspensions. *Starch‑Stärke*, *67*(3-4), pp.319-327.

Rueda, L., d'Arlas, B.F., Zhou, Q., Berglund, L.A., Corcuera, M.A., Mondragon, I. and Eceiza, A., 2011. Isocyanate-rich cellulose nanocrystals and their selective insertion in elastomeric polyurethane. *Composites Science and Technology*, *71*(16), pp.1953-1960.

Sacui, I.A., Nieuwendaal, R.C., Burnett, D.J., Stranick, S.J., Jorfi, M., Weder, C., Foster, E.J., Olsson, R.T., Gilman, J.W., 2014. Comparison of the properties of cellulose nanocrystals and cellulose nanofibrils isolated from bacteria, tunicate, and wood processed using acid, enzymatic, mechanical, and oxidative methods. *ACS applied materials & interfaces*, *6*(9), pp.6127-6138.

Saito, T., Isogai, A., 2004. TEMPO-mediated oxidation of native cellulose. The effect of oxidation conditions on chemical and crystalstructures of the water-insoluble fractions. *Biomacromolecules*, *5*(5), pp.1983-1989.

Saito, T., Kimura, S., Nishiyama, Y., Isogai, A., 2007. Cellulose nanofibers prepared by TEMPO-mediated oxidation of native cellulose. *Biomacromolecules*, *8*(8), pp.2485-2491.

Salajková, M., Berglund, L.A., Zhou, Q., 2012. Hydrophobic cellulose nanocrystals modified with quaternary ammonium salts. *Journal of Materials Chemistry*, *22*(37), pp.19798-19805.

Shatkin, J.A., Wegner, T.H., Bilek, E.T. and Cowie, J., 2014. Market projections of cellulose nanomaterial-enabled products. Part 1: Applications. *TAPPI JOURNAL, Volume 13, Number 5, pp. 9-16.*, *13*(5), pp.9-16.

Siqueira, G., Bras, J., Dufresne, A., 2008. Cellulose whiskers versus microfibrils: influence of the nature of the nanoparticle and its surface

functionalization on the thermal and mechanical properties of nanocomposites. *Biomacromolecules*, *10*(2), pp.425-432.

Srinivas, P.R., Philbert, M., Vu, T.Q., Huang, Q., Kokini, J.L., Saos, E., Chen, H., Peterson, C.M., Friedl, K.E., McDade-Ngutter, C., Hubbard, V., 2009. Nanotechnology research: applications in nutritional sciences. *The journal of nutrition*, *140*(1), pp.119-124.

Tang, J., Sisler, J., Grishkewich, N., Tam, K.C., 2017. Functionalization of cellulose nanocrystals for advanced applications. *Journal of colloid and interface science*, *494*, pp.397-409.

Tang, Y., Yang, S., Zhang, N., Zhang, J., 2014. Preparation and characterization of nanocrystalline cellulose via low-intensity ultrasonic-assisted sulfuric acid hydrolysis. *Cellulose*, *21*(1), pp.335-346.

Terech, P., Chazeau, L., Cavaille, J. Y., 1999. A small-angle scattering study of cellulose whiskers in aqueous suspensions. *Macromolecules*, *32*(6), 1872-1875.

Thakur, M.K., Thakur, V.K., Prasanth, R., 2014. Nanocellulose-based polymer nanocomposites: An introduction. *Nanocellulose Polymer Nanocomposites*, pp.1-15.

Turbak, A.F., Snyder, F.W., Sandberg, K.R., 1983, January. Microfibrillated cellulose, a new cellulose product: properties, uses, and commercial potential. In *J. Appl. Polym. Sci.: Appl. Polym. Symp;(United States)* (Vol. 37, No. CONF-8205234-Vol. 2). ITT Rayonier Inc., Shelton, WA.

Wickholm, K., Hult, E.L., Larsson, P.T., Iversen, T., Lennholm, H., 2001. Quantification of cellulose forms in complex cellulose materials: a chemometric model. *Cellulose*, *8*(2), pp.139-148.

Wilkinson, J.M., 2003. Nanotechnology applications in medicine. *Medical device technology*, *14*(5), pp.29-31.

Wohlhauser, S., Delepierre, G., Labet, M., Morandi, G., Thielemans, W., Weder, C. and Zoppe, J.O., 2018. Grafting polymers from cellulose nanocrystals: synthesis, properties, and applications. *Macromolecules*, *51*(16), pp.6157-6189.

Xie, Y., He, Y., Irwin, P.L., Jin, T., Shi, X., 2011. Antibacterial activity and mechanism of action of zinc oxide nanoparticles against Campylobacter jejuni. *Appl. Environ. Microbiol.*, *77*(7), pp.2325-2331.

Xiong, R., Zhang, X., Tian, D., Zhou, Z., Lu, C., 2012. Comparing microcrystalline with spherical nanocrystalline cellulose from waste cotton fabrics. *Cellulose*, *19*(4), pp.1189-1198.

Xu, S., Girouard, N., Schueneman, G., Shofner, M.L. and Meredith, J.C., 2013. Mechanical and thermal properties of waterborne epoxy composites containing cellulose nanocrystals. *Polymer*, *54*(24), pp.6589-6598.

Yang, J., Han, C.R., Duan, J.F., Ma, M.G., Zhang, X.M., Xu, F., Sun, R.C. and Xie, X.M., 2012. Studies on the properties and formation mechanism of flexible nanocomposite hydrogels from cellulose nanocrystals and poly (acrylic acid). *Journal of Materials Chemistry*, 22(42), pp.22467-22480.

 Yu, J., Ai, F., Dufresne, A., Gao, S., Huang, J., Chang, P.R., 2008. "Structure and mechanical properties of poly(lactic acid) filled with (starch nanocrystal)-graft-poly(ε-caprolactone)," Macromolecular Materials and Engineering, vol. 293, no. 9, pp. 763–770.

Yu, H.Y., Qin, Z.Y., Liu, Y.N., Chen, L., Liu, N. and Zhou, Z., 2012. Simultaneous improvement of mechanical properties and thermal stability of bacterial polyester by cellulose nanocrystals. *Carbohydrate polymers*, *89*(3), pp.971-978.

Zhao, Y., Zhang, Y., Lindström, M.E. and Li, J., 2015. Tunicate cellulose nanocrystals: preparation, neat films and nanocomposite films with glucomannans. *Carbohydrate polymers*, *117*, pp.286-296.

Zimmermann, T., Pöhler, E. and Geiger, T., 2004. Cellulose fibrils for polymer reinforcement. *Advanced engineering materials*, *6*(9), pp.754-761.

Chapter 2

Aims and objectives

Chapter 2. Aims and objectives

The main objective of the PhD was to implement multi-layer structures (bio-sed and fully compostable) based on cellulose nanocrystals produced from natural resources to achieve excellent oxygen and water vapor barrier properties for food shelf-life extension. The Project stemmed from the idea that abundant natural resources such as cellulose, which bear exceptional potential, could be exploited to create more advanced and bio-based laminates in replacement of conventional-based laminates (EVOH, PVDC). From the cellulose, cellulose nanocrystals can be obtained through a "top-down" process. Nanocrystals are intended as tiny crystals whose at least one dimension is equal to or less than 100 nm. CNCs are biodegradable and crystalline materials based on 100% cellulose and they are obtained either by oxidative or acid hydrolysis of the amorphous regions of the cellulose to release the crystalline regions intact. CNCs display extraordinary gas barrier and mechanical properties which meet all the needed requirements to be incorporated into food packaging. This project will contribute to sort out two major challenges such food waste and environmental concerns actually faced and targeted by the world. Not only that, the use of cellulose nanocrystals in packaging will help to alleviate the dependency on oil-based materials (plastics) which are unhealthy for the environment, but it will further reduce the food loss caused by the oxidation phenomenon. In addition, the possibility of employing by-products and biomass to produce cellulose nanocrystals will surely make the novel food packaging compliant with requirements of eco-compatible applications. At the end of this project, 4 µm thick of synthetic oxygen barrier currently used in laminates (EVOH, PVDC) for oxidation-sensitive food products will be replaced with bio-based laminates containing only 1 µm CNCs. The figure 1 below best illustrates the first target of my PhD project.
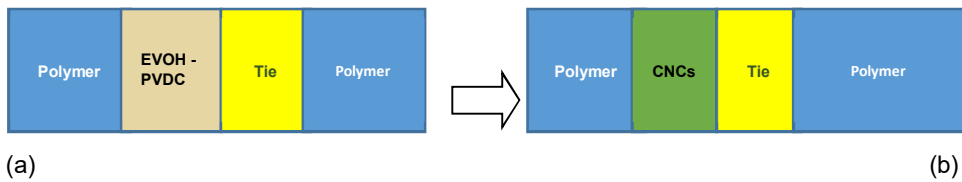
Figure 1. (a) Laminates based on synthetic gas barrier [EVOH/PVDC] (b) Bio-based Laminates blended with CNCs

In parallel, the second objective of my PhD work was an interdisciplinary project called BIOCOMPLACK with the purpose of using those nanoparticles to create a fully compostable packaging in order to extend the food shelf-life (figure 2b). BIOCOMPLACK is a project granted from UE in the European framework project HORIZON 2020. BIOCOMPLACK is a food biopackaging with three main points of innovation:

1. **The production and use of cellulose nanocrystals (CNCs)**

2. **The multilayer structure lamination**

3. **Development of a reinforced PLA**

(a)   **(b)**
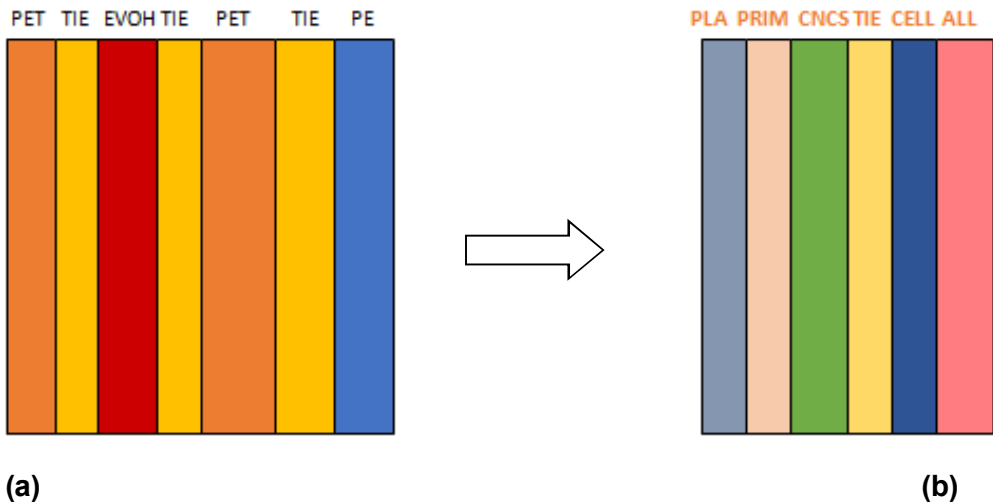
Figure 2. (a) synthetic laminates based on EVOH, (b) fully compostable laminates based on CNCs.

These three innovations will enhance the barrier properties to oxygen (more than 100 times compared with common biopackaging) and water vapour as well as will improve the shelf-life of food. BIOCOMPLACK is an alternative to common bio-packaging products that enhances 300% the shelf-life of food. This international project is born in a consortium integrated by two large enterprises (Sapici and Goglio), two small-medium enterprises (SMEs) (NaturePlast and Tecnopackaging) and a research institution (Packlab, University of Milan) from four different countries which together cover the supply chain of the food packaging industry. BIOCOMPLACK will have strong impact in the society and in the environment. BIOCOMPLACK will be an eco-friendly packaging from natural renewable sources instead of fossil fuels, will reduce the plastic packaging waste thanks to its biodegradability in the nature and will generate at the end of its useful life an added value product, the compost (to improve the quality of soils and provide nutrients). Our BIOCOMPLACK solution will provide a loop cycle of sustainability.

SAPICI

Sapici S.p.a, coordinator of this proposal, will provide to BIOCOMPLACK the adhesive of polyurethane with the cellulose nanocrystals (CNCs) dispersed on it. Established in Italy in 1936, Sapici is a global innovation and full-quality driven developer and manufacturer of advanced and high-performance polyurethane products for such applications as Coating, Flexible Packaging, Industrial Adhesives, Prepolymers, and Inks.

 NATUREPLAST

NaturePlast is a SMEs enterprise specialized in accompanying plastic converters or outsourcers who want to develop and integrate products or packaging into bioplastics. Nature Plast directly manages the supply of raw materials and additives from various suppliers around the world. We certainly now have the broadest portfolio in Europe. The materials that we sell have all been tested by our technical centre (Biopolynov) and have been approved on industrial equipment. Our suppliers have been chosen by several criteria: quality, price, production volumes, availability and certificates of biodegradation and food contact. We will provide the PLA polymer (raw material) to Tecnopackaging for the BIOCOMPLACK project.

TECNOPACKAGING

Located in Zaragoza, Tecnopackaging´s main purpose is conducting R-D-i on advanced polymeric materials and their transformation processes for packaging and industrial plastic applications, targeting companies which operate directly or indirectly in the agri-food, cosmetic, pharmaceutical and industrial sectors.Tecnopackaging integrates the capabilities and skills of various researchers and has the necessary technical equipment for providing customers a comprehensive design of new products, from concept to prototype, validation and development of the first series. In addition, Tecnopackaging develops all its activities keeping in mind an eco-innovative perspective, analysing in each case the different alternatives that would reduce the environmental impact of both their products and/or their processes. The company role in the project will be to supply the PLA film to BIOCOMPLACK project.

UNIMI

The Food Packaging Laboratory (Packlab) of the Department of Food, Environmental and Nutritional Sciences (DeFENS) of the University of Milan has been established since 1985 and it is a laboratory exclusively devoted to packaging research. In these almost 25 years several collaborations have been established with companies in the food as well as in the packaging sector and many relationships have been instituted with other Universities and Research Centers in Italy and abroad. Packlab has an important role in the BIOCOMPLACK project. Packlab will provide the characterization tests needed for the nanocellulose crystals and/or the coated layer and for the final laminated before the scale-up. Packlab also will carry out trials of shelf life studies of target foods and the test to control the food contact compliance of the final product.

GOGLIO NE

Goglio North Europe BV will be the converter of the BIOCOMPLACK food biopackaging. Goglio will manufacture the biobased, biodegradable and compostable packaging, safe for food with long-term preservation thanks to the multilayer structure of PLA film (supplied by Tecnopackaging) and the adhesive of polyurethane with CNCs dispersed on it (supplied by Sapici).

Goglio was founded in Milan in 1850, today Goglio is leader in flexible packaging, rigid plastic accessories such as valves and spouts, and packaging machines.

PhD challenges

Unlike the enormous capabilities displayed and highlighted above, cellulose nanocrystals behave as most biodegradable materials, they are sensitive to water, that compromises their gas barrier properties, and subsequently, this makes them inappropriate for use in wet ambient and/or for fresh foods applications. To overcome that drawback, two solutions were considered valid and plausible, modifying the cellulose nanocrystals to impart them hydrophobic nature or incorporating CNCs in multi-layer laminates to protect them against the humid surrounding. The PhD project was divided into 5 stages as the table below illustrates very clearly.

Activity / Weeks	6	12	18	24	30	36	42	48	54	60	66	72	78	84	90	96	112	118	124	130	136	142	148	156
A1) CNCs production -characterization																								
1) Water uptake, hysteresis zone																								
2) Diffusion and solubility studies																								
A2) Chemical Modification of CNCs																								
1) Reaction trials																								
2) Applications																								
A3) Life cycle assessment																								
1) CNCs coatings onto films																								
2) Lamination with adhesives																								
A4) Food Shelf-life extension																								
1) Trials and applications																								
2) Food shelf-life tests																								
A5) Thesis and Papers Preparation																								

Table 1. Five stages of PhD project

Throughout the reading of the content of this thesis, it will be discovered that apart from the life cycle assessment, the purpose of the project was completely achieved either for the implementation of the bio-based packaging or that of the fully compostable packaging, with great possibility to overstep the lab scale and shift at the industrial scale.

Chapter 3

Results

Chapter 3. Results

IV. Are cellulose nanocrystals "alien particles" to human experience?

V. Implementation of biocomposites by the lamination cellulose nanocrystals

I. The Effect of Moisture on Cellulose Nanocrystals Intended as a High Gas Barrier Coating on Flexible Packaging Materials

I. The Effect of Moisture on Cellulose Nanocrystals Intended as a High Gas Barrier Coating on Flexible Packaging Materials

Ghislain Fotie [1], Riccardo Rampazzo [2,3], Marco Aldo Ortenzi [2,3], Stefano Checchia [2,3,4], Dimitrios Fessas [1,3] and Luciano Piergiovanni [1,3,*]

[1] DeFENS, Department of Food, Environmental and Nutritional Sciences, Università degli Studi di Milano, Via Celoria 2, Milano 20133, Italy; Ghislain.Fotie@unimi.it (G.F.); Dimitrios.Fessas@unimi.it (D.F.)

[2] Department of Chemistry, Università degli Studi di Milano, Via Golgi 19, Milano 20133, Italy; Riccardo.Rampazzo@unimi.it (R.R.); Marco.Ortenzi@unimi.it (M.A.O.); Stefano.Checchia@esrf.fr (S.C.)

[3] CRC Laboratorio di Materiali e Polimeri (LaMPo), Department of Chemistry, Università degli Studi di Milano, Via Golgi 19, Milano 20133, Italy

[4] ESRF–The European Synchrotron, 71 Avenue des Martyrs, Grenoble 38000, France

* Correspondence: Luciano.Piergiovanni@unimi.it

Abstract

Cellulose nanocrystals (CNCs) exhibit outstanding gas barrier properties, which positionthemselves as biobased and biodegradable barrier coating on flexible food packaging materials. However, CNCs have a strong sensitivity to water that can be detrimental to gas barrier properties. In this work, the oxygen and water vapor permeability of polyethylene terephthalate (PET) films coated with CNCs obtained from cotton linters were measured at various relative humidities and the diffusion and solubility coefficients were estimated. The CNCs' moisture absorption and desorption isotherms at 25

°C were collected in the range of relative humidity 0%–97% and analyzed through GAB (Guggenheim-Anderson-de Boer) and Oswin models. The effects of moisture, following the freezable water index, and on the crystal structure of CNCs were investigated by Differential Scanning Calorimetry and by X-ray Powder Diffraction, respectively. These findings provide solutions of coupling CNCs with hydrophobic materials in order to boost their capabilities as barrier packaging materials.

Keywords: cellulose nanocrystals; flexible packaging materials; oxygen barrier; moisture effects.

1. Introduction

In any cellulosic material, the water content and interactions with the material's components have a great influence on its final properties. In particular, the way in which water molecules interact with cellulose and their distribution within the often complex and heterogeneous system of cellulosic materials are critical to their applications. In fact, the manufacturing processes developed for paper, board and regenerated cellulose (cellophane films) include specific operations aimed at the careful removal of water added or present, and several hydrophobic protective layers and ingredients for providing moisture resistance are extensively used nowadays (Biermann, 1996). Sorption isotherms interpretation, particularly through FTIR spectroscopy studies, led to the idea that water molecules are adsorbed to specific sites, both as layered adsorption or as cluster formation. The main potential adsorption sites are the hydroxyl groups and their possible oxidation forms such as the carboxyl groups (Olsson et al., 2004). For specific cellulosic materials, even at relative humidity (RH) values below 100%, it was possible to establish the number (1.0–1.3) of water molecules that adsorb to a single hydroxyl group (Hodge et al., 1996; Peemoeller et al., 1985; Pin et al., 2001). Studies of the diffusion of water molecules in cellulosic materials led to the conclusion that cellulose wetting can be related to acid-base interactions, weak hydrogen bonding and van der Waals forces (dipole-dipole and dispersion forces) (Gardner et al.,

2008). Therefore, the extent of water sorption in cellulosic materials can also depend on the surface free energy of the solid-liquid interface.

At a larger scale, bulk amorphous regions have been pointed out, from as early as 1949, as a favorable place for water adsorption, and the relationship between availability of surface hydroxyl groups and crystallinity of cellulose is well established (Howsmon, 1949; Mihranyan et al., 2004). As a result of the heterogeneous and complex morphology of cellulosic materials, the state of water in cellulose was classified in three different types: free water (type I), freezing bound water (type II) and non-freezing bound water (type III) (Agrawal et al., 2004; Nakamura et al.,1981)

When cellulose based materials are used in packaging applications, water adsorption and desorption phenomena during the commercial life are of great importance because they are able to affect fundamental performance, such as mechanical and diffusional properties. Mechanical resistance, for instance, can be strongly reduced by moisture adsorption leading to the dissolution of the hydrogen bonds which produces tight fibers in papers and boards. This bonding occurs as the wetted fibers can dry in contact with each other, requiring close proximity between adjacent hydroxyl groups (0.25–0.35 nm) (Gardner et al., 2008). At least in paper, this bonding seems more important than the mechanical interlocking of cellulose fibers. Furthermore, the adsorption of hydrophobic components on cellulose fibers during paper manufacturing greatly decreases fiber bonding and can affect the weakness and adhesion as well (Bikerman, 1967), leading to the risk of failure and unsuitability.

The effects of water sorption on the diffusional properties of cellulose, that is gas and water vapor permeability, have been often overlooked in the past, since most cellulosic materials employed in paper and board do not require outstanding barrier properties towards gases and water. Several papers demonstrated the high gas barrier properties provided by the use of cellulose nanocrystals (CNCs) and cellulose nanofibers (CNFs) as coatings applied

onto common plastic films, as well as fillers of common polymers (Aulin et al., 2010; Frounchi and Dourbash, 2009;Fukuya et al., 2014; Gicquel et al., 2017; Li et al., 2013; Minelli et al., 2010). At the same time, moisture can be seriously detrimental to the gas barrier properties of CNC coated films (Belbekhouche et al., 2011; Rampazzo et al., 2017). In general, synthetic or bio-based polymers with hydrophilic behavior and high polarity, show low oxygen and gas permeability when dry, but lose such properties when water molecules plasticize and swell their native structure.These behaviors are well known and widely investigated in polyamide, polyesters, polyvinyl alcohols and bio-polymers (Aulin et al., 2009; Aulin et al., 2010; Auras et al., 2004; Belbekhouche et al., 2011; Lagaron et al., 2001), while less knowledge is available for the effects of moisture on the gas barrier properties of CNCs when used as coatings applied onto conventional plastic films intended for food packaging applications, which is the main goal of this chapter.

2. Materials and Methods

2.1. Materials

The cotton linters used as raw material to produce CNCs were kindly supplied by Innovhub (Milano, Italy). All the chemicals used were purchased from Sigma-Aldrich (Milano, Italy). Polyethylene terephthalate (PET) film, with a thickness of 12 ± 0.5 μm, was provided by Sapici spa, Cernusco sul Naviglio, Italy.

2.2. CNCs Extraction by Ammonium Persulfate Treatment and Coating Process

The CNCs were obtained by the hydrolyzing-oxidative method proposed by Leung and coworkers in 2011 (Leung et al., 2011). The procedure for the obtainment of the CNCs, the purification steps and the coating process onto PET film have been described in our previous works (Li et al., 2015) and

strictly followed in this paper. The yield of CNC production (%) was evaluated from the weight of the freeze-dried products by comparing them with the mass of cellulosic raw materials treated. The thickness of the coating applied onto the film was assessed by a gravimetric method. Four samples (10 × 10 cm^2) were weighed (m_1, g), then the coating was removed by running hot water (~70 °C) and the resulting uncoated film was dried and weighed (m_2, g). The coating thickness (L, cm) was estimated by equation (1):

$$L= (m_1 - m_2)/(\rho \times 100), \tag{1}$$

where ρ = 1.58 g cm^{-3} is assumed as the density of the CNCs.

2.3. Characterization of cellulose nanocrystals and coated PET film

2.3.1. Characterization of cellulose nanocrystals

By dynamic light scattering (DLS) measures (mod. Litesizer 500, Anton Paar, Graz, Austria), the equivalent hydrodynamic diameters of the CNCs were determined, as well as the polydispersity index and intensity and particle number distributions (data not shown). The measurements were performed at 25.0 ± 0.1 °C with a 35 mW laser diode light (λ = 658 nm) and collecting the scattered light at 90°. Before measurements, the samples were diluted to 1:500 (w/w) with distilled water adjusted to pH 8 and maintained at 25 °C through stirring until measurement. The diluted solutions were poured in the measurement cell after 30 s homogenization by an ultrasonic water bath. The actual dimensions of the CNCs were evaluated via Transmission Electron Microscopy (TEM). Drops of aqueous dispersions of CNC (1 wt %) were deposited on carbon-coated electron microscope grids, negatively stained with uranyl acetate and allowed to dry. Samples were analyzed with a Hitachi Jeol-10084 TEM operated (Hitachi, Brugherio, Italy) at an accelerating voltage of 80 kV.

Zeta-potential and Conductivity of the CNCs.

84

Zeta potential (mV) and conductivity (mS cm⁻¹) of the CNCs in the diluted suspension at pH 8 were determined by electrophoretic light scattering (ELS), using the PALS technology (mod. Litesizer 500, Anton Paar, Graz, Austria). Measures were replicated 5 times, at 25.0 ± 0.1 °C, by means of a 35 mW diode laser (λ = 658 nm) and at 15° detection angle.

X-ray Powder Diffraction (XRPD)

X-ray diffraction measurements were performed at the beamline ID15A of the ESRF synchrotron facility (Grenoble, France). The sample for X-ray diffraction was a 13 mm-diameter, 0.5 mm thick pellet obtained by pressing uniaxially 45 mg of CNC flakes. The pellet was mounted on a goniometric head and aligned normal to the incident X-ray beam at a distance of 260.5 mm from the detector, a Pilatus 2M CdTe (Dectris, Baden-Daettwil, Switzerland). Each dataset consists of 50 2D diffraction images recorded by exposing the sample for 5 s. First, the sample was measured in the dry state, i.e., as mounted. Then, 100 mg of water were pipetted on one face of the pellet and allowed to absorb immediately before collecting the second dataset. The injection of 100 mg water and the subsequent diffraction measurement were repeated 60 and 120 minutes after the first measurement. The X-ray wavelength was 0.17712 Å. The wavelength, sample-detector distance, detector tilt, and beam position were calibrated based on the diffraction pattern of CeO_2. Raw diffraction images were scaled, averaged and finally subtracted by the air background before being radially integrated and corrected for the polarization of the incident X-ray beam. Calibration, image processing and radial integration were performed using Python 2.7 and the libraries pyFAI and FabIO (Ashiotis et al., 2015; Knudsen et al., 2013). For each measurement, the Pair Distribution Function (PDF) was calculated as the G(r) described by Keen, 2001 (Keen, 2001) using the program PDFgetX3 (company, city, country) (Juhás et al., 2013). The PDF is a function in real space representing the distribution of interatomic distances in the bulk material and is obtained by Fourier-transforming the total scattering intensity after proper normalisation

and correction (Fischer et al., 2005). The maximum value of momentum transfer used for PDF calculation was $Q_{max} = 27$ Å^{-1}. The diffraction pattern of the dry CNC sample was fitted via the Rietveld method (Rietveld, 1969) using the program Topas 5.0 (Bruker AXS, Karlsruhe, Germany.).

Freezable Water Content (DSC)

The freezable water content of CNCs at various humidity (HU% = g H_2O/g sample) was assessed through differential scanning calorimetry (DSC) (Alamprese et al., 2017). The DSC calorimeter 2920 (TA Instruments, Vimodrone, Italy), operating with 60 microliter sealed cells, was used. The typical sample mass was 30 mg; the reference cell was empty and Indium was used for calibration. Measures were carried out from −60 to 30 °C with 1.0 °C/min scanning rate. This relatively low scanning rate was selected in order to enhance maximum crystallization during cooling. Two cooling-heating cycles were performed. The transitions were reversible in the heating mode (super-cooling effects were observed in the cooling step) and the first cycle heating curves were taken into account. The output signal in mW units was divided by the product of sample mass per heating rate in order to be converted into apparent specific heat and it was scaled with respect to the baseline to obtain the excess (with respect to the water solid state) specific heat trace, Cp^{exc} (J K^{-1} g$^{-1}_{water}$). The heat capacity change during the solid-liquid water transition, $\Delta_{fus}Cp$, was scaled across the signal and was therefore not taken into account in the present work. Thanks to this treatment, the area beneath the recorded peaks directly corresponds to the relevant transition enthalpy $\Delta_{fus}H$. The freezable water content was assessed according the ratio $\Delta_{fus}H/\Delta_{fus}H°$, $\Delta_{fus}H°$ being the pure (free) water enthalpy (333.59 J g^{-1} at 0 °C). Errors were evaluated based on at least three replicates and were under 5%.

Water Sorption Isotherm

The water adsorption and desorption isotherms (at 25 - 1 °C) of CNCs were roughly determined by the standard static gravimetric method developed by

the European Cooperation Project COST 90 (Tsami et al., 1990), in triplicate, using saturated salt solutions to establish the RH values of 20.9%, 27.3%, 35.1%, 51.3%, 59.9%, 66.1%, 79.0% and 85.6%. In the desorption mode the Knudsen thermogravimetry approach was also used. Details of the method are reported elsewhere (Alamprese et al., 2017). This method is continuous and each measurement produces the overall desorption isotherm with high reproducibility also in the low water activity ranges but can be applied only in the desorption mode (Fessas and Schiraldi, 2005; Schiraldi et al., 2013). A TG-DSC instrument (TG-DSC 111, SETARAM, Caluire, France) operating with a typical sample mass of 30 mg was used. The GAB (Van den Berg, 1981, 1984) and Oswin (Oswin, 1946) Equations (2) and (3) respectively, were tentatively applied to data for the adsorption and desorption of water by CNCs and shown in the following equation:

$$m = M_o \, CKa_w/[(1 - K \, a_w)(1 - K \, a_w - CK \, a_w)], \qquad (2)$$

where m is moisture content (g H_2O/g d.m.), a_w is the water activity. M_o, K, C describe the sorption properties of the structure. M_o is the monolayer water content; the parameters K and C are the degree of freedom of water content and difference between layers (upper and monolayer) respectively and they depend on the temperature.

$m = c_1 \, (a_w/(1-a_w)) \, c_2$, where c_1 and c_2 are empirical constants.

2.3.2. Characterization of CNCs-coated PET film Optical Properties of Coated Film

The transparency of the CNCs coated PET was measured at 550 nm, according[(3)] to the ASTM D 1746-70, by means of a UV-VIS spectro-photometer (mod. L650, Perkin-Elmer, Milano, Italy). The haze (%) of the same samples was measured according to ASTM D 1003-61 with the same instrument equipped with a 150 mm integrating sphere. Each sample was replicated three times, analyzing at least four spots on each replicate

Water Contact Angles

Static contact angles of the coated film were determined after conditioning the samples at three different RH values (57%, 81% and 97%). The sessile drop method was used by gently dropping a droplet of 4.0 ± 0.5 μL of water onto the film. The measurements were performed at room temperature (RH about 40%) on five different positions for each sample. The equilibrium angle was achieved in 2–3 seconds and remained constant for at least 10–15 seconds; due to the short time of the measurement, we assumed that the CNCs coating did not change its original activity water value. The instrument used was an OCA 15 Plus angle goniometer (Data Physics Instruments GmbH, Filderstadt, Germany), equipped with a high-resolution CCD camera, a high-performance digitizing adapter (Data Physics Instruments GmbH, Filderstadt, Germany) and SCA20 software (Data Physics Instruments GmbH, Filderstadt, Germany) for contact angle measurements.

Gas and Water Vapour Permeability

All the oxygen and water vapor permeability measures were performed by an isostatic permeabilimeter (mod. Multiperm, PERMTECH S.r.l., Pieve Fosciana, Italy) according to ASTM standard methods (D-3985 and F-1249 respectively). The oxygen permeability (PO2, cm^3 m^{-2} d^{-1} bar^{-1}) of CNCs coated PET film was measured at 25 °C under 80%, 70%, 50%, 30%, 20% and 10% RH on the coated side of the film, both increasing and decreasing the RH value. The water vapor transmission rates (WVTR, g m^{-2} d^{-1}) were measured at 25 °C under 90%, 80%, 70%, 60%, 50% and 40% RH on the coated side of the film (being at 0% RH on the other side). The oxygen permeability coefficients of the CNCs coating alone (KPO2, cm^3 μm m^{-2} d^{-1} bar^{-1}) were assessed using equation (4) (Krank, 1979), assuming that the PET surface did not interact with the coating layer above with thickness L (μm), and that the interface between them negligibly affected the permeation measure.

$$L/[KPO2_{\text{(CNCs coating)}}] = [1/PO2_{\text{(coated PET film)}}] - [1/PO2_{\text{(uncoated PET film)}}]. \quad (4)$$

From the isostatic permeation curves obtained, the oxygen diffusion coefficients (D, $cm^2\ s^{-1}$) in the coating at each RH value were estimated according to equation (5) (Hernandez el., 1999; Lee et al., 2008);

$$D = L^2/(7.2 \times t_{(1/2)}), \quad (5)$$

where L is the thickness (cm) and $t_{1/2}$ (s) is the time required to reach half of the maximum permeability value. From the permeability and diffusion coefficients (KPO2 and D), the oxygen solubility in the CNCs coating (S, bar^{-1}) were estimated at each RH value, based on equation (6):

$$S = KPO2/D \quad (6)$$

3. Results

3.1. CNCs Production and Coating onto PET Film

Cellulose nanocrystals were obtained from cotton linters by the hydrolyzing-oxidative method, already used in previous works (Mascheroni et al., 2016; Rampazza et al., 2017), with a yield of about 50%; the morphological and main chemical characteristics of the CNCs were identical to the ones already described and are recalled in Table 1. As mentioned in the Materials and Methods section, the dimensions of cellulose nanocrystals were determined via transmission electron microscopy and confirmed the values obtained previously (Table 1). A TEM image of CNCs is reported in Figure 1. The coating process was also the same as described in previous papers and the tests carried out confirmed the continuity and the uniformity of the CNCs layer coated onto the PET substrate. Therefore, only a few characteristics of the coated film are reported in Table 1.

Property of CNCs	Value[1]
Hydrodynamic diameter (nm)	101.15 ± 3.65
Average dimensions (length, L) from TEM measures	139 ± 33
Average dimensions (diameter, D) from TEM measures	16 ± 5
Aspect ratio (L/D)	9 ± 4
Zeta potential (mV)	-44.40 ± 4.12
Conductivity (mS cm^{-1})	0.095 ± 0.024
Polydispersity index	22.95 ± 0.63
aw after freeze drying	0.26 ± 0.01
Property of CNCs coated PET film	
aw after coating and drying	0.46 ± 0.05
Thickness of PET film (µm)	12.0 ± 1
Thickness of CNCs coating (nm)	756.3 ± 22.3
Transparency (T% at 550 nm)	85.67 ± 0.3
Haze (%)	1.89 ± 0.1
Optical contact angle (water) at 57% RH	11.23 ± 0.41
Optical contact angle (water) at 81% RH	9.33 ± 0.56
Optical contact angle (water) at 97% RH	8.05 ± 0.31

Table 1. Main characteristics of cellulose nanocrystals and of the CNCs coated PET film.

[1] Mean values of at least 3 replicates ± standard deviations.
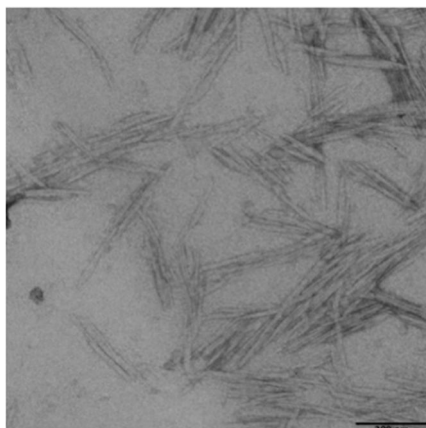
Figure 1. TEM micrograph of the CNCs (cellulose nanocrystals) obtained.

It is worth underlining that the water optical contact angles measured on coated film decreased linearly (R_2 = 1.0) from 57% to 97% RH, showing a clear growth of hydrophilic behavior of the CNCs surface. Previous measures (Rampazzo et al., 2017) on the same CNCs coated film at 35% RH, had shown a much higher value of 23.6 ± 4.9—not linearly correlated to the contact angles measured in these trials—as preliminary evidence of a dramatic change of the structure, occurring above a threshold of humidity content.

In general, the CNCs coated film obtained had an appearance and performance very similar to the previously obtained films and to many common flexible packaging materials.

3.2. Water and Gas Permeability of Coated PET Film

The water vapor transmission rates (WVTR, g m^{-2} d^{-1}) were measured in duplicate at 25 °C, decreasing the RH on the coated side from 90% to 40% for each sample. The inset of Figure 2 shows the progressive and linear decrease of water transmission across the coated film, according to the water vapor pressure established by the conditions of the measures (temperature and ΔRH). Figure 2 depicts the superimposed isostatic curves of water diffusion at the different driving forces, from which it should be possible to estimate the diffusion coefficient (D), once $t_{1/2}$ (the time required to reach half

of the maximum diffusion) has been estimated. The vertical black bar shows that the $t_{1/2}$ of all the curves are reached at the same time, denoting the same diffusion coefficient of water permeating through the coated film at the various driving forces considered.
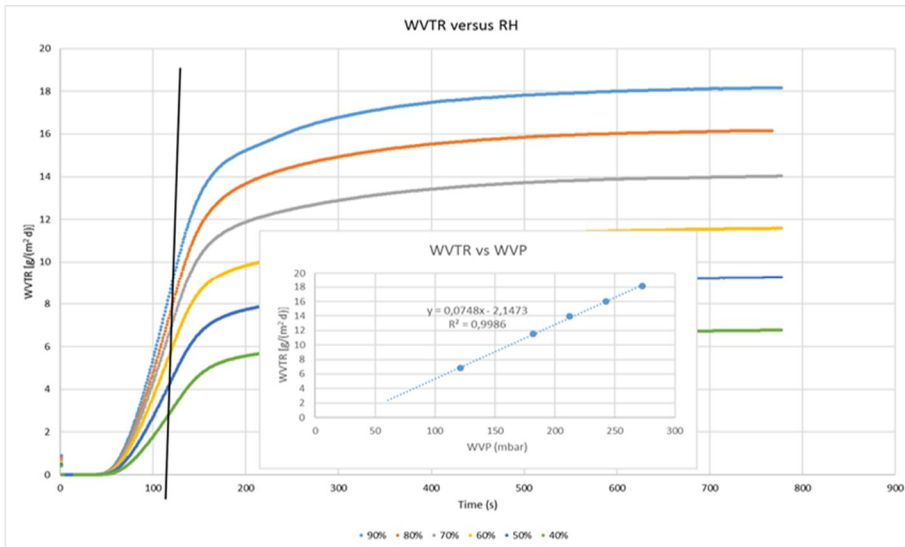
Figure 2. Isostatic curves of water diffusion at 25 °C under different driving forces through the CNCs coated PET film.

The oxygen permeability of the CNCs coated PET film was also measured at various RH values in triplicate and at 25 °C, progressively changing the relative humidity on the coated side of the films from 7.7% up to 80% and then going back from 80% to 7.7% on each sample. Figure 3 reports the average values (± relative standard deviation) of oxygen permeability during the adsorption run (blue curve) and the desorption run (orange curve). Significant differences are present along the range 40%−80% between the two behaviors (in adsorption and desorption) and the values increase more than 90 times from the minimum to the maximum RH value.
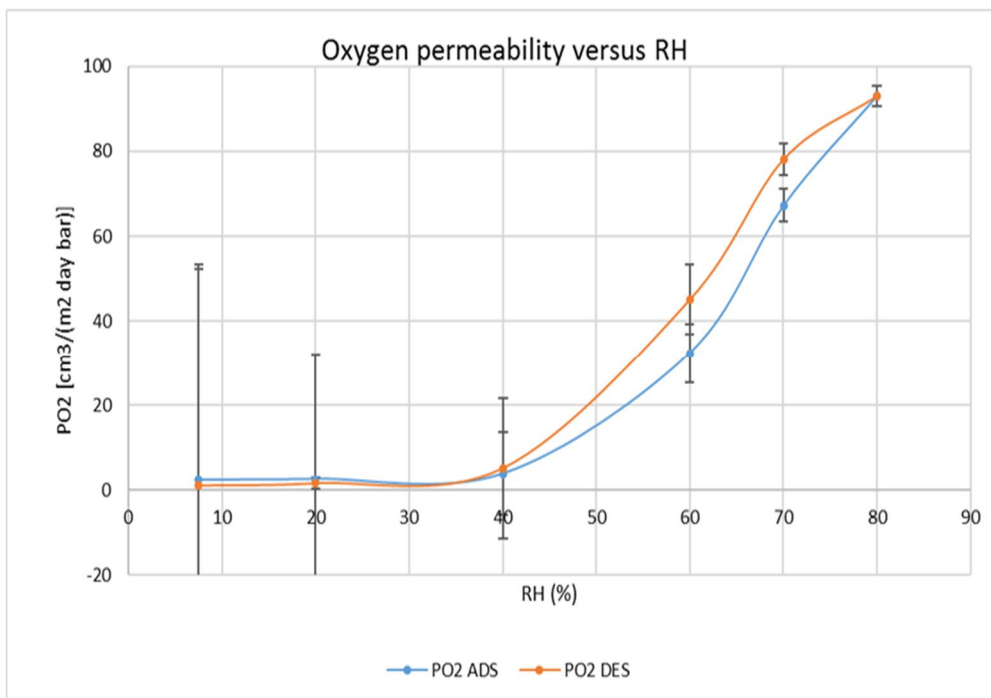
Figure 3. Oxygen permeability at 25 °C under different relative humidity (RH) values, both in adsorption and desorption, through the CNCs coated PET film.

The isostatic permeabilimeter used has provided—also for oxygen permeability measures—sharp curves of diffusion (oxygen transmission rate versus time, data not shown) which permitted us to estimate, from the oxygen permeability coefficient of the CNCs coating layer alone (excluding the PET contribution), the diffusion (D) and solubility (S) coefficients (Equations (4)/(6)).

These fundamental parameters of the diffusional behavior of oxygen inside the cellulose nanocrystals (mean values ± standard deviation) are proposed in Figures 4 and 5, as function of relative humidity values, showing large differences.
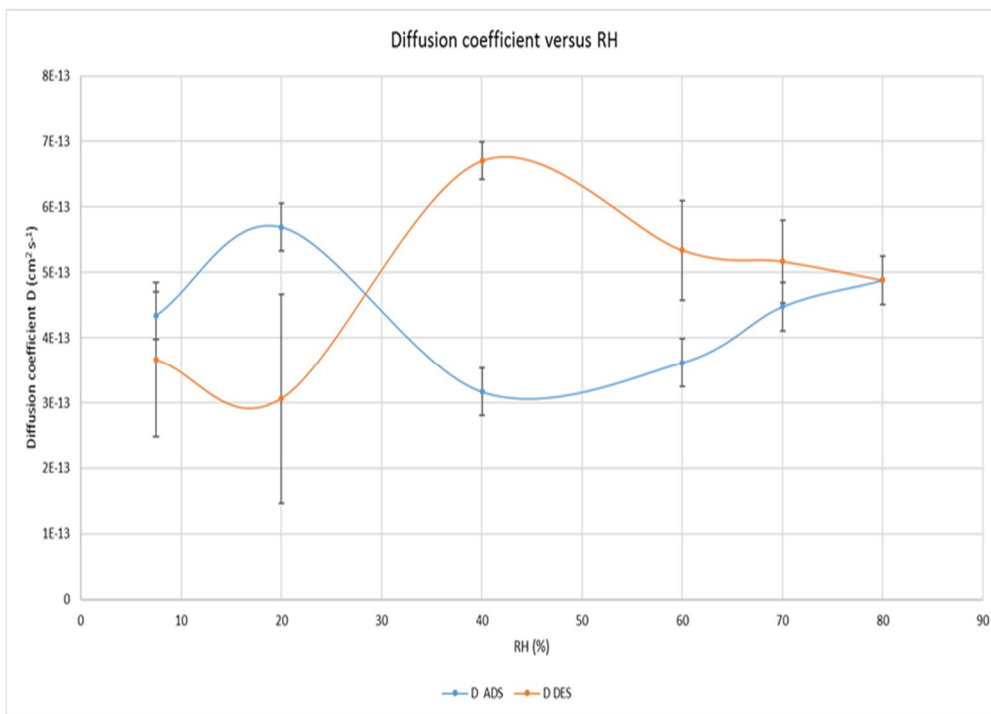
Figura 4. Oxygen diffusion coefficients under different RH values, both in adsorption and desorption, through the CNCs coated PET film.

While the diffusion coefficients are quite different when measured in adsorption and desorption, with the largest and statistically significant differences between 40 and 60% RH values, the solubility coefficients remain quite constant until 70% and show much lower differences between adsorption and desorption which, however, are significant ($p < 0.05\%$) at 70% RH only.
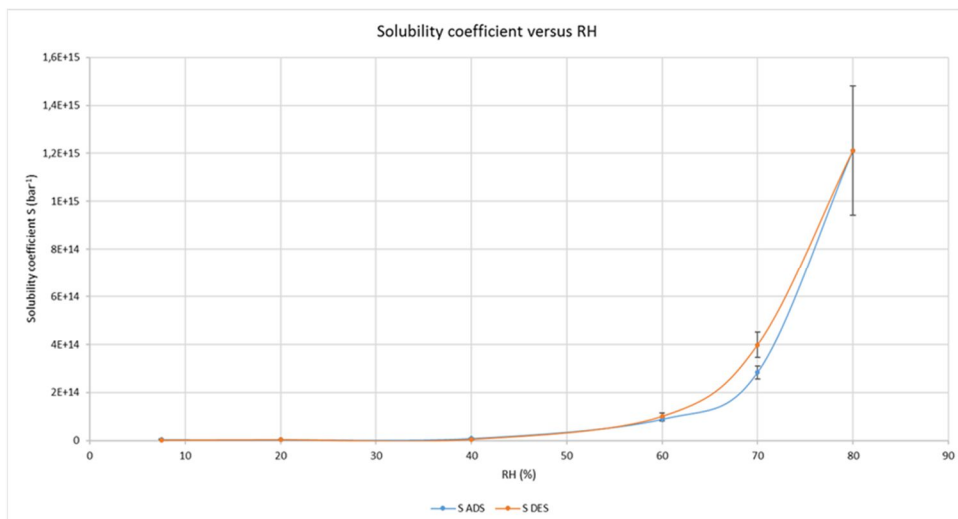
Figure 5. Oxygen solubility coefficients under different RH values, both in adsorption and desorption, through the CNCs coated PET film.

3.3. Characterization of isolated cellulose nanocrystals

CNCs Freezable Water Content

In Figure 6 the DSC measurements are presented in order to assess the freezable water amount in the CNCs samples. We observe a typical behavior for water engaged in polysaccharide substrates (shift of fusion temperature due to colligative effects etc.) (Fessas and schiraldi, 2001). The profiles also indicate that the water crystal size distribution (the width of the peaks almost follow their height) is almost uniform. The freezable water results obtained following the relative enthalpies (see Materials and Methods) are reported in Table 2.

CNCs Humidity % (g H2O/g sample)·100	Freezable water (%) ± 5%
85	100
75	100
52	75
46	65
8	0

Table 2. CNCs freezable water content assessed by DSC.
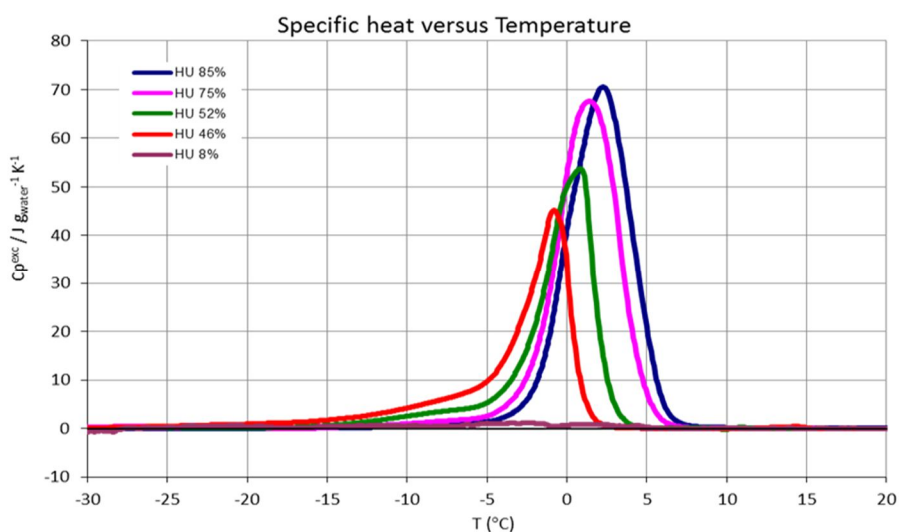
Figure 6.DSC measurements of CNCs at different humidity values.

CNCs Water Sorption Isotherms

In Figure 7 we can observe the sorption isotherms of CNCs. The static gravimetric method used for roughly estimating the sorption behavior of CNCs gave satisfactory results in the middle-high region of water activity aw (or relative humidity RH) values, with low standard deviations. It is very likely that

the values collected at lower RH were less accurate; on the other hand, the desorption isotherms obtained with the Knudsen thermogravimetry method fulfilled this gap. Indeed, we observed that these curves were highly reproducible and in agreement with the static method in the middle-high region of aw. In Figure 7 we also report the adsorption data obtained with the static method. Despite the uncertainties, it is interesting to highlight the hysteresis observed by the two static method curves which denotes a different behavior in adsorption and desorption steps than usually observed for similar systems. In order to be compared, the GAB equation was tentatively applied to these experimental data (excluding the points with high uncertainty, R_2, respectively = 0.989, 0.810) both for the adsorption and desorption of water by CNCs. For the validation of the GAB model, K should be between 0 and 1, and C between 0 and 2 or higher for an isotherm of type III, as in this case. The OSWIN model also fitted well with the experimental data but, is less useful for the interpretation of the water-CNCs interaction. The coefficients are reported in Table 3.

Coefficient	Adsorption	Desorption
	GAB equation	
R_2	0.989	0.810
k	1.27	1.95
C	0.14	0.35
Mo	0.45	0.08
	OSWIN equation	
c_1	1.3	1.23
c_2	1.57	1.90
R_2	0.97	0,90

Table 3. Empirical coefficients of GAB and OSWIN models fitting the experimental isotherms.
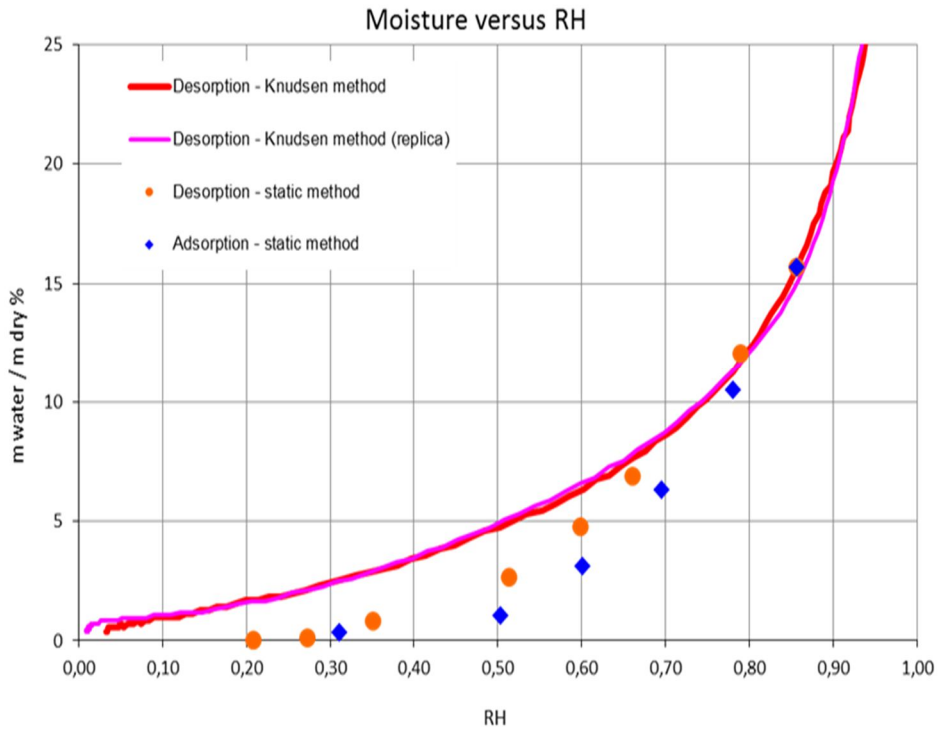
Figure 7. CNCs adsorption and desorption isotherm at 25 °C according to the standard static gravimetric method, and desorption isotherms according the Knudsen thermogravimetry method.

X-ray Diffraction Patterns

In Figure 8 the panel (a) illustrates the diffraction pattern of the dry CNC sample. Panel (b) in the same figure shows the meltdown of the diffraction peaks of the CNC pellet between the four different hydration stages. Finally, the panel (c) shows the decay of the amplitude of the PDF, which directly represents the distribution of atom pairs through space in the bulk material as a function of their interatomic distance.

a) XRPD patterns vs hydration

b) Crystalline phases in dry CNC

c) PDF vs hydration

d) Cellulose I_β phase
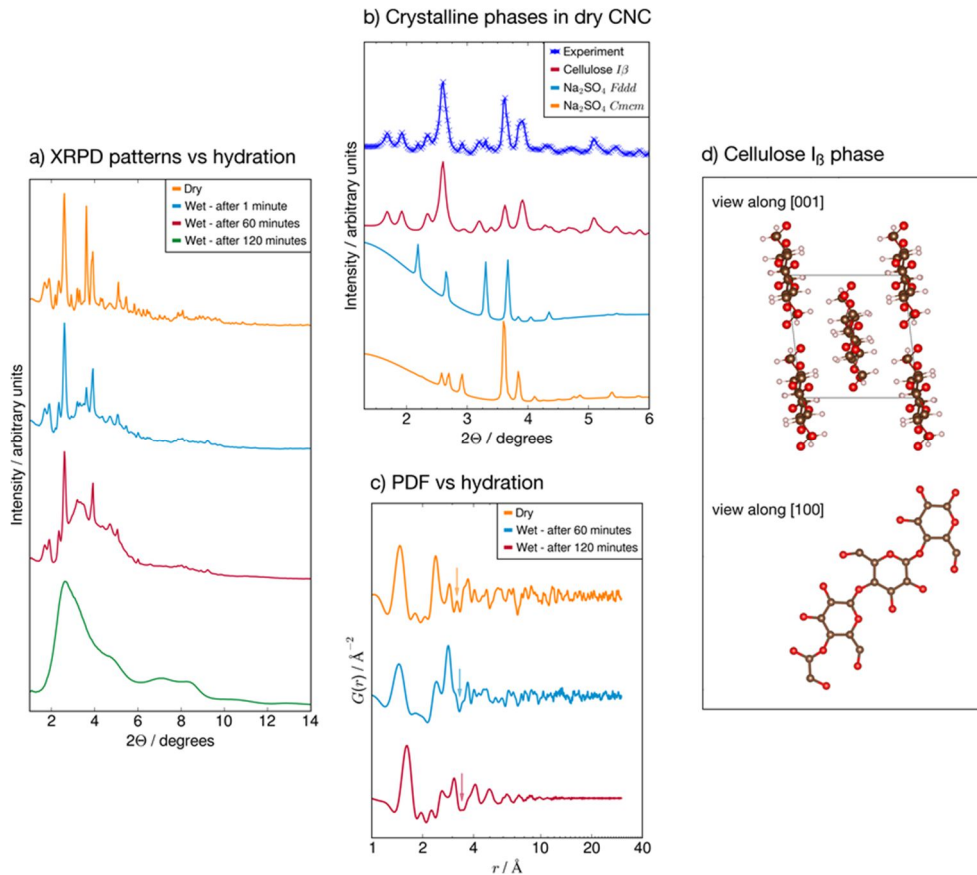
Figure 8. Raw XRPD (X-Ray Powder Diffraction) patterns of CNCs in the dry state and after successive exposures to 100% RH (**a**), breakdown of the XRPD pattern of the dry CNCs sample into the constituent crystalline phases (**b**), The PDF curves of the dry sample and of the wet sample at the second and third hydration (**c**) and a view of the crystal structure of CNC along the crystallographic directions **{001}** and **{100}** (**d**).

4. Discussion

4.1. Permeability of CNCs Coated Film

The water vapor transmission rate measures were carried out starting from 90% of RH and then decreasing the humidity on the coated side, step by step until 40%, and a very linear relationship between water transmission and driving force occurred (inset of Figure 2). It is noticeable that each previous measure did not affect the following one at a lower humidity. Thus, it is

reasonable to assume that the water molecules adsorbed by the coating layer of CNCs were effectively removed by the conditioning steps applied by the instrument between measures, and that each permeability measure has been conducted in the expected conditions. Otherwise, it would not have been possible to obtain such a linear relationship.

This assumption contributes to the interpretation of the results obtained for oxygen permeability assessment at various RH values. As proved in our previous papers (Mascheroni et al., 2016; Rampazzo et al., 2017), at RH value close to zero, the oxygen permeability of very thin CNCs coating is much lower than the PET substrate. To get the same permeability, a PET thicker than 8.0 mm would be necessary.

The determinations, carried out in triplicate on different samples of coated films, were performed increasing at first and then decreasing the relative humidity, i.e. in an adsorption and desorption way. As expected, the oxygen permeability increased exponentially during the increase of RH values, reaching values which are no longer of interest for CNCs application as a barrier layer of flexible packaging materials for perishable food products. The most interesting and novel results deal with the measures carried out in desorption, after the achievement of 80% of RH and going back to dry conditions (7.7%). The relative standard deviations of the measures confirm that the oxygen transmission in desorption is different from that in adsorption; especially in the range between 70 and 50%. The calculation of diffusion coefficients (in Figure 4) is further confirmation of this behavior, showing the largest differences in the range 60%–40% of RH whereas, below and above these limits, the uncertainties of the measure exclude statistical differences. Moreover, since the solubility of oxygen in CNCs seems slightly affected by RH values of up to 70% (in Figure 5), with negligible discrepancies between adsorption and desorption (except at 70% RH), it is reasonable to conclude that moisture has a different effect on oxygen solubility and oxygen diffusion along the cellulose nanocrystals layer.

Generally, polymer crystallization influences diffusivity more than solubility (Pollyakova et al., 2001; Weinkauf et al., 1990). This is in accordance with the concepts of free-volume, as well as cooperative movement of gas molecules and polymer chains (Mokwena et al., 2012), in which diffusion of small gas molecules through a semicrystalline polymer, is viewed as a movement through the amorphous regions, with an increased tortuosity given by platelet-like crystallites. Obviously, a higher thickness would increase the barrier effect even more. In bio-polymers, however, the negative correlation between crystallinity and diffusion coefficient is not always confirmed. Guinault et al. (2012) showed that oxygen diffusion coefficient was accelerated upon crystallization of poly (lactic acid), while the solubility coefficient decreased, remaining constant in the amorphous phase. This phenomenon was attributed to the presence of a rigid amorphous fraction, which holds larger free volume.

The experimental evidence and the, somehow, contradictory literature analysis suggested the focus should be kept as much as possible on understanding the interactions between CNCs and water molecules.

4.2. Freezable Water and Water Sorption Isotherms

The above observations are in line with the DSC and the sorption data. Indeed, we observed that the amount of freezable water increases considerably with respect to the sample humidity. For instance, for sample humidity of 46%—that corresponds to about 85% in terms of water/dry matter ratio—the freezable water is 65%, i.e. 35% of water is strongly engaged in interactions with the substrate. Taking into account the sorption picture (see Figure 7) that is in an upper range of 25% in terms of water/dry matter ratio we argue that the majority of the water is strongly engaged in interactions in all the experimental RH ranges of the water vapor transmission rate measures. In this strong interaction environment, the RH variation corresponds in water/dry ratio variation sufficiently to affect the oxygen permeability. Furthermore, looking at the desorption profile, the variation of

water/dry ratio is enhanced to the RH 90%–40% range, while for lower RH becomes modest (flat part of the desorption curve). This is coherent with the results showed in Figure 3 (oxygen permeability vs RH). Finally, the hysteresis effects observed (see Figure 7) are also in line with the above considerations.

The GAB model obtained has 0 <C< 2 which means that the isotherm of the CNCs may be of the type III and the OSWIN model actually fitted sharply the relationship between the moisture content and the water activity, sustaining the experimental results.

4.3. Crystallinity by WAXD Analyses

X-ray diffraction measurements explained the hydration behaviour of CNCs at the crystal structure level at 100% RH and, particularly, the changes in short-range and long-range interactions that make the cellulose nanocrystals (whiskers) accommodate a large amount of absorbed water.

The diffraction pattern of the dry CNCs sample shows a highly crystalline phase corresponding to the Iβ polymorph of cellulose (space group $P112_1$), which consists of chains of pyranosidic rings directed along the c-axis (panel (d) in Figure 8), and in which the sharp reflections (012) and (102) point to the random orientation of the crystallites in the sample (French, 2014). In addition to the cellulose phase, the dry CNCs sample contains 22% wt of Na_2SO_4, as evidenced by the diffraction pattern showing two different Na_2SO_4 polymorphs with space groups Cmcm and Fddd (Tanaka et al., 1991; Zachariasen, et al., 1932). Panel (a) in Figure 8 illustrates the contribution of each of the three phases to the experimental powder pattern of the dry CNCs sample.

Panel (b) in the same figure shows the meltdown of the diffraction peaks of the CNCs pellet between the four different hydration stages, each of them exposed the CNCs pellet to 100% RH by absorption of 100 mg of water. Immediately after the first hydration (blue line, second from top), the sharp Bragg peaks of the Iβ phase are retained, while a higher background around scattering angle 2θ = 4° signals the partial amorphisation of cellulose;

predictably, embedded Na_2SO_4 was dispersed upon contact with the absorbed water, as evidenced by the drop in the intensity of the peaks at 2θ ~ 2.20°, 3.60°. Upon swelling the pellet again by absorbing another 100 mg of water after 60 minutes (red curve, third from top), the amorphous regions in the sample expanded at the expense of the crystalline part; the most intense Bragg peaks of cellulose are still visible but the large amorphous bump now dominates the diffraction pattern. After the third and last exposure to water (green curve, bottom), all the Bragg peaks vanished and the diffraction pattern only showed a broad, amorphous feature.

The loss of structural coherence can be evidenced even more clearly by the decay of the amplitude of the PDF (panel (c) in Figure 8), which directly represents the distribution of atom pairs through space in the bulk material as a function of their interatomic distance.

While the PDF curves relative to the dry sample (orange line, top) and after 60 minutes (blue line, middle) have discernible peaks up to r = 40 Å, the PDF collected after 120 minutes (red line, bottom) is flat for every interatomic distance above r = 12 Å. The smearing of the interatomic distances at the nanometer scale is indicative of the broad distribution of inter-chain distances in the cellulose crystallites brought about by hydration. At the same time, several intra-chain interatomic distances within 10 Å are preserved but show crucial changes that are directly relatable to structural changes in CNCs upon hydration. At the second hydration, after 60 minutes (blue line, middle), the peak at r = 2.50 Å becomes broader and weaker than in the dry sample: besides the disappearance of the underlying Na–O distances as Na_2SO_4 is dispersed in water, this suggests a broader distribution of the distances between neighbouring pyranosidic rings; the sharp peak at 2.87 Å, on the other hand, is specific to intra-ring interatomic distances and changes only slightly with respect to dry CNCs. The disappearance of the peak at r = 3.17 Å suggests that the benzyl alcohol moieties engage in different H-interactions and they no longer sit in the same plane as the C-alpha (see the {100}

projection in panel (d)). The third hydration, after 120 minutes, results in the general broadening of the PDF features which broaden even within r = 10 Å; beyond this distance, corresponding to two pyranosidic rings, the PDF is then completely flat and corresponds to the complete loss of structural coherence.

5. Conclusions

The multidisciplinary approach to understanding the water-cellulose nanocrystals interaction resulted in a complex scenario, leading to a unique conclusion about the importance of preserving the gas barrier properties exhibited by CNCs, by limiting as much as possible the moisture adsorption. In the case of practical applications such as food-packaging materials, the presence of a hydrophobic and sealable polymeric layer protecting the CNCs coating seems essential. However, an identical issue concerns synthetic polymers, like polyvinyl alcohol (PVOH) or ethylene vinyl alcohol copolymer (EVOH), which are even less of a barrier than CNCs.

We observed that at low humidity the amount of freezable water decreases considerably indicating relevant interaction with the substrate, despite the accessible surface area being limited by the crystallinity of cellulose nanoparticles. The freezable water, however, seems not strictly related to the oxygen barrier, since we measured very low permeability values up to about 40% RH, where the freezable point appears higher than 50%.

The water adsorption by CNCs is relevant and continues to follow an isotherm of type III. This phenomenon provokes the loss of structural coherence, as clearly evidenced by the X-Ray diffraction patterns, and the sharp increase of oxygen diffusion and solubility, leading to permeability values of no interest for packaging applications.

Author Contributions: G.F., D.F., R.R., M.A.O., S.C., L.P. conceived and designed the experiments, performed the experiments, analyzed the data, contributed reagents/materials/analysis tools; L.P., D.F., S.C. and M.A.O. wrote the paper."

Conflicts of Interest: The authors declare no conflict of interest.

6. References

Agrawal, A.M., Manek, R.V., Kolling, W.M., Neau, S.H., 2004. Water distribution studies within microcrystalline cellulose and chitosan using differential scanning calorimetry and dynamic vapor sorption analysis. J. Pharm. Sci. 93, 1766–1779.

Alamprese, C., Cappa, C., Ratti, S., Limbo, S., Signorelli, M. Fessas, D., Lucisano, M., 2017. Shelf life extension of whole-wheat breadsticks: Formulation and packaging strategies. Food Chem, 230, 532–539.

Ashiotis, G., Deschildre, A., Nawaz, Z., Wright, J.P., Karkoulis, D., Picca, F.E., Kieffer, J., 2015. The fast azimuthal integration python library: Pyfai. J Appl Crystallogr. 48, 510–519.

Aulin, C., Ahola, S., Josefsson, P., Nishino, T., Hirose, Y., Osterberg, M., Wagberg, L., 2009. Nanoscale cellulose films with different crystallinities and mesostructures-their surface properties and interaction with water. Langmuir. 25, 7675–7685.

Aulin, C., Gallstedt, M., Lindstrom, T., 2010. Oxygen and oil barrier properties of microfibrillated cellulose films and coatings. Cellulose. 17, 559–574.

Auras, R., Harte, B., Selke, S., 2004. Effect of water on the oxygen barrier properties of poly (ethylene terephthalate) and polylactide films. J. Appl. Polym. Sci. 92, 1790–1803.

Belbekhouche, S., Bras, J., Siqueira, G., Chappey, C., Lebrun, L., Khelifi, B., Marais, S., Dufresne, A., 2011. Water sorption behavior and gas barrier

properties of cellulose whiskers and microfibrils films. Carbohyd. Polym. 83, 1740–1748.

Biermann, C.J., 1996. Handbook of pulping and papermaking; Academic press: New York, USA.

Bikerman, J.J., 1967. Causes of poor adhesion: Weak boundary layers. Ind. Eng. Chem. 59, 40–44.

Clausen, P., Signorelli, M., Schreiber, A., Hughes, E., Plummer, C.J., Fessas, D., Schiraldi, A., Månson, J.-A.E., 2009. Equilibrium desorption isotherms of water, ethanol, ethyl acetate, and toluene on a sodium smectite clay. J. Therm. Anal. Calorim. 98, 833–841.

Crank, J., 1979. The mathematics of diffusion; Oxford university press: Oxford, UK.

Engelund, E.T., Thygesen, L.G., Svensson, S., Hill, C.A., 2013. A critical discussion of the physics of wood–water interactions. Wood Sci. Technol., 47, 141–161.

Fessas, D., Schiraldi, A., 2001. State diagrams of arabinoxylan-water binaries. Thermochim. Acta. 370, 83–89.

Fessas, D., Schiraldi, A., 2005. Water properties in wheat flour dough ii: Classical and knudsen thermogravimetry approach. Food Chem, 90, 61–68.

Fischer, H.E., Barnes, A.C., Salmon, P.S., 2005. Neutron and x-ray diffraction studies of liquids and glasses. Rep. Prog. Phys., 69, 233.

French, A.D., 2014. Idealized powder diffraction patterns for cellulose polymorphs. Cellulose. 21, 885–896.

Froix, M.F., Nelson, R., 1975. The interaction of water with cellulose from nuclear magnetic resonance relaxation times. Macromolecules, 8, 726–730.

Frounchi, M., Dourbash, A., 2009. Oxygen barrier properties of poly(ethylene terephthalate) nanocomposite films. Macromol. Mater. Eng. 294, 68–74.

Fukuya, M.N., Senoo, K., Kotera, M., Yoshimoto, M.; Sakata, O., 2014. Enhanced oxygen barrier property of poly(ethylene oxide) films crystallite-oriented by adding cellulose single nanofibers. Polymer. 55, 5843–5846.

Gardner, D.J., Oporto, G.S., Mills, R., Samir, M.A.S.A., 2008. Adhesion and surface issues in cellulose and nanocellulose. J. Adhes. Sci. Technol. 22, 545–567.

Gicquel, E., Martin, C., Yanez, J.G., Bras, J., 2017. Cellulose nanocrystals as new bio-based coating layer for improving fiber-based mechanical and barrier properties. J. Mater. Sci. 52, 3048–3061.

Guinault, A., Sollogoub, C., Ducruet, V., Domenek, S., 2012. Impact of crystallinity of poly (lactide) on helium and oxygen barrier properties. Eur. Polym. J. 48, 779–788.

Hernandez, R.J., Gavara, R., 1999. Plastics packaging: Methods for studying mass transfer interactions: A literature review, Pira International: Frankfurt, Germany.

Hodge, R., Edward, G.H., Simon, G.P., 1996. Water absorption and states of water in semicrystalline poly (vinyl alcohol) films. Polymer. 37, 1371–1376.

Howsmon, J.A., 1949. Water sorption and the poly-phase structure of cellulose fibers. Text. Res. J. 19, 152-162.

Ioelovich, M., Leykin, A., 2010. Study of sorption properties of cellulose and its derivatives. Bioresources. 6, 178–195.

Juhás, P., Davis, T., Farrow, C. L., & Billinge, S. J., 2013. PDFgetX3: a rapid and highly automatable program for processing powder diffraction data into total scattering pair distribution functions. *Journal of Applied Crystallography*, *46*(2), 560-566. Keen, D.A., 2001. A comparison of various commonly used correlation functions for describing total scattering. J Appl Crystallogr, 34, 172–177.

Knudsen, E.B., Sørensen, H.O., Wright, J.P., Goret, G., Kieffer, Fabio J., 2013. Easy access to two-dimensional x-ray detector images in python. J Appl Crystallogr. 46, 537–539.

Kohler, R., Alex, R., Brielmann, R., Ausperger, B., 2006. A new kinetic model for water sorption isotherms of cellulosic materials. Macromol. Symp. 244, 89–96.

Lagaron, J., Gimenez, E., Gavara, R., Saura, J., 2001. Study of the influence of water sorption in pure components and binary blends of high barrier ethylene–vinyl alcohol copolymer and amorphous polyamide and nylon-containing ionomer. Polymer, 42, 9531–9540.

Lee, D.S., Yam, K.L., Piergiovanni, L., 2008. Food packaging science and technology, CRC Press: Boca Raton.

Leung, A., Hrapovic, S., Lam, E., Liu, Y.L., Male, K.B., Mahmoud, K.A., Luong, J.H.T., 2011. Characteristics and properties of carboxylated cellulose nanocrystals prepared from a novel one-step procedure. Small. 7, 302–305.

Li, F., Biagioni, P., Bollani, M., Maccagnan, A., Piergiovanni, L., 2013. Multi-functional coating of cellulose nanocrystals for flexible packaging applications. Cellulose. 20,2491–2504.

Mascheroni, E., Rampazzo, R., Ortenzi, M.A., Piva, G., Bonetti, S., Piergiovanni, L., 2016. Comparison of cellulose nanocrystals obtained by sulfuric acid hydrolysis and ammonium persulfate, to be used as coating on flexible food-packaging materials. Cellulose. 23, 779–793.

Mazeau, K., Heux, L., 2003. Molecular dynamics simulations of bulk native crystalline and amorphous structures of cellulose. J. Phys. Chem. B. 107, 2394–2403.

Mihranyan, A., Llagostera, A.P., Karmhag, R., Strømme, M., Ek, R., 2004. Moisture sorption by cellulose powders of varying crystallinity. Int. J. Pharmaceut. 269, 433–442.

Minelli, M., Baschetti, M.G., Doghieri, F., Ankerfors, M., Lindström, T., Siró, I., Plackett, D., 2010. Investigation of mass transport properties of microfibrillated cellulose (mfc) films. J. Membr. Sci. 358, 67–75.

Mokwena, K.K., Tang, J., 2012. Ethylene vinyl alcohol: A review of barrier properties for packaging shelf stable foods. Crit. Rev. Food Sci. Nutr., 52, 640–650.

Nakamura, K., Hatakeyama, T., Hatakeyama, H., 1981. Studies on bound water of cellulose by differential scanning calorimetry. Text. Res. J., 51, 607–613.

Olsson, A.-M., Salmén, L., 2004. The association of water to cellulose and hemicellulose in paper examined by ftir spectroscopy. Carbohyd. Res. 339, 813–818.

Oswin, C., 1946. The kinetics of package life. Iii. The isotherm. J. Chem. Technol. Biotechnol. 65, 419–421.

Pani, P., Schiraldi, A., Signorelli, M., Fessas, D.,2010. Thermodynamic approach to osmo-dehydration. Food biophys. 5, 177–185.

Peemoeller, H., Sharp, A., 1985. Nmr study of cellulose-water systems: Water proton spin-lattice relaxation in the rotating reference frame. Polymer. 26, 859–864.

Ping, Z., Nguyen, Q., Chen, S., Zhou, J., Ding, Y., 2001. States of water in different hydrophilic polymers—dsc and ftir studies. Polymer, 42, 8461–8467.

Polyakova, A., Stepanov, E.V., Sekelik, D., Schiraldi, D.A., Hiltner, A., Baer, E., 2001. Effect of crystallization on oxygen-barrier properties of copolyesters based on ethylene terephthalate. J. Polym. Sci. Part B Polym. Phys. 39, 1911–1919.

Rampazzo, R., Alkan, D., Gazzotti, S., Ortenzi, M.A., Piva, G., Piergiovanni, L., 2017. Cellulose nanocrystals from lignocellulosic raw materials, for oxygen

barrier coatings on food packaging films. Packag. Technol. Sci., doi:10.1002/pts.2308.

Rietveld, H., 1969. A profile refinement method for nuclear and magnetic structures. J Appl Crystallogr, 2, 65–71.

Schiraldi, A., Signorelli, M., Fessas, D., 2013. Knudsen thermogravimetry approach to the thermodynamics of aqueous solutions. J. Chem. Thermodyn., 62, 79–85.

Tanaka, K., Naruse, H., Morikawa, H., Marumo, F., 1991. Phase-transition process of na2so4 (iii) to na2so4 (i) and anharmonic thermal vibration. Acta Crystallogr. Sect. B Struct. Sci. 47, 581–588.

Tsami, E., Marinos-Kouris, D., Maroulis, Z., 1990. Water sorption isotherms of raisins, currants, figs, prunes and apricots. J Food Sci, 55, 1594–1597.

Van den Berg, C. Vapour sorption equilibria and other water-starch interactions. PhD thesis, Wageningen University, Wageningen, The Netherlands, 1981.

Van den Berg, C., 1984. Description of water activity of foods for engineering purposes by means of the gab model of sorption. Eng. Food. 1, 321.

Villalobos, R., Hernández-Muñoz, P., Chiralt, A., 2006. Effect of surfactants on water sorption and barrier properties of hydroxypropyl methylcellulose films. Food Hydrocolloids. 20, 502–509.

Weinkauf, D.H., Paul, D.R., 1990. Effects of structural order on barrier properties. In Barrier polymers and structures, American Chemical Society: Washington, DC, USA. Volume 423, pp. 60–91.

Zachariasen, W., Ziegler, G., 1932. The crystal structure of anhydrous sodium sulfate na2so4. Z. für Kristallogr. Cryst. Mater. 81, 92–101.

Zografi, G., Kontny, M., Yang, A., Brenner, G., 1984. Surface area and water vapor sorption of macrocrystalline cellulose. Int. J. Pharmaceut. 18, 99–116

7. Figure captions page

8. Table captions page

II. Carbon dioxide diffusion at different relative humidity through coating of cellulose nanocrystals for food packaging applications

II. Carbon dioxide diffusion at different relative humidity through coating of cellulose nanocrystals for food packaging applications

Ghislain Fotie, Luana Amoroso[b], Giuseppe Muratore[b], Luciano Piergiovanni[a].*

[a]DeFENS, Department of Food, Environmental and Nutritional Sciences - PackLAB Università degli Studi di Milano, Via Celoria 2, 20133, Milan, Italy.

[b]Department of Agricultural, Food and Environment (Di3A), Università degli studi di Catania, Via Santa Sofia 100, 95123 Catania, Italy.

Abstract

In this paper, the investigation was focused on the CO_2 permeability through CNCs coating at various RH values, comparing with the O_2 one, aiming to evaluate the potential usage in all the applications of modified atmosphere packaging for intermediate-low moisture foods where the role of carbon dioxide is essential for shelf life extension. For this purpose, PET films were coated with characterized CNCs, obtained from cotton linters, and the CO_2 permeance was measured as a function of increasing RH values (from 0% to 80%). After calculating the diffusion and solubility coefficients, and estimating the CO_2/O_2 selectivity, the possible evolution of different modified atmospheres has been theoretically calculated. The results obtained, let hypothesize that, in consequence of a very high CO_2/O_2 permeability selectivity, the CNCs coated films can be useful in some modified atmosphere packaging applications, in a range of RH typical of many medium-high RH food products.

Keywords: cellulose nanocrystals; carbon dioxide barrier; moisture effects; modified atmosphere packaging.

1. Introduction

An intensive research and a general wide interest in the cellulose nanomaterials (CNM) have greatly increased over the last years, up to the point that the "ISO Technical Committee (ISO/TC 229) for Nanotechnologies" recently published a standard vocabulary, (ISO, 2017) for cellulose nanomaterials, whose indications are strictly followed in this paper. CNMs are anticipated to have significant commercial impact because for their renewable nature and unique properties. They are believed to have potential applications in a wide range of products including those that currently use non-renewable, oil-based materials or ingredients. In particular, the interest in possible packaging applications of cellulose nano-crystals (CNCs) and cellulose nano-fibrils (CNFs) is continuously and very rapidly growing all around the world (Hubbe et al., 2017; Johansson et al., 2012; Li et al., 2015; Rebouillat and Pla, 2013; Reig and Ballester, 2014; Riedl and Lacroix, 2014). In addition to the biodegradability and their origin in renewable sources, there is a strong interest in the potential for activating feasible paradigms of circular economy, related to the chance of producing CNCs and CNFs from cellulose-containing biomasses of food companies or by-products of packaging materials industries.

Actually, very attractive properties can be detected when the size of cellulose molecules is broken down into the nanoscale (Dufresne, 2017). Extraordinary gas barrier functionalities and improved mechanical properties, differently expressed by CNCs and CNFs, lead to very promising applications in bio-based flexible packaging and cellulosic materials for food products. The perspective of optimizing diffusional properties with the purpose of packaging material minimization and possible shelf life extension seems, in particular, a very interesting and current strategy for food packaging innovation, and for high sustainability targets. Several researches have been carried out on the gas barrier properties of cellulose nano-crystals and cellulose nano-fibrils (Aulin et al., 2010; Gicquel et al., 2017; Li et al., 2013; Minelli et al., 2010).

In all our previous works, which were carried out on CNCs, obtained from different raw materials and coated onto conventional and bio-based films for food packaging, we always found permeance values much lower than those of conventional synthetic barrier layers, even if very thin coatings were applied (less than 1 μm) (Fotie at al., 2017; Li et al., 2013a; Li et al., 2013b; Mascheroni et al., 2016; Rampazzo et al., 2017).

These peculiar and interesting barrier properties of CNCs coatings are not totally surprising, taking into account the main requirements for getting low gas permeability through polymers (Ashley, 1985; Freeman and Stewart, 2002; McKeen, 2017; Siracusa, 2012; Yam, 2010). In fact, it is well known that highly polar polymers have low gas permeability; having high cohesive energy and strong chain-to-chain attractions, their void volume is small and diffusional phenomena are limited (Salame, 1986) at low humidity. Cellulose can be defined a polar polymer since it has many polar oxygen–hydrogen (−OH) groups, with small differences in whatever crystalline forms (Gardiner & Sarko, 1985), even if net dipoles, i.e. a result of opposite charges, are absent.

Un-saturations which lead to a greater ease of chains rotation and consequently to high gas diffusion, are completely absent in cellulose molecules. Short lateral chains which hinder the close packing of macromolecules, increasing free volume and enhancing permeability, as well, are absent in the linear polymers such as cellulose. On the contrary, the crosslinking that restrains the segmental mobility of the polymer and makes the diffusion process slower is extensively possible due to the crystalline conformation of cellulose, through hydrogen bonds between chains alongside and intramolecular. The crystallinity degree that in whatever polymer leads to tortuous path in the diffusion pathway of permeants is always high in cellulose nanocrystals: depending on the different source and preparation process used, the crystallinity index reaches even 80-90% (McKeen, 2017). Finally, the glass transition temperature, which when higher than service temperature is consistent with very stiff chains and gives relatively better barrier properties,

is well above 200 °C in the cellulose biopolymers (Fakhraai et., 2005; Gajdoš et al., 2000).

All that is currently known about morphology and chemical properties of polymers, which positively affect high barrier performance, is noticeable in cellulose and, particularly in cellulose nano-crystals.

At the same time, however, it has been noted that the lack of intramolecular hydrogen bonding in the surface chains of cellulose makes possible extensive interactions with water molecules. Various studies dealing with these kind of phenomena showed that the water content and interactions with the material's components have a great influence on final properties of cellulosic materials (Engelund et al., 2013; Froix and Nelson, 1975; Ioelovich and Leykin, 2010). For more than 70 years, bulk amorphous regions have been indicated to be an ideal place for water adsorption, and the relationship between the availability of surface hydroxyl groups and crystallinity of cellulose is well established (Howsmon, 1949; Mihranyan et al., 2004).

The moisture sensitivity is a serious critical point for preserving the outstanding gas barrier properties of CNCs coatings, particularly if they are expected to be used in food packaging applications. Actually, we always observed a strong reduction of oxygen barrier properties at medium-high relative humidity values (Fotie et al., 2017; Rampazzo et al., 2017) and recently (Fotie et al., 2017), by a multidisciplinary approach, we tried to better understand the basics and the entity of water-cellulose nanocrystals interaction. Starting from about 40% of equilibrium relative humidity (RH), we assessed a 65% of freezable water in the CNCs and the XRPD (X-Ray Powder Diffraction) patterns gave clear indications of loss of structural coherence in the increasing of the RH values, and that the amorphous regions in the sample expanded at the expense of the crystalline part.

In this paper, the investigation was continued and focused on both the O_2 and CO_2 permeability of CNCs coatings at various relative humidity values. A

potential application for such a high barrier material is in fact, the modified atmosphere packaging of food products, where the role of carbon dioxide is essential for shelf life extension of perishable foods that have medium or high relative humidity values.

2. Materials and Methods

2.1. Materials

The cotton linters used for CNCs production were obtained from Innovhub (Milan, Italy), the chemical reagents were purchased from Sigma-Aldrich (Milan, Italy) and the 12 μm thick polyethylene terephthalate (PET) film, used as coating substrate, was achieved by Sapici spa (Cernusco sul Naviglio, Italy).

2.2. CNCs Obtainment and Coating Deposition

The Leung and co-workers' method was followed for the CNCs preparation, throughout the oxidative hydrolysis process by ammonium persulfate (APS) 1 molar, in the ratio APS (cm^3)/cotton linters (g) 100:1 (Leung et al., 2011). The yield of CNCs production (%) was calculated as the ratio of freeze-dried CNCs weight (g) and cellulosic content of 100g of raw materials. The steps of CNCs purification and the coating application on PET films, were followed as described in previous works (Mascheroni et al., 2016; Rampazzo et al., 2017); the coating suspension was a CNCs 4% (m/m), adjusted at pH 8 with NaOH 1M. For the thickness assessment of CNCs coating, a gravimetric method was used. After weighing 4 samples (M1, g) of 100 cm^2, the coating was washed out under hot water (~70 °C) and the resulting uncoated PET films were dried and weighed (M2, g). The coating thickness (L, cm) was estimated by equation (1): L= (M1-M2)/ (ρ× 100) (1)

where ρ = 1.58 g cm^{-3} is assumed as the density of the CNCs (Mazeau and Heux, 2003).

2.3. Characterization of CNCs morphology and coating uniformity

Either equivalent hydrodynamic diameters of the dispersed CNCs, and particle number distributions were determined by dynamic light scattering (DLS) measurements (mod. Litesizer500, Anton Paar, Graz, Austria). The measurements were performed at 25.0 ± 0.1 °C with a 35 mW laser diode light (λ = 658 nm) and collecting the scattered light at 15°and 90°. Prior to proceeding with the measurements, the samples were diluted at 3 different concentrations with distilled water adjusted to pH 8 and maintained at 25 °C through stirring until measurement. The diluted solutions were flowed in the measurement cell after 30 s homogenization by ultrasonic (UP 200St, Hielscher ultrasonics GMBH, Teltow, Germany) in a cool water bath to prevent overheating. The dimensions of the CNCs were next evaluated via Transmission Electron Microscopy (TEM). Drops of aqueous dispersions of CNCs (1%) were settled on carbon-coated electron microscope grids, negatively stained with uranyl acetate and left to dry. Samples were analysed with a Hitachi Jeol-10084 TEM operated (Brugherio, Italy) at an accelerating voltage of 80 kV.

Surface structure of the PET coated films was also evaluated by Atomic Force Microscope. Three different samples were measured with Tosca™400 AFM (Anton Paar, Graz, Austria) in tapping mode. Three randomly selected positions were measured for each sample. All images were recorded with the same scan size of 5 x 5 µm and resolution 500 x 500. Surface roughness (Sq, root mean square) has been calculated from AFM images following standard procedure (ISO 25178). The transparency of the CNCs coated PET was also measured at 550 nm, according to the ASTM D 1746-70, by means of a UV-VIS spectro-photometer (mod. L650, Perkin-Elmer, Milano, Italy). Each sample was replicated three times, analyzing at least four spots on each replicate.

2.4. CNCs Zeta potential and Conductivity.

Zeta potential (mV) and conductivity (mS cm^{-1}) of the CNCs in the diluted suspension at 3 different concentrations at pH 8 were performed by electrophoretic light scattering (ELS), using the PALS technology (mod. Litesizer 500, Anton Paar, Graz, Austria). Measures were replicated 5 times, at 25.0 ± 0.1 °C, by means of a 35 mW diode laser (λ = 658 nm) and at 15° detection angle.

2.5. O_2 and CO_2 Permeance at various Relative Humidities

Oxygen and Carbon dioxide permeance measures were performed by an isostatic permeabilimeter (mod. Multiperm, PERMTECH S.r.l., Pieve Fosciana, Italy) according to ASTM standard method D-3985. The gasses' permeance (P_G, cm^3 m^{-2} d^{-1} bar^{-1}) of CNCs coated and uncoated PET films were measured at 25 °C under 80%, 70%, 60%,40%, 20% and 0% RH on the coated side of the film, both increasing and decreasing the RH values for CO_2 and just increasing RH for O_2 and uncoated PET film. The CO_2 permeability coefficients at different RH ($KP_{CO2/CNCs}$, cm^3 μm m^{-2} d^{-1} bar^{-1}) of the CNCs coating alone were estimated from the average values of both increasing and decreasing RH, using equation (2) (Crank, 1979), and assuming that the PET surface did not interact with the CNCs coating layer of thickness L (μm) and considering that the interface PET-CNCs minimally affected the carbon dioxide permeation.

$$L / [KP_{CO2/CNCs} \text{ (CNCs coating)}] = [1 / P_{CO2} \text{ (coated PET film)}] - [1 / P_{CO2} \text{ (uncoated PET film)}] \quad (2)$$

From the isostatic CO_2 permeation curves obtained from the permeance measures, the apparent diffusion coefficients ($D_{CO2/CNCs}$, cm^2 s^{-1}) in the coating, at each RH value were evaluated by using this equation (3) (Hernandez & Gavara, 1999; Rampazzo et al., 2017):

$$D_{CO2/CNCs} = L^2 / (7.2 \times t_{(1/2)}) \quad (3)$$

where L is the thickness (cm) and $t_{(1/2)}$ (s) is the time required to reach half of the maximum permeance value. Actually, this lag-time was measured on the coated film, not on the coating alone. However, we know that the limiting factor for CO_2 permeation is the CNCs coating and assumed as meaningless the barrier contribution of the bare (uncoated) substrate. From eq. (2), in fact, we estimated that the CO_2 permeance of the uncoated PET is 125-1500 times higher than the coating (see Table 2). Therefore, we assumed eq. (3) as a reliable estimation of apparent CO_2 diffusion coefficient of the CNCs coating. From the permeability and diffusion coefficients ($KP_{CO2/CNCs}$ and $D_{CO2/CNCs}$), the gases solubility in the CNCs coating ($S_{CO2/CNCs}$, bar^{-1}) were also calculated at each RH value as follows (eq. 4):

$$S_{CO2/CNCs} = KP_{CO2/CNCs} / D_{CO2/CNCs} \qquad (4)$$

For determining the selectivity parameter (P_{CO2}/P_{O2}) at different RH values, the average permeance values obtained increasing and decreasing RH, were used.

3. Results and Discussion

3.1. CNCs Production and Coating onto PET Film

The cellulose nanocrystals obtained resulted very similar to the ones already described in previous works (Mascheroni et al., 2016; Rampazzo et al., 2017), for their morphological and main chemical characteristics, which are reported in Table 1 and in the TEM image of Figure 1a. The coating process, carried out with a 4% CNCs suspension in water at pH 8, were very similar as reported in previous papers. The roughness, assessed by AFM, and the transmittance measured at 550 nm, confirmed the uniformity of the CNCs layer coated onto the PET film, for a thickness lower than 1 μm. In Table 1 and in the AFM image of Figure 1b these results are summarized.

Hydrodynamic diameter (nm), by DLS	101.15 ± 3.65 (n=3)
Zeta potential (mV), by ELS	−44.40 ± 4.12 (n=3)
Conductivity (mS cm^{-1}), by ELS	0.095 ± 0.024(n=3)
Thickness of CNCs coating (nm)	756.3 ± 22.3 (n=3)
Transparency of the CNCs coated PET film (T% at 550 nm)	85.67 ± 0.3 (n=2)
Roughness of the CNCs coated PET film (Sq)	14.5±4.9 (n=9)

Table 1. Main characteristics of cellulose nanocrystals and CNCs coated PET film (± s.d.)
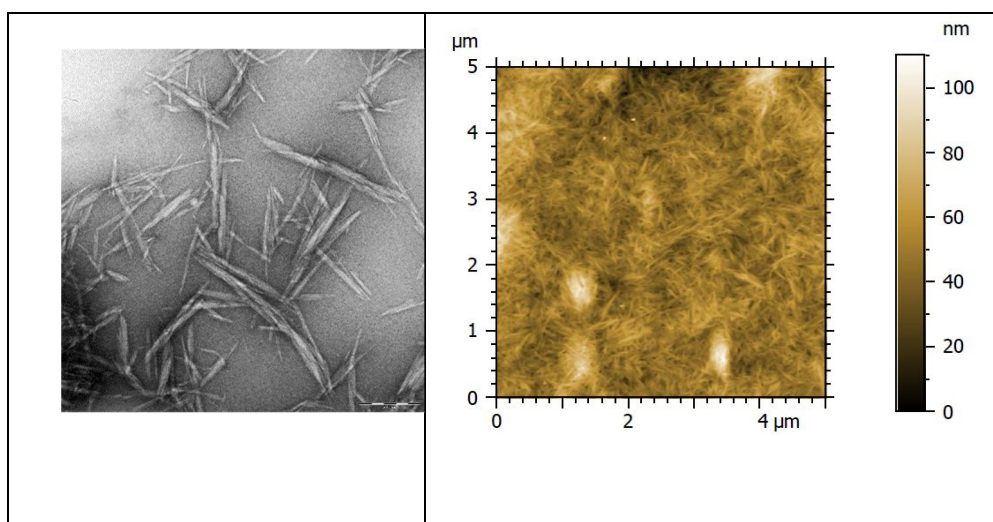
Figure 1. TEM picture of cellulose nanocrystals in the suspension used for coating (a) and AFM picture of the coating applied onto PET film (b)

3.2. O_2 and CO_2 Permeance of the coated film, at various Relative Humidities

The oxygen and carbon dioxide permeance of PET film, as a function of RH, is state of the art (Zhang et al., 2001; Auras et al., 2004). In our previous paper (Fotie et al. 2017) we have already shown the negligible differences, observed in measuring the oxygen permeance of the CNCs coated PET film, increasing

122

and decreasing the relative humidity. Therefore, in this case we assessed the carbon dioxide permeance, both increasing (ads) and decreasing (des) the RH value, for CNCs coated PET film only. The overall results are reported in Table 2, as average values $\pm$ standard deviation, and also in this case the permeance values in adsorption and desorption are quite similar, so in Figure 2 the global averages values are shown.

	0% RH	20% RH	40% RH	60% RH	70% RH	80% RH
Uncoated PET O_2 permeance (*ads*)	128.5* $\pm$ 6.4 (n=3)	123.4 $\pm$ 6.2 (n=3)	115.2 $\pm$ 5.8 (n=3)	109.7 $\pm$ 5.5 (n=3)	107.1 $\pm$ 5.4 (n=3)	104.9 $\pm$ 5.2 (n=3)
Uncoated PET CO_2 permeance (*ads*)	597.7 $\pm$ 29.9 (n=3)	541.1 $\pm$ 27.0 (n=3)	514.1 $\pm$ 25.7 (n=3)	500.0 $\pm$ 25.0 (n=3)	500.1 $\pm$ 25.0 (n=3)	501.1 $\pm$ 25.0 (n=3)
CNCs Coated PET O_2 permeance (*ads*)	0.38 $\pm$ 0.4 (n=2)	1.03 $\pm$ 0.07 (n=2)	2.05 $\pm$ 0.14 (n=2)	23.07 $\pm$ 3.1 (n=2)	56.41 $\pm$ 5.1 (n=2)	83.97 $\pm$ 2.9 (n=2)
CNCs Coated PET CO_2permeance (*ads*)	4,75$\pm$4.6 (n=3)	338,83 $\pm$ 152.1 (n=3)	474,53 $\pm$ 54.0 (n=3)	494,74 $\pm$ 14.8 (n=3)	494,2 $\pm$ 14.7 (n=3)	494,21 $\pm$ 13.4 (n=3)
CNCs Coated PET CO_2permeance (*des*)	4,82 $\pm$ 4.2 (n=3)	244,281 $\pm$ 73.5 (n=3)	480,68 $\pm$24.0 (n=3)	491,65 $\pm$14.7 (n=3)	492,10$\pm$ 12.8 (n=3)	494,21 $\pm$13.4 (n=3)

Table 2. Oxygen and Carbon dioxide permeance at 25 °C under different relative humidity (RH) values, through the CNCs-coated and uncoated PET film (cm^3 m^{-2} d^{-1} bar^{-1}, average $\pm$ s.d.) *(ads): increasing RH from 0 to 80 %; (des): decreasing RH from 80 to 0 %; * RH = 8%*
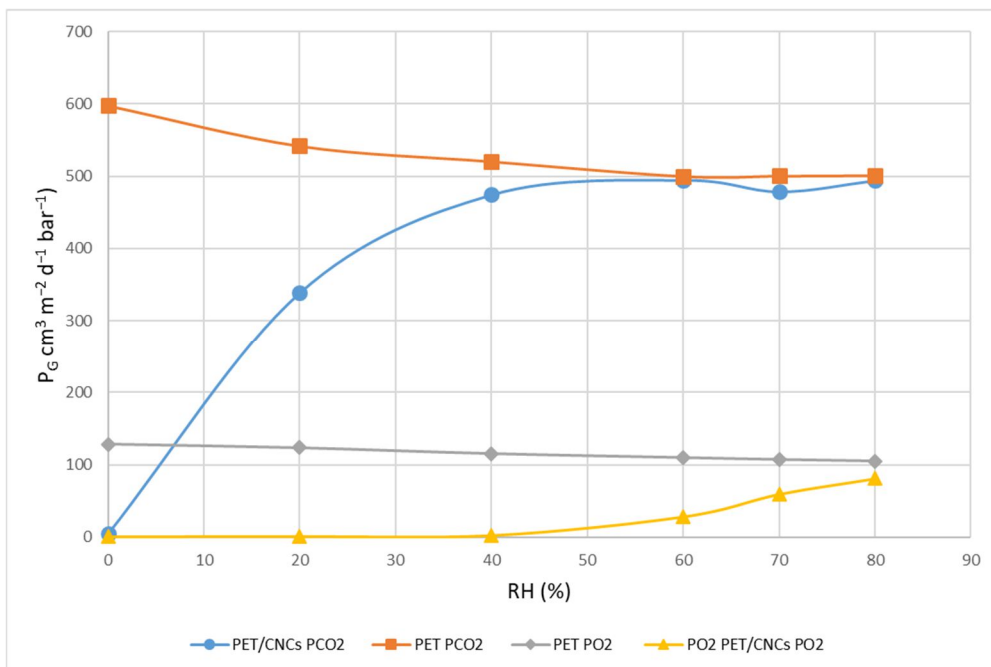
Figure 2. Global average values of O_2 and CO_2 permeability for CNCs-coated and uncoated PET film.

The carbon dioxide barrier of the CNCs coating decreases very greatly with increasing the relative humidity, much faster than the oxygen barrier. At around 50% RH the resistance to carbon dioxide permeance is meaningless and the permeance values is very close to the one of uncoated PET. The same phenomenon appears for oxygen just above 80% RH.

This unexpected and quite peculiar behaviour of CO_2 permeability throughout the cellulose nanocrystals coating, obviously affects the so-called "selectivity", the ratio between the permeance of CO_2 and O_2 (Van Krevelen and Nijenhuis, 2009), which increases more than 55 times from 0 to about 25% relative humidity, slowly decreasing thereafter, and going back to typical values (about 6-7) just for RH above 70%. This trend is reported in Figure 3, showing the peak in selectivity at approximately 25% RH.
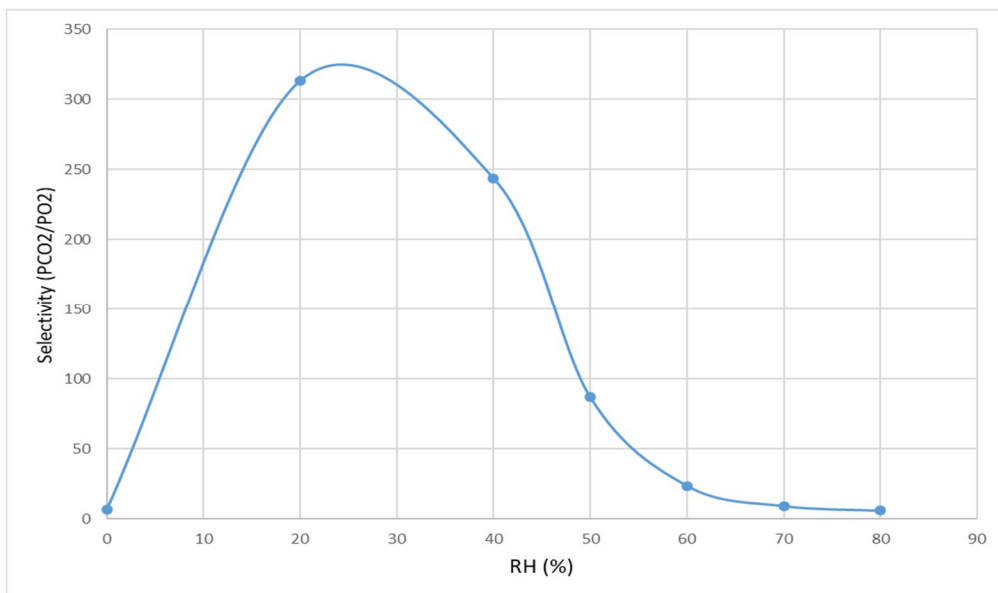
Figure 3. Trend of PCO2/PO2 ratio (selectivity) according to relative humidity

Herreraet al. (2014) investigatedvarious gases permeability and selectivity of cellulose nanocrystals films (layers) deposited by spin coating and obtained by acid hydrolysis using both sulphuric and hydrochloric acid. For the PCO_2/PO_2 ratio, they found values in the range 2.4 - 11.2, presumably at 0% RH (temperature and RH of measure not published).

In order to better understand the role of RH on the carbon dioxide transmission across the CNCs coating, and thereafter on selectivity, the permeability ($KP_{CO2/CNCs}$), diffusion ($D_{CO2/CNCs}$) and solubility ($S_{CO2/CNCs}$) apparent coefficients, in the cellulose nanocrystals thickness only, were assessed at relative humidity from 0 to 80%. According to the gas permeation theory, in fact, permeability is influenced by these two main factors: diffusion and solubility of gases, which are mostly related respectively to the crystallinity of the structure and to the nature of the gas (Barrer and Rideal 1939; Hernandez and Gavara 1999).

The related values are reported in Table 3 as average - standard deviation, while in Figures 4a and 4b, the trends of apparent diffusion and solubility coefficients (average values) are shown as function of RH values.
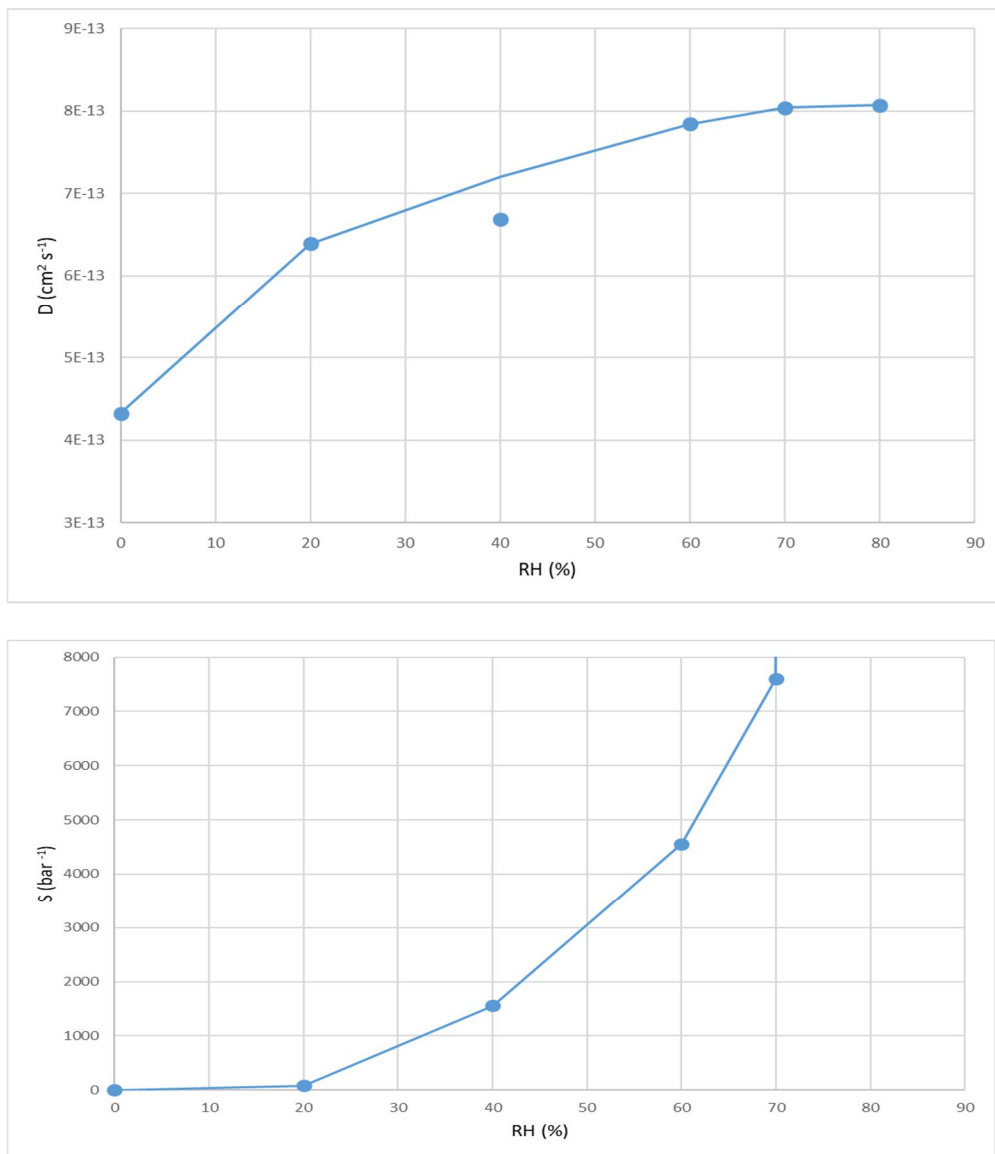
Figure 4. Trends of apparent diffusion (a) and solubility (b) coefficients of carbon dioxide in CNCs at 25°C, as function of RH values

	0% RH	20% RH	40% RH	60% RH	70% RH	80% RH
Apparent permeability coefficient ($KP_{CO2/CNCs}$, cm^3 µm m^{-2} d^{-1} bar^{-1})	3.18 ± 2.9 (n=6)	397.3 ± 272 (n=6)	10219 ± 8590 (n=6)	17141 ± 8234 (n=6)	20137 ± 10119 (n=6)	21663 ± 4814 (n=3)
Apparent diffusion coefficient ($D_{CO2/CNCs}$, cm^2 s^{-1})	4.32 E-13 ± 5.1 E-14 (n=6)	6.39 E-13 ± 1.1 E-13 (n=6)	6.69 E-13 ± 9.2 E-14 (n=6)	7.84 E-13 ± 1.6 E-14 (n=6)	8.04 E-13 ± 9.0 E-15 (n=6)	8.07 E-13 ± 6.2 E-15 (n=6)
Apparent solubility coefficient ($S_{CO2/CNCs}$, bar^{-1})	1.01 ± 0.9 (n=5)	78.2 ± 42.9 (n=5)	1555 ± 1070 (n=3)	4714 ± 3779 (n=5)	7596 ± 6717 (n=5)	219640 ± 236151(n=3)

Table 3. Permeability ($KP_{CO2/CNCs}$), diffusion ($D_{CO2/CNCs}$) and solubility ($S_{CO2/CNCs}$) apparent coefficients of carbon dioxide in the CNCs coating at 25 °C, under different relative humidity (RH) values.

From the overall data presented, is quite evident the huge increase in CO_2 permeability of CNCs layer, from 0 to 70-80% relative humidity. In the same range of RH values, diffusion and solubility show different trends: the increase of $D_{CO2/CNCs}$ is less than double and it seems to be terminated around 50-60 %RH, while the apparent solubility coefficient $S_{CO2/CNCs}$ increases more than 1000 times and in an exponential way approximately.

When the evaluation of gas permeability is performed on very hydrophilic coatings such as CNCs, in presence of the humidity, it is appropriate to

consider a three-dimensional interaction profile that is configured between water, cellulose nanocrystals and gas.

In the absence of water (0% RH), we only have the CNCs-gas interaction; therefore, it can be assumed that the permeance of CO_2 is faster than that of O_2, due to the smaller kinetic diameter (Mehio et al., 2014) and higher condensability of CO_2 which facilitate its transmission through any polymer; the value of common selectivity is around 6-7.In the presence of moisture, it can be hypothesized that there would be an interaction between the gas and water and between water and cellulose nanocrystals, i.e. the water could affect the CNCs structure.

At low humidity, since the CNCs shape has not yet been modified, a part of the water will occupy the free volume of the CNCs network, probably assuming a pH value close to the one at which the coating suspension has been dried (pH 8), and affecting the permeability due to the gas solubility in the media. Since the pH value, before coating, was adjusted with sodium hydroxide, it is reasonable to presume a residual of anions, able to affect the pH value of the media, even upon a small hydration. Increasing the RH value, we can assume that the water also swells the coating, increasing the distance among the nanocrystals chains and, progressively, changes and modifies the conformational organization of the crystalline network.

The observed increase in the apparent diffusion coefficient ($D_{CO2/CNCs}$) from 0 to 40-50% RH is consistent with this interpretation and might be related to a moderate and initial swelling of CNCs network, while the fast increase of apparent solubility $S_{CO2/CNCs}$ explains the very high value of the selectivity parameter. In fact, carbon dioxide is much more soluble in water than oxygen, especially at high pH values, leading to a very high permeability of CO_2. About this, it is advisable to report that the pH value of the CNCs suspension can be modulated in a certain range; therefore, this seems a useful chance for modulating permeability and selectivity of the coated film in real packaging applications.

The further increase of RH, however, is certainly related to a progressive loss of coherence of the structure, already observed in previous work (Fotie et al., 2017), which equally, and significantly affects both the O_2 and the CO_2 permeability that increase, reaching the PET permeability that acts as limiting factor and decreases the selectivity ratio to standard values of uncoated PET. In fact, at 50% RH for carbon dioxide and above 80% RH for oxygen, the gas barrier of CNCs coating is completely lost. It is worth noting, however, that the barrier properties of CNCs coating are always completely recovered by the drying phase of the coated film, without any defect in the original performance.

In any case, the opportunity of having such a high ratio between carbon dioxide and oxygen permeation, might be useful in many circumstances, where respiring or fermented or toasted food products are packaged. Although carbon dioxide is useful in various modified-atmosphere packaging applications, a residual CO_2 accumulation in some packages can be detrimental to the quality or the integrity of the package (Lee, 2016).

3.3. Modified atmosphere evolution modelling

Taking into account the potential interest in having such high selectivity values, the possible evolution of various modified atmospheres has been theoretically calculated. The volume concentrations (%) of oxygen, carbon dioxide and nitrogen were forecasted on the basis of gas volumes transmission expected, every 30 minutes, by the permeance data at 4 different relative humidity, and for 3 different atmospheres. All the variables taken into account for the computing are proposed in Table 4 (P_{N2} figures are estimations based on common selectivity values). The expected gas volumes transmission was estimated taking into account 600 cm^2 of permeable surface, 1L of initial unfilled volume (UFV) and the initial relative concentrations of oxygen, nitrogen and carbon dioxide, as from MAP_1, MAP_2 and MAP_3. We have also assumed that the gas volumes permeated inside the

ideal package did not change during time for phenomena different from permeability. By iterative calculation, the permeated amounts, new UFV value and corresponding gas concentrations every 30 minutes were accounted as follows:

$$UFV^n = \underline{\ }\ vO_2^n\underline{\ }\ vN_2^n\underline{\ }\ vCO_2^n - UFV^{n-1}$$

$$\%O_2^n = 100 \times (vO_2^n\underline{\ }\ vO_2^{n-1})/\ UFV^n$$

$$\%N_2^n = 100 \times (vN_2^n\underline{\ }\ vN_2^{n-1})/\ UFV^n$$

$$\%CO_2^n = 100 \times (vCO_2^n\underline{\ }\ vCO_2^{n-1})/\ UFV^n$$

Where vO_2^n, vN_2^n, vCO_2^n are the volumes of O_2, N_2 and CO_2, respectively, permeated in the time of iterative forecasting interval (30 minutes), positive (-) for gas volume permeated inside, while negative ($-$) for gas permeated outside. This theoretical-iterative approach was experimentally verified in a previous work (Piergiovanni et al., 1993).

In Figures 5 the speculative atmosphere changes are reported during a possible 24 hours' storage at 25 °C, assuming that the coating immediately equilibrates with the environmental humidity, and no interaction between the gases and a food product inside, take place during the storage time. The relative humidity values have been selected as central point of the common classes of intermediate (IMF, aw = 0.90 – 0.60), low moisture (LMF, aw = 0.60 – 0), and for dry foods (aw ≈ 0), while the three different modified atmospheres tested were representative of high (MAP$_1$), low carbon content (MAP$_3$), and assuming a possible residue of oxygen (MAP$_2$).

Permeable surface (cm^2)		600			
Unfilled volume (cm^3)		1000			
Time of iterative forecasting (min)		30			
MAP$_1$	CO_2(%)	60	**RH 0%**	P_{CO2}*	4.7
	O_2(%)	0		P_{O2}*	0.4
	N_2(%)	40		P_{N2}*	0.1
MAP$_2$	CO_2(%)	60	**RH35%**	P_{CO2}*	474
	O_2(%)	5		P_{O2}*	2.4
	N_2(%)	35		P_{N2}*	0.5
MAP$_3$	CO_2(%)	20	**RH70%**	P_{CO2}*	494
	O_2(%)	0		P_{O2}*	59.4
	N_2(%)	80		P_{N2}*	13.5

Table 4. Parameters used for forecasting the modified atmosphere evolution *(cm^3 m^{-2} d^{-1} bar^{-1}, at 25°C)
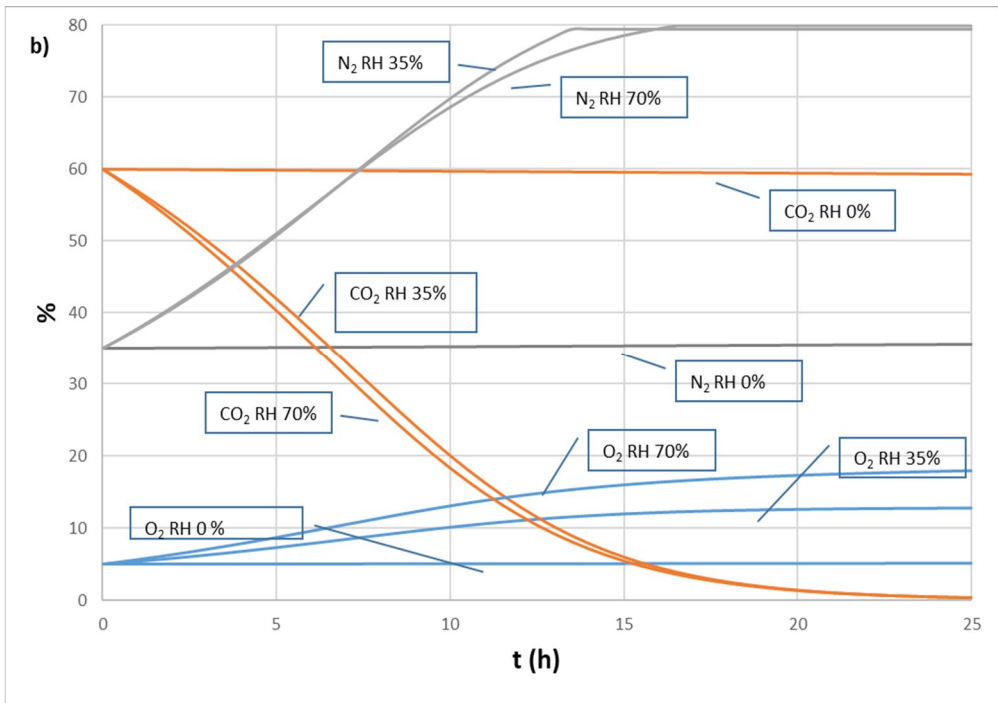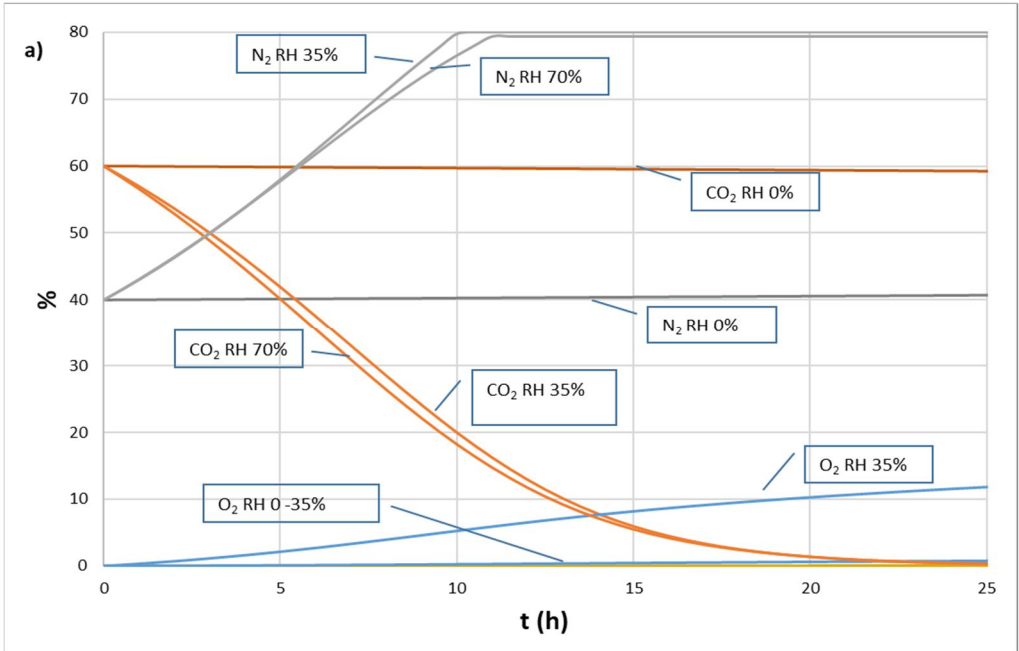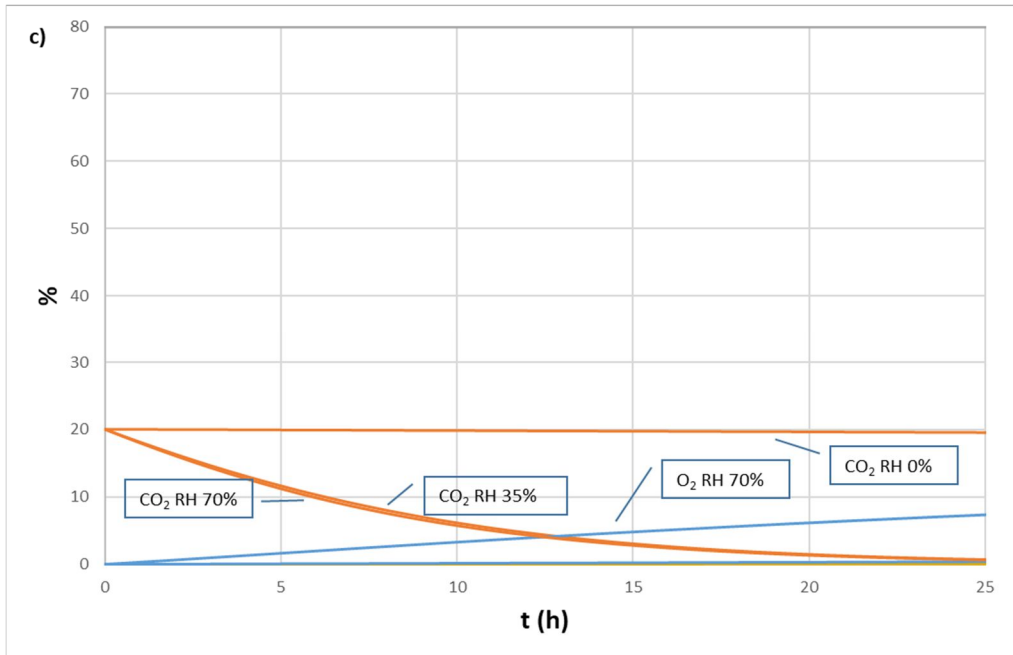
Figure 5. Theoretical evolution of three different modified atmospheres [a) MAP$_1$; b) MAP$_2$; c) MAP$_3$] compositions, according to different relative humidity values (0, 35 and 70% RH).

It is quite evident how selectivity can affect the modified atmosphere evolution, at different relative humidity and in different way depending on the atmosphere composition. The influence of the food relative humidity, as well as the environmental conditions, is thus quite important both for the carbon dioxide exit and for the oxygen entrance. These results, which need an experimental confirmation in real packaging applications or in reliable model systems, might be useful for a smart design of modified atmosphere food packaging applications, aimed at targeted shelf life for different food products.

4. Conclusions

A deep investigation on the oxygen and carbon dioxide permeability at different relative humidity values, revealed a huge sensitivity of the CO_2 diffusion through the cellulose nanocrystals coated onto a PET film, already at RH values around 20% and above. Increasing the relative humidity, the

carbon dioxide permeance greatly increased, much more than oxygen permeance and well before any indication of loss of structural coherence of the CNCs layer. Because of this behaviour, the permeability selectivity (the ratio of CO_2 and O_2 permeance) reached very, very high values in a range of RH, which are typical of many low and intermediate moisture food products. The solubility of CO_2 and the pH of the coating used, have been assumed as the main explications of this unexpected behaviour of the coated film. The carbon dioxide solubility, in particular, is strongly dependent on the pH of permeated matrix and the pH of the coating preparations is adjustable in a certain range, evoking a potential tool for O_2/CO_2 selectivity and CO_2 permeance design. This lead to the hypothesis that such CNCs coated films can be useful in some active or passive modified atmosphere packaging applications. Several commodities, like fruits, lettuce, potato, artichoke and many others are sensitive to relatively low CO_2 concentrations, leading to symptoms of CO_2 injury, including off-flavour development, discoloration and internal tissue breakdown. In such cases, as well as for some fermented or toasted products, the application of a CNCs coatings may be beneficial for preserving the food quality.

5. Acknowledgements

6. References

Ashley, R. J., 1985. Permeability and plastics packaging. *Polymer Permeability*; Comyn, J., Ed.; Springer: Dordrecht, The Netherlands, 269–308.

Aulin, C., Gallstedt, M., Lindstrom, T., 2010. Oxygen and oil barrier properties of microfibrillated cellulose films and coatings. *Cellulose*, 17, 559–574.

Auras, R., Harte, B., Selke, S., 2004 Effect of water on the oxygen barrier properties of poly(ethylene terephthalate) and polylactide films. *Journal of Applied Polymer Science*, 92, 1790-1803.

Barrer, R. M., Rideal, E. K., 1939. Permeation, diffusion and solution of gases in organic polymers. *Transaction of the Faraday Society*, 35, 628.
Crank, J. 1979. The Mathematics of Diffusion; Oxford University Press: Oxford, UK.

Dhoot, S. N., Freeman, B. D., Stewart, M. E., 2002. Barrier Polymers. *Encyclopedia of Polymer Science and Technology*. John Wiley & Sons, Inc.
Dufresne, A., 2017 Nanocellulose: From Nature to High Performance Tailored Materials. De Gruyter GmbH.

Engelund, E. T., Thygesen, L. G., Svensson, S., Hill, C. A., 2013. A critical discussion of the physics of wood–water interactions. *Wood Science and Technology*, 47, 141–161.

Fakhraai, Z., Valadkhan, S., Forrest, J. A., 2005. Qualitative discrepancy between different measures of dynamics in thin polymer films. *The European Physical Journal E – Soft Matter and Biological Physics*, 18 (2), 143-148.

Fotie, G., Rampazzo, R., Ortenzi, M., Checchia, S., Fessas, D., Piergiovanni, L., 2017. The Effect of Moisture on Cellulose Nanocrystals Intended as a High Gas Barrier Coating on Flexible Packaging Materials. *Polymers,* 9, 415.

Froix, M. F. Nelson, R., 1975. The interaction of water with cellulose from nuclear magnetic resonance relaxation times. *Macromolecules*, 8, 726–730.

Gajdoš, J., Galić, K., Kurtanjek, Ž., Ciković, N., 2000. Gas permeability and DSC characteristics of polymers used in food packaging. *Polymer Testing*, 20, 49-57.

Gardiner, E. S., Sarko, A., 1985. Packing analysis of carbohydrates and polysaccharides. 16. The crystal structures of celluloses IV_I and IV_{II}. *Canadian Journal of Chemistry*, 63, 173-180.

Gicquel, E., Martin, C., Yanez, J. G., Bras, J., 2017. Cellulose nanocrystals as new bio-based coating layer for improving fiber-based mechanical and barrier properties. *Journal* of *Materials Science,* 52, 3048–3061.

Hernandez, R. J., Gavara, R., 1999. Plastics Packaging: Methods for Studying Mass Transfer Interactions: a Literature Review. Pira International: Frankfurt, Germany.

Herrera, M. A., Mathew A. P., Oksman, K., 2014. Gas permeability and selectivity of cellulose nanocrystals films (layers) deposited by spin coating. *Carbohydrate Polymers*, 112, 494-501.

Howsmon, J. A., 1949. Water sorption and the poly-phase structure of cellulose fibers. *Textile Research Journal,* 19, 152–162.

Hubbe, M. A., Ferrer, A., Tyagi, P., Yin, Y., Salas, C., Pal, L., Rojas, O. J., 2017. Nanocellulose in Thin Films, Coatings, and Plies for Packaging Applications: A Review. *BioResources*, 12(1), 2143-2233.

Ioelovich, M., & Leykin, A., 2010. Study of sorption properties of cellulose and its derivatives. *Bioresources*, 6, 178–195.

ISO B., 2017. ISO/TS 20477. Cellulose nanomaterials - Standard terms and their definition for cellulose nanomaterial.

ISO, B., 2012. 25178–2: Geometric Product Specification, Surface Texture (Areal). Part 2: Terms, Definitions and Surface Texture Parameters. *British Standards Institute: London, UK*.

Johansson, C., Bras, J., Mondragon, I., Nechita, P., Plackett, D., Simon, P., Svetec, D. G., Virtanen, S., Baschetti, M. G., Breen, C., Clegg, F., Aucejo, S., 2012. Renewable Fibers and Bio-Based Materials for Packaging Applications: a Review of Recent Developments. *Bioresources*, 7(2), 2506-2552.

Khan, A., Huq, T., Khan, R. A., Riedl, B., Lacroix, M., 2014 Nanocellulose-Based Composites and Bioactive Agents for Food Packaging. *Critical Reviews in Food Science and Nutrition*, 54 (2), 163-174.

Lee, D. S., 2016. Carbon dioxide absorbers for Food Packaging Applications. *Trends in Food Science & Technology*, 57, 146-155.

Li, F., Biagioni, P., Bollani, M., Maccagnan, A. Piergiovanni, L.,2013a. Multi-functional coating of cellulose nanocrystals for flexible packaging applications. *Cellulose*, 20, 2491–2504.

Li, F., Biagioni, P., Finazzi, M., Tavazzi, S., Piergiovanni, L., 2013b. Tunable green oxygen barrier through layer-by-layer self-assembly of chitosan and cellulose nanocrystals *Carbohydrate Polymers*, 92,2128-2134.

Li, F., Mascheroni, E., Piergiovanni, L., 2015. The Potential of NanoCellulose in the Packaging Field: A Review. *Packaging Technology and Science*, 28 , 475-508.

Mascheroni, E., Rampazzo, R., Ortenzi, M. A., Piva, G., Bonetti, S., Piergiovanni, L., 2016. Comparison of cellulose nanocrystals obtained by sulfuric acid hydrolysis and ammonium persulfate, to be used as coating on flexible food-packaging materials. *Cellulose*, 23, 779-793.

Mazeau, K., Heux L., 2003. Molecular Dynamics Simulations of Bulk Native Crystalline and Amorphous Structures of Cellulose. *The Journal of Physical Chemistry*, 107 (10), 2394–2403.

McKeen, L. W., 2017. Introduction to Plastics and Polymers. *Permeability Properties of Plastics and Elastomers* (Fourth Edition). William Andrew Publishing, 21-40.

Mehio, N., Dai, S., Jiang, D., 2014. Quantum Mechanical Basis for Kinetic Diameters of Small Gaseous Molecules. *The Journal of Physical Chemistry A,* 118 *(6),* 1150-1154.

Mihranyan, A., Llagostera, A. P., Karmhag, R., Strømme, M., Ek, R.,2004. Moisture sorption by cellulose powders of varying crystallinity*. International Journal of Pharmaceutics*, 269, 433–442.

Minelli, M., Baschetti, M. G., Doghieri, F., Ankerfors, M., Lindström, T., Siró, I., Plackett, D.,2010. Investigation of mass transport properties of microfibrillated cellulose (mfc) films. *Journal of. Membrane Science*, 358, 67–75.

Piergiovanni, L., Fava, P., Moro, M., 1993. Shelf-life extension of Taleggio cheese by modified atmosphere packaging. *Italian journal of food science,* 5(2), 115-127.

Rampazzo, R., Alkan, D., Gazzotti, S., Ortenzi, M. A., Piva, G. Piergiovanni, L., 2017. Cellulose Nanocrystals from Lignocellulosic Raw Materials, for Oxygen Barrier Coatings on Food Packaging Films. *Packaging Technology and Science*, 30, 645-661.

Rebouillat, S, Pla, F., 2013. State of the Art Manufacturing and Engineering of Nanocellulose: A Review of Available Data and Industrial Applications. *Journal of Biomaterials and Nanobiotechnology*, 4, 165-188.

Reig, C.S., Lopez, A. D., Ramos, M. H., Ballester, V. A. C., 2014. Nanomaterials: a Map for Their Selection in Food Packaging Applications. *Packaging Technology and Science*, 27, 839–866.

Salame, M., 1986. Prediction of gas barrier properties of high polymers. *Polymer Engineering & Science,* 26, 1543-1546.

Siracusa, V., 2012. Food Packaging Permeability Behaviour: A Report. *International Journal of Polymer Science,*1687-9422.

Van Krevelen, D. W., Nijenhuis, K., 2009. Properties of polymers - Their correlation with chemical structure; their numerical estimation and prediction from additive group contributions (4th ed.). Elsevier, Netherlands, Chapter 18.

Yam, K. L., 2010. The Wiley Encyclopedia of Packaging Technology. Wiley & Sons, Inc., New York, 103: 109.

Zhang, Z., Britt, I. J.,Tung, M. A., 2001. Permeation of oxygen and water vapor through EVOH films as influenced by relative humidity. *Journal of Applied Polymer Science*, 82.

7. Figure captions page

8. Table captions

III. Green functionalization and characterization of cellulose nanocrystals

III. Green functionalization and characterization of cellulose nanocrystals

Abstract

The functionalization of the cellulose nanocrystals occurred by adsorption and esterification forming non-covalent and covalent bonds on the CNCs surface through the grafting of chemical coumpounds. A reported method called Solreact was used for a solvent-free esterification of cellulose nanocrystals by using citric and sorbic acids which acted not only as a grafting agent but also as a solvent during the covalent grafting process. The esterification of the CNCs was driven by the in-situ solvent exchange by water evaporation.
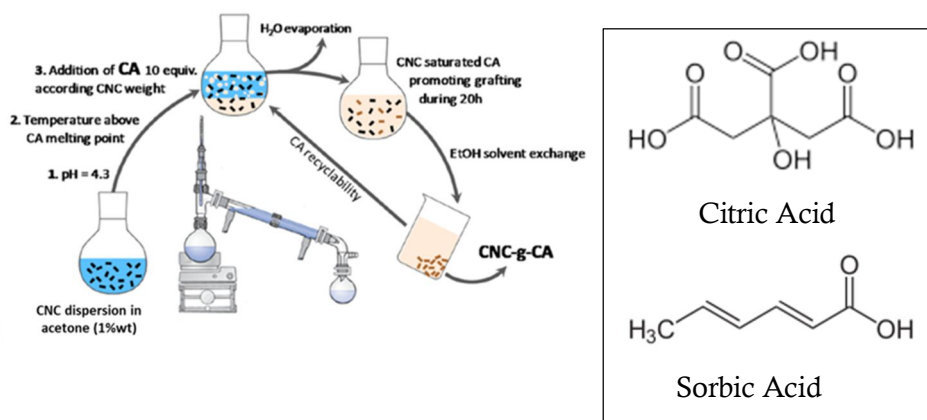
Figure 1. Esterification of cellulose nanocristals with citric and sorbic acid by solreact technique.

Through the characterization of modified CNCs, FTIR analysis revealed the ester groups formed on the CNCs after the adsorption and esterification which confirmed the effectiveness of the functionalization. Oxygen permeability of coated plastic films with modified and unmodified CNCs were assessed as well.

1. Introduction

In recent years, nanocellulose (nanocrystals of cellulose and cellulose nanofibrillated) has garnered a lot of scientists' attention all over the world. This interest in nanocellulose is related to its exceptional and unique properties that could find applications in various sectors (automotive, aeronautics, packaging) (Kim et al., 2015). In fact, the nanocellulose derives from the hydrolysis of cellulose since, is the most abundant natural polymer on the planet (Dufresne et al., 2013). Cellulose is made up of chains of glucose units connected by 1-4 beta-glucoside bonds sand with a structure made of amorphous and crystalline regions. That crystalline part when isolated, has a rod-like shape and more importantly, displays an extraordinary barrier to gases (O_2, CO_2...) and grease and improved mechanical properties (rigidity and tensile strength) when a very thin layer of it is coated onto plastic films (Li et al., 2013). Furthermore, the nanocellulose is biodegradable-biocompostable, renewable and moreover it can be extracted from natural matrices (cotton linter, wood pulp...) and by-products (soy hulls, rice husks, etc). Nowadays, an "ideal food package" must tie all the criteria required for food quality and safety in a fair manner, meeting concomitantly environmental and safety requirements in a circular economy (Geissdoerfer et al., 2017). However, the hydrophilic nature of the CNCs is an obstacle for their incorporation in complex matrices containing hydrophobic materials and also hampers their use as fillers for polymer nanocomposites (Oksman et al., 2006). The humid ambient provokes the conformational change of the crystalline network of the CNCs which is detrimental to gas barrier and mechanical properties (Fotie et al., 2017). One of the effective strategies to alleviate the effect of the humidity on the CNCs organization is that to resort to the functionalization. Recently, it was reported several successful attempts of modifications such as adsorption of single molecules, covalent grafting of molecules, covalent grafting of chain of polymers on the cellulose nanocrystals surface. The adsorption can be electrostatic interaction

(Kaboorani and Riedl, 2015) or interaction by affinity of surfactants (OH…OH) (Tardy et al., 2017). The covalent grafting of single molecules can be esterification, silylation, isocyanate derivatives coupling and succinic anhydride (Braun and Dorgan, 2008; Braun et al., 2012, Pei et al., 2010, Siqueira et al., 2009); moreover, the covalent grafting of polymers chain can occur through radical and ring opening polymerization (Habibi et al., 2008). In this chapter, it was demonstrated the possibility of using food additives for novel functionalizationto confer a hydrophobic character to the CNCs surface through esterification and adsorption while keeping the integrity of their crystalline core in the strict consideration of the 12 principles of green chemistry (Poliakoff et al., 2002).

2. Materials and Methods

Preparation and production of cellulose nanocrystals (CNCs)

CNCs used in my work were wood-based CNCs (-OH and –SO_3H content) provided by the Canadian company called CelluForce. Glycerol monostearate, citric and sorbic acids, ethanol were all bought from Sigma Aldrich, France.

Modification by adsorption onto cellulose nanocrystals surface

3g of wood CNCs and 3g of GMS were added in ethanol at 3 wt% and the latter solution was brought at pH 7then stirred at room temperature for 3h. As the reaction takes place, GMS particles are adsorbed on the CNCs surface irreversibly. Afterwards, the residual part of GMS was washed out in ethanol at 30°Cx15 min and 10000 rpm for 4 times and the purified GMS-CNCs were obtained.

Modification by esterification of cellulose nanocrystals surface

The method called Solreact was used for a solvent-free esterification of cellulose nanocrystals by using citric and sorbic acid not only as a grafting agent above their melting point. Sol-react technique was performed with

wood-based CNCs and citric-sorbic acid (CNCs-Cit-Sorb). 3g of wood CNCs were dispersed in 100 mL of water (Sonication 2min, 50%, 5) in a 500mL round-bottom flask and the pH was adjusted to 4. After, the solution was heated and maintained at 150°C under hot oil bath then, 31g of sorbic acid and 53g of citric acid were added in the dispersed CNCs and placed in the distillation system for promoting the chemical absorption. The latter solution was stirred for 8 hours, and the water evaporated. At the end of the reaction, the product obtained was purified from unreacted acid by 5 times dispersion-centrifugation with a large excess of ethanol (10000 rpm, 30°C, 15').

CNCs Hydrodynamic diameter and Z potential-conductivity

Hydrodynamic diameter of the dispersed CNCs was determined by dynamic light scattering (DLS) measurements (mod. Litesizer500, Anton Paar, Graz, Austria). The measurements were assessed at 25.0 ± 0.1 °C with a 35 mW laser diode light (λ = 658 nm) and collecting the scattered light at 15°and 90°. Before any measurements, the samples were diluted at 3 different concentrations with distilled water adjusted to pH 8 and maintained at 25 °C. Zeta potential (mV) and conductivity (mS cm-1) of the CNCs in the diluted suspension at 3 different concentrations at pH 8 were performed by electrophoretic light scattering (ELS), using the PALS technology (mod. Litesizer 500, Anton Paar, Graz, Austria). Data were obtained through 5 time-replication, at 25.0 ± 0.1 °C, by means of a 35 mW diode laser (λ = 658 nm) and at 15° detection angle. Contact angle assessment of coated PLA with CNCs Static contact angles of the coated film were determined after the conditioning of the CNCs coated PLAfilms at 30°C. The sessile drop method was used by precisely dropping a droplet of 4.0 ± 0.5 μL of water onto the film. The measurements were performed at room temperature (RH about 40%) on five different positions for each sample. The instrument used was an OCA 15 Plus angle goniometer (Data Physics Instruments GmbH, Filderstadt, Germany), equipped with a high-resolution CCD camera, a high performance digitizing adapter (Data Physics Instruments GmbH, Filderstadt, Germany)

and SCA20 software (Data Physics Instruments GmbH, Filderstadt, Germany) for contact angle measurements.

FTIR spectroscopy analysis

FTIR spectroscopy was performed on oven-dried CNCs by Perkin Elmer 264 instrument (Spectrum 100), equipped with ATR, at room temperature. The data were collected over 64 scans with a resolution of 4 cm^{-1}.

Elemental analysis

Elemental analysis was carried out by the "service Central d'Analyse of the "Centre Ntional de la Recherché Scientifique" (Vernaison, France). Carbon, hydrogen and oxygen contents of modified and unmodified CNCs were evaluated with the precision of the measurement higher than the standard deviation, therefore, it is ± 0.2 wt% at maximum. From the collected data, the degree of the substitution that corresponds to the number of grafted hydroxyl groups per glucose unit was calculated by the following equation:

$$DS = \frac{\text{Cglu} - \text{Xc} * \text{PMglu}}{PMglu * Ca - Cca}$$

Where Cglu is the carbon mass of 1 glucose unit (72g/mol) and PM glu is the total mass of the carboxylic acid (162 g/mol), Ca is total mass of the carboxylic acid and Cca is the carbon mass of the carboxylic acid. The analyses were performed twice to obtain the average result.

Assessment of the CNCs coatings thickness

The thickness of the coating applied onto the film was assessed by a gravimetric method. Four samples (10 ×10 cm2) were weighed (m1, g), then the coating was removed by running hot water (~70 °C) and the resulting

uncoated film was dried and weighed (m2, g). The coating thickness (L, cm) was estimated by Equation (1): L = Δm/ (ρ × 100),

Where ρ = 1.58 g cm-3 is assumed as the density of the CNCs and Δm=m1-m2.

O$_2$ and WVTR permeability measurements

Both oxygen and water vapor permeabilities were performed by an isostatic permeabilimeter (mod. Multiperm, PERMTECH S.r.l., Pieve Fosciana, Italy) according to ASTM standard methods (D-3985 and F-1249 respectively). The oxygen and water permeation of coated and uncoated PLA films were measured at 25 °C and 50 & 80% RH.

3. Results and discussion

FTIR spectra of modified and neat CNCs

The FTIR results are illustrated by the graph 1 and the proof of the chemical modification is easily identifiable with the presence of ester groups (-COOR) at the peak of wavelength 1746.21 cm^{-1}
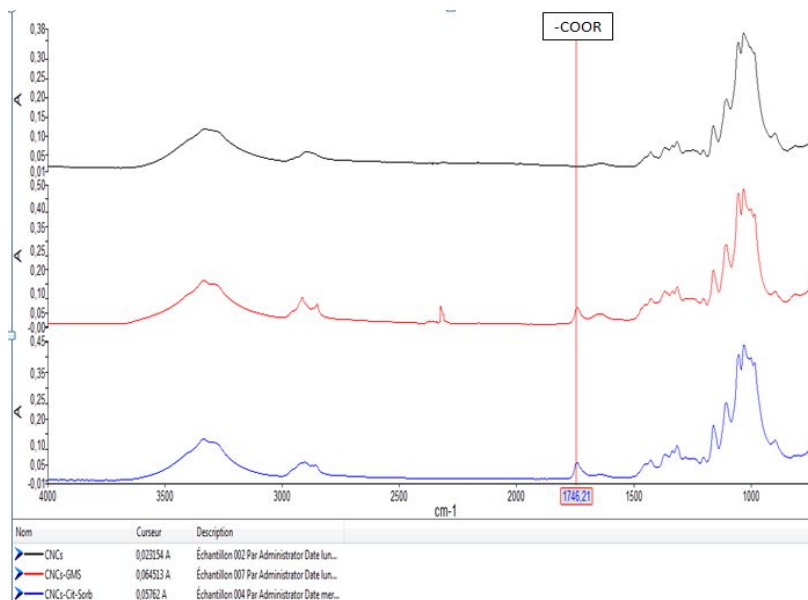
Figure 2. FTIR spectra of neat and modified cellulose nanocrystals

FTIR spectra of CNCs clearly show the typical absorption band of ester groups for modified CNCs (CNCs-GMS and CNCs-Cit-Sorb), which is absent in the standard CNCs spectra. The peak recognizable in the inset of graph 1 is referable, according to Lam (Lam et al. 2013), to C=O stretching peaks of the ester group (1746.21 cm-1).

Hydrodynamic diameter and z-potential

The table shows similar values of the hydrodynamic diameter however; their respective z-potential is different from each other. The Z potential of the neat CNCs (unmodified) is much higher because of the negative charges called sulfate half esters (-SO3H) groups present on their surface while modified CNCs have a part of their negative charges occupied (covered) by grafting compounds and that justifies the reduction in the absolute Z potential.

Cellulose nanocrystals	Hydrodynamic diameter (µm)	Z-potential (mV)	Conductivity (mS cm^{-1})
Wood CNCs(unmodified)	0.28±0.01	-45±1.2	0.07±0.01
CNCs-GMS(modified)	0.22±0.08	-38±1.1	0.24±0.03
CNCs-Cit-Sorb(modified)	0.25±0.06	-25±1.1	0.14±0.03

Table 1. Hydrodynamic diameter, Z potential and conductivity of unmodified and modified CNCs

Elemental Analysis

After the esterification of the cellulose nanocrystals with citric acid and sorbic acid, the % of the sulfur (S) decreased because of the occupation of its site

by the grafting structure. That is another proof of the effectiveness of the functionalization.

Atoms	Neat CNCs	CNCs-Cit-Sorb
C	39.77%	41.4%
O	50.48%	50.12%
H	6.29%	6.13%
S	0.80%	< 0.20%

Table 2. Percentage of atoms (C, O, H, S) in unmodified and modified CNCs

The table 2 below shows the oxygen and water permeabilities results performed on coated-CNCs (neat and modified) PLA at 25°C in 2 different relative humidities (RH). The automatic coating was performed by the green bar to provide 1µm thickness of 2.8 wt% CNCs onto the corona-treated PLA polymers (25 µm thick).

Oxygen and water vapor transmission rate of coated PLA film

RH (%)	PO_2 (cm^3 m^{-2} d^{-1} bar^{-1})			WVTR(g m^2 d^{-1})		
	PLA-CNCs	PLA-CNCs-GMS	PLA-CNCs-Cit-Sorb	PLA-CNCs	PLA-CNCs-GMS	PLA-CNCs-Cit-Sorb
50	279.6±5.2	359.10±2.2	178.8±2.1	32.01±2	33.7±2	31.4±1.2
80	519±4	508.94±3.4	478.1±3.2	62.2±3.1	65.2±1.	61.49±1.2

Table 3. Water vapor transmission rate and oxygen permeability of coated and uncoated PLA film

After the esterification, coated polymers with esterified CNCs resulted to be improved in oxygen barrier at around 40% but the WVTR did not gain any improvements. Modified CNCs obtained by the adsorption of GMS did not obtain higher gas barrier on PLA in comparison with the unmodified ones.

Grammage and water contact angle of coated PLA

The water contact angle slightly increased in PLA films coated with modified CNCs, about 40% increase for both types of modified CNCs compared to the neat ones.

Coated and uncoated PLA	PLA Thickness (μm)	Coating deposition (g/m²)	CNCs concentration solution (%)	Water contact angle (°)
PLA	25	-	-	74±2
PLA-CNCs-GMS	25	1	2.8	17±1
PLA-CNCs-Cit-Sorb	25	1	2.8	14±1
PLA-CNCS	25	1	2.8	8.8±1.1

Table 4. Water contact angle and grammage of uncoated and coated PLA film

4. Conclusions

From the data, the chemical modifications of the cellulose nanocrystals through adsorption and esterification were successfully implemented and the oxygen barrier properties were significantly improved for polymers coated with modified cellulose nanocrystals (CNCs-Cit-Sorb).

5. References

Braun, B. and Dorgan, J.R., 2008. Single-step method for the isolation and surface functionalization of cellulosic nanowhiskers. *Biomacromolecules*, *10*(2), pp.334-341.

Braun, B., Dorgan, J.R. and Hollingsworth, L.O., 2012. Supra-molecular ecobionanocomposites based on polylactide and cellulosic nanowhiskers: synthesis and properties. *Biomacromolecules*, *13*(7), pp.2013-2019.

Dufresne, A., 2013. Nanocellulose: a new ageless bionanomaterial. *Materials today*, *16*(6), pp.220-227.

Fotie, G., Rampazzo, R., Ortenzi, M., Checchia, S., Fessas, D. and Piergiovanni, L., 2017. The effect of moisture on cellulose nanocrystals intended as a high gas barrier coating on flexible packaging materials. *Polymers*, *9*(9), p.415.

Geissdoerfer, M., Savaget, P., Bocken, N.M. and Hultink, E.J., 2017. The Circular Economy–A new sustainability paradigm? *Journal of cleaner production*, *143*, pp.757-768.

Habibi, Y., Goffin, A.L., Schiltz, N., Duquesne, E., Dubois, P. and Dufresne, A., 2008. Bionanocomposites based on poly (ε-caprolactone)-grafted cellulose nanocrystals by ring-opening polymerization. *Journal of Materials Chemistry*, *18*(41), pp.5002-5010.

Kaboorani, A. and Riedl, B., 2015. Surface modification of cellulose nanocrystals (CNC) by a cationic surfactant. *Industrial Crops and Products*, *65*, pp.45-55.

Kim, J.H., Shim, B.S., Kim, H.S., Lee, Y.J., Min, S.K., Jang, D., Abas, Z. and Kim, J., 2015. Review of nanocellulose for sustainable future materials. *International Journal of Precision Engineering and Manufacturing-Green Technology*, *2*(2), pp.197-213.

Li, F., Biagioni, P., Bollani, M., Maccagnan, A. and Piergiovanni, L., 2013. Multi-functional coating of cellulose nanocrystals for flexible packaging applications. *Cellulose*, *20*(5), pp.2491-2504.

Oksman, K., Mathew, A.P., Bondeson, D. and Kvien, I., 2006. Manufacturing process of cellulose whiskers/polylactic acid nanocomposites. *Composites science and technology*, *66*(15), pp.2776-2784.

Pei, A., Zhou, Q. and Berglund, L.A., 2010. Functionalized cellulose nanocrystals as biobased nucleation agents in poly (l-lactide) (PLLA)–Crystallization and mechanical property effects. *Composites Science and Technology*, *70*(5), pp.815-821.

Poliakoff, M., Fitzpatrick, J.M., Farren, T.R. and Anastas, P.T., 2002. Green chemistry: science and politics of change. *Science*, *297*(5582), pp.807-810.

Siqueira, G., Bras, J. and Dufresne, A., 2009. New process of chemical grafting of cellulose nanoparticles with a long chain isocyanate. *Langmuir*, *26*(1), pp.402-411.

Tardy, B.L., Yokota, S., Ago, M., Xiang, W., Kondo, T., Bordes, R. and Rojas, O.J., 2017. Nanocellulose–surfactant interactions. *Current opinion in colloid & interface science*, *29*, pp.57-67.

6. Figure captions   page

7. Table captions

IV. Are Cellulose nanocrystals 'alien particles' to human experience?

IV. Are Cellulose nanocrystals 'alien particles' to human experience?

Luciano Piergiovanni[a], GhislainFotie[a], Luana Amoroso[b], Begum Akgun[a], Sara Limbo[a]

[a]PackLAB- DeFENS, Department of Food, Environmental and Nutritional Sciences, Università degli Studi di Milano, Via Celoria 2, 20133, Milan, Italy

[b]Department of Agricultural, Food and Environment (Di3A), Università degli Studi di Catania, Via Santa Sofia 100, 95123, Catania, Italy

Abstract

A wide family of cellulose-based additives are authorized worldwide as fillers and thickening agents in foods, pills and tablets, and microcrystalline cellulose (MCC) is, among these, the most importantone. Since MCC manufacturing is similar to the main production route of cellulose nanocrystals (CNCs), it is reasonable to wonder whether the MCC would contain CNCs as minor components. In this Short Communication we provided first results about the occurrence of CNCs in MCC, observed by dynamic light scattering and transmission electron microscopy after serial filtrations of MCC suspensions. The incidence of cellulose nanoparticles has been proved in several different trials in our ongoing works on diverse MCC samples and the nanoparticles isolated showed shape and dimensions similar to those commonly produced by acidic hydrolysis at laboratory level. Therefore, the presence of CNCs in many products is considered as a certainty. The foods and the pharmaceuticals we have been consuming so far, do indeed contain traces of CNCs to such an extent that this wide presence in consumed products should be taken into account when considering possiblelimitations of the use of these nanoparticles infood contact materials manufacture.

1. Introduction

A general, strong prejudice on the use of nanomaterials in food contact materials (FCM) persists all around the world and the European legislation, since 2011, established that in the manufacture of FCM "substances in nano-form should be used only if explicitly authorized" even ignoring for these applications the functional barrier concept (Commission Regulation EU, 2011).It is worth reminding that according to EU Recommendation 2011/696, nanomaterial means a *natural, incidental or manufactured material containing particles, in an unbound state or as an aggregate or as an agglomerate and where, for 50 % or more of the particles in the number size distribution, one or more external dimensions is in the size range 1 nm - 100 nm* (Commission Recommendation, 2011).

Even though a precautionary policy may be understandable when considering novel substances or inorganic/metallic species, these limitations definitely affect the possible development of innovative, more sustainable and high performance packaging materialsthat include cellulose nanoparticles. On the other side, fundamental and applied research has already demonstrated the great potential of cellulose nanoparticles, both cellulose nanocrystals (CNCs) and microfibrillated cellulose (MFC), in the improvement of fundamental properties of FCM (Dufresne, 2017; Hubbe et al., 2017; Li et al., 2015). In particular, CNCs have been shown to be very interesting barrier coatings, capable of further reducing the gas permeability than synthetic polymers (e.g. EVOH) to a much thinner thickness (Fotie et al., 2017; Li et al., 2013).In addition, no studies to date have demonstrated any dangerousness of the CNCs (Li et al., 2015; Seabra et al., 2018) and recent results suggested that cellulose nanoparticles might potentially beused as useful antimicrobial packaging materials as well as regulators of lipid absorption; in particular,used as food additives or supplement,they might provide a safe and non-chemical means of reducing fat absorption, thus allowing weight loss (DeLoyd et al., 2018; Silva et al., 2019).

CNCs are nanoparticles whose shape and dimensions are largely influenced by the type of cellulosic sources and processes used for their fragmentation. However, they are generally reported as rod-like particles, with length of 100-200 nm and width of 5-10 nm (Li et al., 2015). Such dimensions are practically excluded from any diffusional migration phenomena. It has been demonstrated, in fact, that measurable migration may occur only for nanoparticles up to approximately 3.5 nm in diameter. For 10 nm diameter particles, an apparent diffusion coefficient (D) of $1.1E^{-35}$ cm^2 $s^{-1}$was theoretically calculated in a LDPE host matrix. Such extremely low D results in almost null mobility of the migrants and undeterminable risk of migration (Bott et al., 2014). In this context, the only real risk is that cutting, breaking, or similar mechanical stresses of the packaging materials containing CNCs, can lead to a release of nanocellulose in the food.

In foods and in pharmaceutical products (pills and tablets), the presence of cellulose is very common because a wide group of cellulose-based additives is authorized worldwide as thickening, filler and functional agents.Recently, European Food Safety Authority (EFSA) has re-evaluated 10 different chemically modified and unmodified celluloses as food additives, concluding that there was no need for a numerical Admitted Daily Intake (ADI) and that there would be no safety concern about the reported uses (Younes et al., 2018). Among all these additives, microcrystalline cellulose (MCC)is certainly the most important. MCC is a cellulose-based, powder-like product, known since the '50s, whose global annual production is currently around 120,000 tonnes (Battista and Smith, 1962; Vanhatalo, 2017). In general, wood and cotton powder are common sources for the production of MCC, although other biomasses have been proposed for its production (Yusrina et al., 2018). In any cases, MCC manufacturing is quite similar to the main route for CNCs production and generally consists of a chemical acidic hydrolysis, possibly followed by ultra-sonication.

Therefore, it is reasonable to wonder whether the MCC would containCNCs as minor components. The aim of this short communication is reportingfirstresults obtained seeking for the presence of CNCs in different types of MCC, focusing also on the needs for more extended and deeper investigation in this field.

2. Materials and Methods

Two different types of cellulose microcrystalline were used: MCC for column chromatography, Merck KGaA, Darmstad Germany and MCC, USP (United State Pharmacopeia) approved, Blackburn Distribution, Nelson UK. Ultrapure Milli-Q® water, 0,22 µm filtered, 18.2 MΩcm, 3ppb TOC (MilliporeMerckKGaA, Darmstad Germany), was used in all the steps of suspensions preparation and filtration.

To check the possible CNCs presence in MCC, 7 water suspensions of the two MCC, in the concentrations ranging from0 to 9% (m/v), were submitted to a serial filtrations protocol. Paper filters with nominal cut-off 8-12, 5-8 and 1 µm (Sartorius Stedim, Varedo Italy) and Polyvinylidene Fluoride (PVDF) hydrophilic membranes filters (Durapore®MilliporeMerckKGaA, Darmstad Germany) with nominal cut-off 0.22 µm were used in the serial filtrations. The last filtered supernatants were analysed by dynamic light scattering (DLS) for equivalent hydrodynamic diameters, polydispersity and light scattering intensities using a Litesizer500, Anton Paar, Graz, Austria; the DLS measurements were performed at 25.0 ± 0.1 °C, with a 35 mW laser diode light (λ = 658 nm) and collecting the scattered light at 90° (side scattering angle). The last supernatants, possibly containing particles with expected dimensions lower than 0.22 µm, were freeze-dried for transmission electron microscopy (TEM) observations (LEO 912AB, Zeiss, Oberkochen, Germany) at an accelerating voltage of 80 kV, in order to characterize the morphology and the dimensions of the isolated particles.

3. Results and Discussion

Whatever the MCC concentrations in the different water suspensions filtered, it was always detected, by DLS measurements, equivalent hydrodynamic diameters around 100-150 nm in the supernatants obtained after the last filtration under the 0.22 µm cut-off, as it is shown in Figure 1, with a relatively low level of polydispersity around 20%. In order to confirm the presence of nanoparticles in MCC only, i.e. excluding the presence in the water or due to the procedure used, the filtered Milli-Q® water (MCC concentration 0%) was also tested. The diameters recorded in this case are inconsistent and not reliable values because of the cumulant fit error very high (poor fitting of the correlation function), the high number of runs needed to get a result and the very low mean intensity was recorded (Figure 2). Moreover, the presence of nanoparticles appeared roughly proportional to the initial MCC concentration as it is shown by the increasing scattering intensity (DLS, kcounts/s), at least in the range shown in Figure 2.
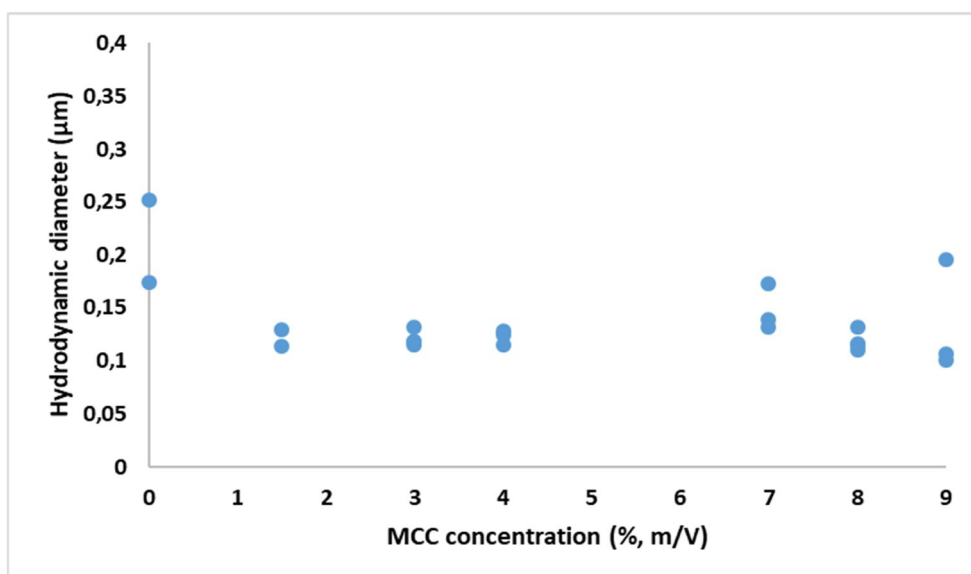
Figure 1. Particle size, equivalent hydrodynamic diameters, measured by DLS for different

MCC concentrations, after the serial filtration protocol (n=3).
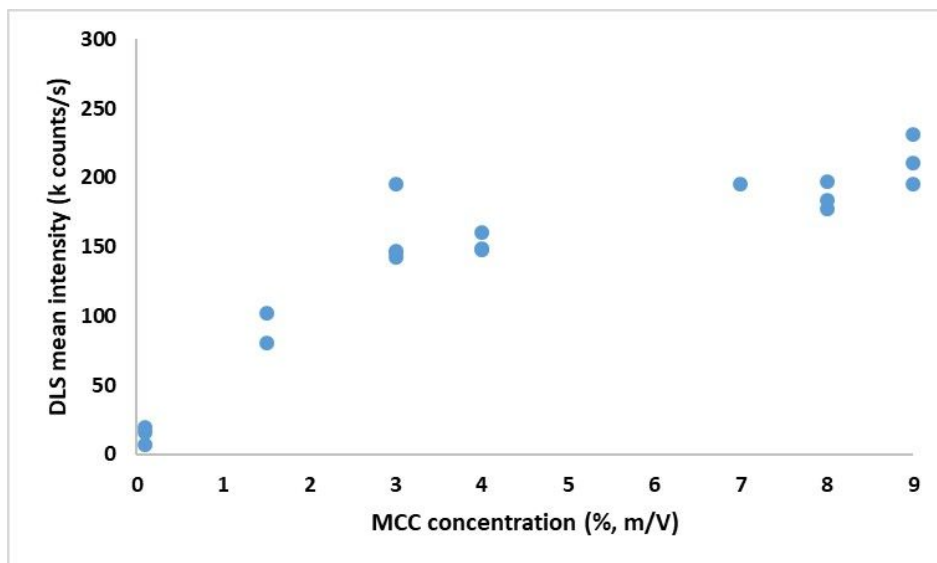
Figure 2. Scattering intensity from DLS measurements for different MCC concentrations, after the serial filtration protocol (n=3).

TEM observations, carried out on the freeze dried supernatants from the last filtration (0.22 µm cut-off), confirmed both the presence of CNCs in MCC, and the dimensions estimated by DLS. Also the typical spindle shape of the cellulose nanocrystals was revealed through TEM observations; the dimensions estimated from Figure 3 are approximately 150-250 nm in length and 20-50 nm in width; dimensions and aspect ratio are consistent with those, commonly measured on CNCs obtained by acidic hydrolysis.

The freeze-dried material obtained through the serial filtration has been also analysed by Fourier-transform infrared (FTIR) spectroscopy with a Perkin Elmer instrument (Spectrum 100), equipped with attenuated total reflectance (ATR) accessory, and the results (data not shown) confirmed the cellulosic nature of the isolated. First results, to be confirmed, revealed a concentration in the order of parts per million (ppm) of cellulose nanocrystals in the MCC samples tested.
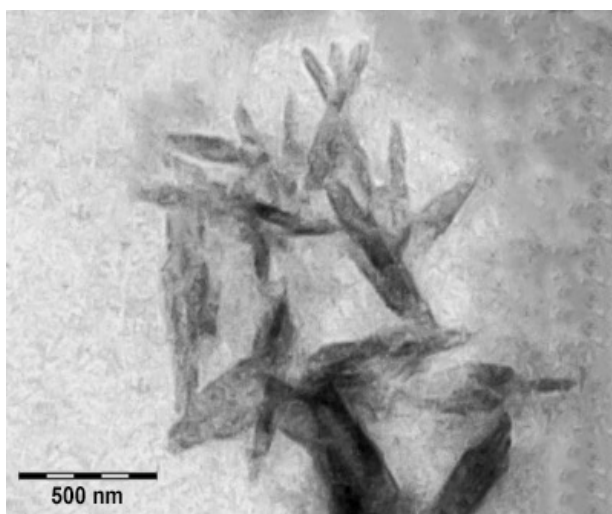
Figure 3.A representative 500 nm scale TEM imageof primary size and morphology of CNCs revealed after serial filtration of MCC suspension.

Works are currently in progress in order to verify the possibility that additional amounts of nanocrystals might be produced from MCC by pH, time and temperature values, typical of gastric digestion. Moreover, a further fundamental undergoing research program isto find out an accurate procedure to estimate the CNCs amount in different media. In fact, it is worth reminding that a reliable procedure to assess quantitatively the CNCs, is an essential pre-requisite for planning migration tests of possible FCM which contain, as fillers or coatings, cellulose nanocrystals.

4. Conclusion

In conclusion, itshould be considered the presence of CNCs in many foods and pharmaceutical products as a certainty; the foods we have been consuming so far contain traces of CNCs, to suchan extent that this wide presence in consumed products should be taken into account when

considering possible limitations of the use of these nanoparticles in FCM manufacture.

A thorough investigation is in progressin order to set up a reliable procedure able to quantify the concentration of the cellulosenanoparticles by means of a combination of electron microscopy, imaging techniques and other appropriate methodologies based on dynamic light scattering. The physicochemical characterization of such organic nanocrystals in terms of shape, dimensions and especially concentration and stability in different media represents a fundamental and challenging stage of the scientific assessment of the risk for the application of nanotechnologies in food and feed chain.

5. References

Battista, O.A., Smith P.A., 1962. Microcrystalline Cellulose. *Industrial &Engineering Chemistry*.54(9):20-9.

BottJ., Störmer A., Franz R., 2014. A model study into the migration potential of nanoparticles from plastics nanocomposites for food contact. *Food Packaging and Shelf Life*. 2(2):73-80.

Commission Recommendation of 18 October 2011 on the definition of nanomaterial Text with EEA relevance. *Off J Eur Union*. 275, 20.10. p. 38-40.

Commission Regulation (EU) No 10/2011 of 14 January 2011 on plastic materials and articles intended to come into contact with food. *Off J Eur Union*. 12, 15.1, p. 1–89.

DeLoid, G.M., Sohal, I.S., Lorente, L.R., Molina, R.M., Pyrgiotakis, G., Stevanovic, A., Zhang, R., McClements, D.J., Geitner N.K., Bousfield, D.W., Ng, K.W., Loo, S.C.J., Bell, D.C., Brain, J, Demokritou, P., 2018. Reducing Intestinal Digestion and Absorption of Fat Using a Nature-Derived Biopolymer: Interference of Triglyceride Hydrolysis by Nanocellulose. *ACS Nano*. 12:6469−6479.

Dufresne, A., 2017. Nanocellulose: from nature to high performance tailored materials. Walter de Gruyter GmbH & Co KG.

Fotie, G., Rampazzo, R., Ortenzi, M., Checchia, S., Fessas, D., Piergiovanni, L., 2017. The Effect of Moisture on Cellulose Nanocrystals Intended as a High Gas Barrier Coating on Flexible Packaging Materials. *Polymers*.9(9):415.

Hubbe, M.A., Ferrer, A., Tyagi, P., Yin Y., Salas, C., Pal, L., Rojas, O.J., 2017. Nanocellulose in thin films, coatings, and plies for packaging applications: A review. *BioResources*.12(1), 2143-2233.

Li, F., Biagioni, P., Bollani, M., Maccagnan, A., Piergiovanni, L., 2013. Multi-functional coating of cellulose nanocrystals for flexible packaging applications. *Cellulose*. 20: 2491–2504.

Li, F., Mascheroni, E., Piergiovanni, L., 2015. The potential of nanocellulose in the packaging field: A review. *PackagTechnol Sci*. 28:475–508.

Seabra, A.B., Bernardes, J.S., Fávaro, W.J., Paula, A.J., Durán, N., 2018. Cellulose nanocrystals as carriers in medicine and their toxicities: A review. *CarbohydPolym*.118:514-527.

Silva, F., Gracia, N., McDonagh, B.H., Domingues, F.C., Nerín, C., Chinga-Carrasco, G., 2019. Antimicrobial activity of biocomposite films containing cellulose nanofibrils and ethyl lauroylarginate. *J. Mater. Sci*.54:12159–12170.

Vanhatalo, K., 2017. A new manufacturing process for microcrystalline cellulose (MCC). *Doctoral Dissertations 152*.Aalto University publication series, Finland.

Younes, M., Aggett, P., Aguilar, F., Crebelli, R., Di Domenico, A., Dusemund, B., et al., 2018.Re-evaluation of celluloses E460(i), E460(ii), E461, E462, E463, E464, E465, E466, E468 and E469 asfoodadditives. *EFSA Journal*. 16(1):5047.

Kharismi, R. R. A. Y., Suryadi, H. 2018. Preparation and Characterization of Microcrystalline Cellulose Produced from Betung Bamboo (Dendrocalamus asper) through Acid Hydrolysis. *Journal of Young Pharmacists*, *10*(2), S79.

6. Figure captions   page

V. Implementation of biocomposites by lamination cellulose nanocrystals

V. Implementation of biocomposites by lamination cellulose nanocrystals

Abstract

In this work, cellulose nanocrystals (CNCs) used were CNCso3h extracted from wood pulp by sulfuric acid (H_2SO_4), CNCcooh extracted from cotton linters by ammonium persulfate (APS) and CNCcoor obtained by esterification between cellulose nanocrystals. When coated onto plastic polymers, these CNCs greatly enhance the gases barrier properties at 0% RH. However, in humid conditions, CNCs capabilities to block diffusion paths in a polymer matrix are lost; therefore, the chemical modification of cellulose nanocrystals and lamination are required to protect the coatings from the wet environment. PLA, PET, PE, PP, OPP and OPA filmswere selected, coated with CNCs and finally laminated. Coated (CNCs-P) and laminated (P-CNC-P) polymers were characterized by gas permeability measurements at 23°C and 50%&80%. It is worth noting that significant improvements of gas barrier were achieved after the lamination. This paper provides insights on the choice of cellulosic nanomaterials for the design and development of advanced and sustainable food packaging.

Key words: Cellulose Nanocrystals, Food Packaging, Cellulose Nanomaterials Coatings, Plastic Polymers

1. Introduction

Cellulose nanocrystals (CNCs) surface chemistry and shape may be utterly different depending on the type of the extraction and the raw materials used. Generally, CNCs extraction consists of an acidic or oxidative hydrolysis of cellulosic sources (cotton linters, by-products, wood pulp…). As reported in many papers, CNCs extracted by hydrochloric acid (HCl) are uncharged (Araki et al., 2001) while those obtained by sulfuric acid (H_2SO_4) contain sulfate half ester charges (Beck-Candanedo et al., 2005; Cherhal et al.,2015; Reid et al., 2016) and those extracted by 2,2,6,6-Tetramethylpiperidin-1-yloxyl(TEMPO)and ammonium persulfate (APS) contain carboxylic charges on their surface (Leung et al., 2011; Habibi et al., 2006). It is worth mentioning that, the superficial chemical charges dictate the dispersibility of the CNCs in solvent or water (Reid et al., 2016; Shimizu et al., 2014) and the strength of adhesion during the interaction CNCs/polymer (Cheng et al., 2015). Due to their many aspects, tiny size and high crystallinity, CNCs may be implemented in food packaging in particular as coatings onto polymers with a consequent enhancement of gas barrier properties. Li et al., (2015) achieved extraordinary reduction in oxygen permeability at 0% RH of several plastic films coated with water-dispersed CNCs while keeping their transparency unchanged.In addition, it has been shown that in dry conditions, with a thickness of about 1 µm, CNCs coatings show gas barrier higher than those obtained from 3-4 µm thickness of common synthetic barriers; such asEthylene vinyl alcoholcopolymer (EVOH) and Polyvinylidene chloridehomoplymer(PVDC) currently used for extension of oxidation sensitive foods (Li et al., 2015; Rampazzo et al., 2017). However, it was also revealed that the interaction polymer/CNCs is not similar and therefore, further investigation must be conducted to have a broad knowledge on the polymers and CNCs chemistry for being ascertained by their chemical affinity and adhesionthroughout the coating process. In recent studies, it has been demonstratedthe relevance of the CNCs barrier against gases was

compromised in humid atmosphere with a subsequent increase in permeation gases. From the reported findings, CNCs being very biodegradable and hydrophilic materials tend to integrate waterfollowed by a gradual disentanglement of their crystalline lattice, which then facilitates the gases to cross the coated plastic films even dramatically (Fotie et al., 2017). Several attempts have been made in order to alleviate that inconvenienceby producing more hydrophobic CNCs through their surface chemical modifications such as esterification, carbamation, sylation, amidation and surfactant absorption (Eyley and Thielemans, 2014; George and Sabapathi, 2015; Lam et al., 2012; Bendahou et al., 2015). Although, some researchers successfully implemented hydrophobic CNCs, however, the gas barrier properties of the coated polymers with those modified crystals were improved but not at acceptable and relevant standards for being implemented in packaging (Arrieta et al., 2014; Fortunati et al., 2012; Ferrer et al., 2012). In food packaging, the lamination technique has long been used to blend various materials of different properties in order to obtain complex multi-layers' structures which comply with all the requirements in terms of gas barrier (oxygen, carbon dioxide, water vapor), grease barrier and sealable-mechanical properties. As mentioned above, one of the common synthetic laminated polymers currently used for shelf-life extension is the EVOH whose structure is strongly sensitive to water and behavior similar to CNCs in wet environment (Zhang et al., 2001). For overcoming that drawbak, the lamination technique has been adopted to protect EVOH layers from surrounding environment and promoted their use in more today's food packaging applications (Shah et al., 2012). In this work, laminated multi-layers' plastics based on the CNCs were successfully implemented by the confinement of the CNCs coating between water-repellent and sealable materials. The combination of modified cellulose nanocrystals and the lamination is likely the best strategy of alleviating the water sensitivity of CNCs coatings and to favor their applications in food packaging. The application of

such bio-based polymers will bring a huge contribution in developing more advanced and sustainable food packaging by making our environment healthy and promoting a circular economy.

2. Materials and Methods

Materials

Plastic films such as 12 µm PET (polyethylene-terephthalate), 75 µm PE (polyethylene), 40 µm PP (polypropylene), 15 µm OPA (oriented polyamide), 30 µm OPP (oriented polypropylene), 25µm PLA and POLURFLEX 2644/ 58-01: two-component polyurethane solvent based adhesive system [mixing ratio 100:10:83 (OH: NCO: Solvent)] and 13 sec viscosity 25°C were all provided by Sapici spa, Cernusco sul Naviglio, Italy.Cellulose nanocrystals (CNCs) obtained by acid hydrolysis of the wood pulp were bought from CelluForce 609, Rang 12C.P.1010 Windsor (Quebec).

Methods

Charges density assessment

Both Z potential and conductometric titration were used to characterize water-suspended cellulose nanocrystals in terms of charges density and colloidal stability. Zeta potential (mV) and conductivity (mS cm^{-1}) of the CNCs in the diluted suspension at pH 8 were determined by electrophoretic light scattering (ELS), using the PALS technology (mod. Litesizer 500, Anton Paar, Graz, Austria). Measures were replicated 5 times, at 25.0 ± 0.1 °C, by means of a 35 mW diode laser (λ = 658 nm) and at 15° detection angle. Conductometric titration was used to evaluate weak and strong acids in the three suspended samples: CNCcooh, CNCcoor, CNCso3h. 15 mg of CNCs were suspended in 200 mL of distilled water and sonicated for 5 min. The pH of the the suspension was then brought to 3 with HCl 0.1 M before the titration. The handheld apparatus was constituted of a pHmeter and conductivity meter

(Multi 3620 IDS) and a titrator (Si Analytics Model Titronic 300). 100 mL increments of NaOH 0.01 M were dispensed in diluted CNCs and stirred for 1 min before collecting the electric conductivity (µS/cm). While the sodium hydroxide is added through the titration, the conductivity first decreases to reach a constant and stable plateau for a moment and after, it increases to reach a constant value of electric conductimetric.

CNCs morphology assessment

Apparent dynamic diameter of water-dispersed CNCs 1 wt% at pH 5.5 was measured by using the PALS technology (mod. Litesizer 500, Anton Paar, Graz, Austria). Measures read at 90° detection angle by dynamic light scattering (DLS) (90° and 25.0 ± 0.1 °C, by means of a 35 mW diode laser (λ = 658 nm) were replicated 5 times. The actual dimensions of the CNCs were evaluated via Transmission Electron Microscopy (TEM).

FTIR Analysis

The FTIR spectroscopy was performed with a Perkin Elmer instrument (Spectrum 782 Cellulose (2016) 23:779–793 123 100), equipped with ATR accessory, at room temperature. The analysis was performed on oven-dried cellulose initially brought to pH 7 and on CNCs-coated polymers (P-CNC) as well. The data were collected over 64 scans with resolutions of 4 cm-1. The three types of cellulose nanocrystals were analyzed (CNCcooh, CNCcoor and CNCso3h).

CNCs coatings of polymers (P-CNC)

All Polymers were previously treated by corona treatment to increase their surface energy and promote their blending with CNCs. Polymers were then coated with water-dispersed CNCs at 6 wt%. Coated polymers were dried in dried conditions for 48 h and the thickness of the coating applied onto the film was assessed by a gravimetric method. Four samples (10 × 10 cm2) were weighed (m1, g), then the coating was removed by flowing hot water (~70 °C) and the resulting uncoated film was dried and weighed (m2, g).

The coating thickness (L, cm) was estimated by Equation (1): $L = (m_1 - m_2)/(\rho \times 100)$

Z potential of uncoated and CNCs-coated polymers

The potential Z of coated and uncoated PET film was measured by Surpass (model, Surpass TM 3, Anton Paar, Graz, Australia). Streaming potential and current are measured while 0.01M KCl solution flows through a chamber of a parallelepiped shape. A double-sided tape adhesive was previously cut around the holder to make sure the tape was exactly as large as the holder. The holder was stuck on the sample with the side of the sample to be measured at the bottom and pieces of uncoated and coated PET film were cut. Finally, the spins were hand-rotated for parallel adjustments of the sample holders clockwise and with dynamometric screwdriver to be sure that the cell was leak proof. The sample holder was finally mounted in the right position and blocked with safe levers. The Knob was used to adjust the gap which had to be around 100 μm. The pH was changed during the measurement with the solution of 0.05 M NaOH and 0.05M HCl. Prior to performing the measurements, the calibration of pHmeter and conductivity meter was required. It might also be useful to remove air bubbles and rinse the samples with the solution to collect reliable data. Furthermore, the temperature of solution has to be taken under control because of intense turbulences which occur during the measurements. For each pH, the Z potential was measured 4 times in 3 replications

Optical Properties of Coated Film

The transparency of the CNCs coated polymers was measured at 550 nm, according to the ASTM D 1746-70, by means of a UV-VIS spectro-photometer (mod. L650, Perkin-Elmer, Milano, Italy). The haze (%) of the coated polymers was measured according to ASTM D 1003-61 with the same instrument equipped with a 150 mm integrating sphere. Each sample was replicated three times, analyzing at least four spots on each replicate.

Contact Angles Assessment

Dynamic contact angles of the plastic film coated the 3 types of cellulose nanocrystals were determined. The sessile drop method was used by gently dropping a droplet of 4.0 ± 0.5 µL of liquid onto the coated film. Two liquids such as the water and formammide were used to measure the contact angle. Measurements were run at room temperature (40%RH) on five different positions for each sample for about 200 sec. The instrument used was an OCA 15 Plus angle goniometer (Data Physics Instruments GmbH, Filderstadt, Germany), equipped with a high-resolution CCD camera, a high-performance digitizing adapter (Data Physics Instruments GmbH, Filderstadt, Germany) and SCA20 software (Data Physics Instruments GmbH, Filderstadt, Germany) for contact angle measurements.

Gas Permeability Measurement

All the oxygen and carbon dioxide permeability measurements of coated and laminated polymers were performed by an isostatic permeabilimeter (mod. Multiperm, PERMTECH S.r.l., Pieve Fosciana, Italy) according to ASTM standard methods (D-3985 and F-1249 respectively). The oxygen and carbon dioxide permeability (PO_2, cm^3 m^{-2} d^{-1} bar^{-1}) of CNCs coated and laminated polymers were measured at 25 °C under 50% and 80% RH on the coated side of the film.

Corona-treatment of CNCs-coated polymers and lamination

Prior to proceeding with the lamination, coated polymers with the three types of cellulose nanocrystals were subjected to corona-discharge to promote the oxidation of cellulose nanocrystals surface to improve the grafting of adhesives during the lamination. Two-component polyurethane solvent based adhesive system [mixing ratio 100:10:83 (OH: NCO: Solvent)] and 13 sec viscosity 25°C.

3. Results and Discussion

3.1. Cellulose nanocrystals

Cellulose nanocrystals dimensions were all simiar but the hydrodynamic diameter of CNCso3h were slightly smaller than those oxidized and esterified.

CNCs properties	CNCso$_3$h	CNCcooh	CNCcoor
Hydrodynamic diameter (nm)	130,55±2,35	176,78±3,52	175,02±0,53
Z potential	-29,6±0,71	-35,65±0,21	-36,3±0,42
Conductivity (mS cm^{-1})	1,31±0,05	0,82±0,04	1,37±0,07
Polydispersity index (%)	27,53	25,24	25,3

Table 1. Properties of dispersed cellulose nanocrystals

FTIR results of dried cellulose nanocrystals

From the figure 1, it can be noticed very easily the presence of peak at wavelength 1746 cm-1 which, can be attributed to esters groups present on the esterified CNCcoor, that is a strong proof of the functionalization of the cellulose nanocrystals during the chemical modification between cellulose nanocrystals.
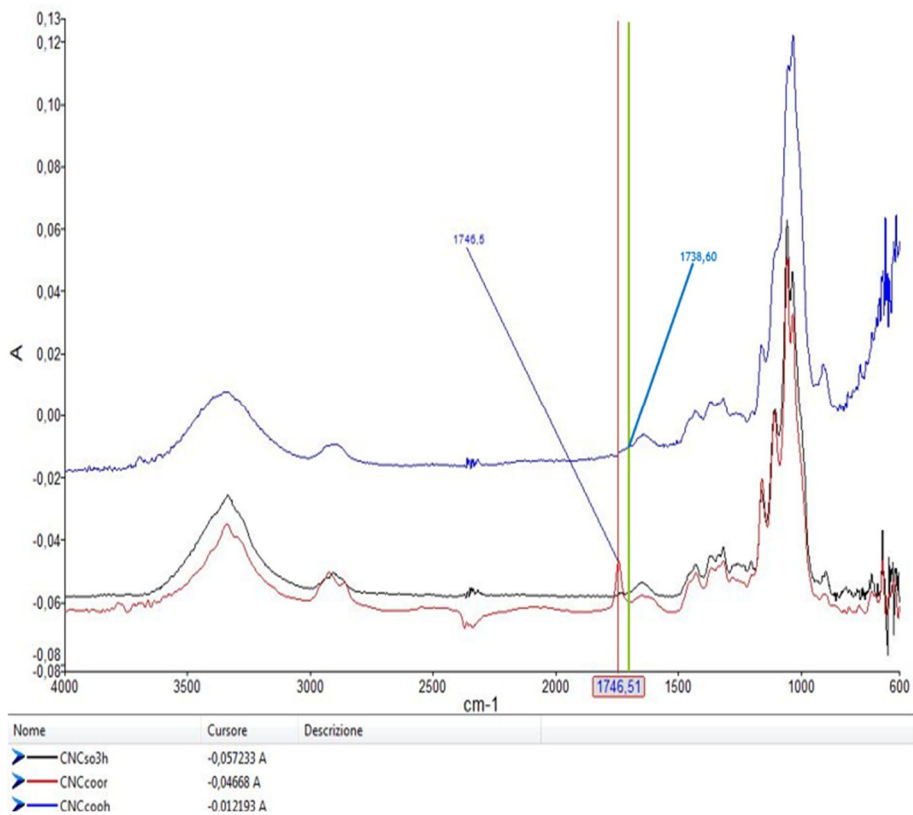
Figure 1. FTIR spectra of the types of cellulose nanocrystals

Z potential versus pH of dispersed cellulose nanocrystals

From the figure 2, it can be noted that independently on the pH, the Z potential values of the esterified CNC (CNCcoor) are the highest ones but are constant from pH 6 to 10. In constrast, Z potential values of CNCso3h are the lowest and constant while those of CNCcooh are fluctuatingwith pH change. That behavior, was expected since the CNCcooh deprotonate to CNCcoo-while, ester and hydroxyl are more stable with pH change. As a result of that, the pH of the CNCcooh dispersion must be brought to 8 before the coating processsto obtain a good stability in water and strong adhesion with plastic polymers.
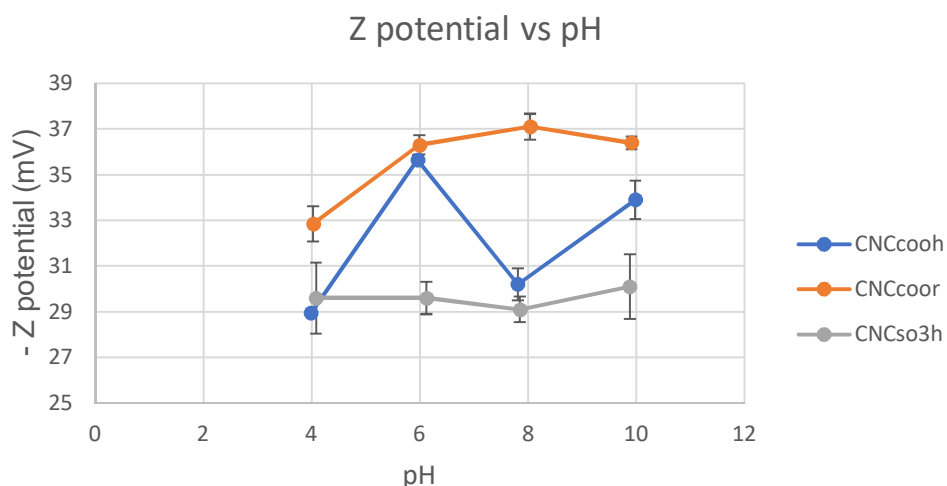
Z potential vs pH

Figure 2. Z potential values versus pH of CNC with carboxylic (CNCcooh), sulfate half ester (CNCso3h) and ester groups (CNCcoor).

Charges density by conductometric titration

The concentration of strong and weak acid derived from the conductometric titration was 0,27 and 0,52 mmol/kg-1for the CNCcooh, 0,24 and 0,30 mmol/kg-1 for CNCso3h and 0,31 and 0,63 mmol/kg-1 (table 1). It can be confirmed that the esterified CNC (CNCcoor) have the highest charges density that contribute to their functionalization with polymers.

Samples (n=3)	Strong acid (mmol/kg-1)	Weak acid (mmol/kg-1)
CNCso3h	0,24±0,02	0,30±0,04
CNCcooh	0,27±0,02	0,52±0,07
CNCcoor	0,31±0,04	0,63±0,06

Table 2. Strong and weak acids of the three types of cellulose nanocrystals

3.2. CNCs-coated PET films (P-CNC)

Z potential of CNCs coated and uncoated PET film versus pH
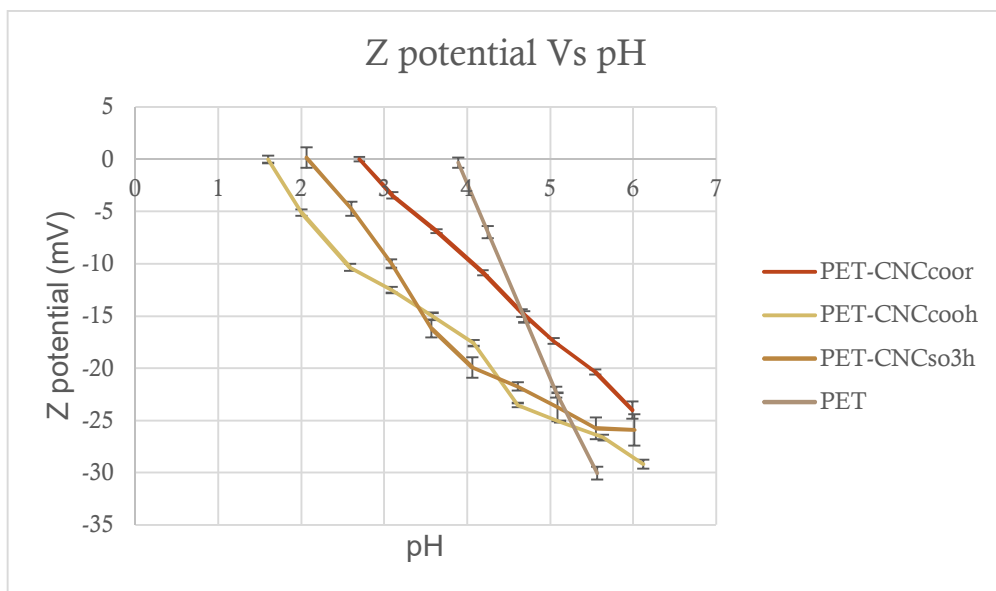
Figure 3. Z potential values versus pH of PET film coated with the three types of cellulose nanocrystals (n= 3)

Z potential and contact angle were employed to assess the hydrophobicity uncoated and CNCs-coated PET fim. From the data, PET films coated with the 3 types of cellulose nanocrystals showed similar threshold, z potential increases with the increase in pH. Uncoated PET film has its isoelectric point at pH 4 while PET films coated with CNCso3h, CNCcooh and CNCcoor have their isoelectric point at pH 1.6, 2.08 and 2.7 respectively. Potential z close to 4 indicates that the material is more hydrophobic and apolar.

In contrast, the hydrodynamic water contact showed a different threshold. There is an immediate decay in water contact angle of PET films coated with esterified CNCs. PET films coated with CNCso3h and CNCcooh have similar trends and decay rate over measurement time.
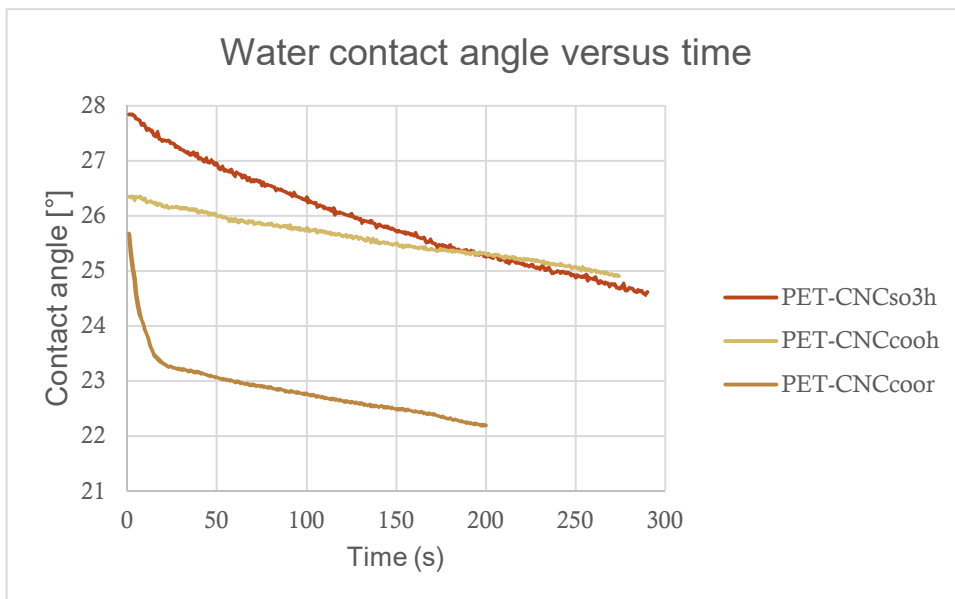
Figure 4. Water contact angle values versus time of PET film coated with the three types of cellulose nanocrystals.

FTIR results of Corona-treated and untreated CNCs-coated PET film

From the figures 5, 6 and 7, the peaks formed during the corona-reatment can be observed. The ozone treatment usually oxidizes the chemical groups of the cellulose nanocrystals surface. However, the oxidation is less pronounced for the already-oxidized cellulose nanocrystals (CNCcooh) while the chemical modification of esterified CNCs (CNCcoor) and CNCso3h surface are much more visible on esterified CNCs. After the corona treatment of coated polymers, the lamination was implemented with solvent-based polyurethanic adhesive at room temperature and the layers were blended and left dried for 7 days before the delamination test and the gas permeability measurements.
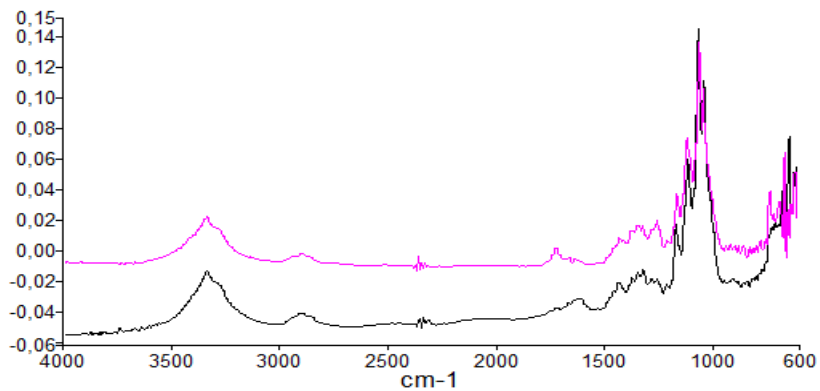
Figure 5. PET-CNCcooh (green) and corona treated PET-CNCcooh (black)
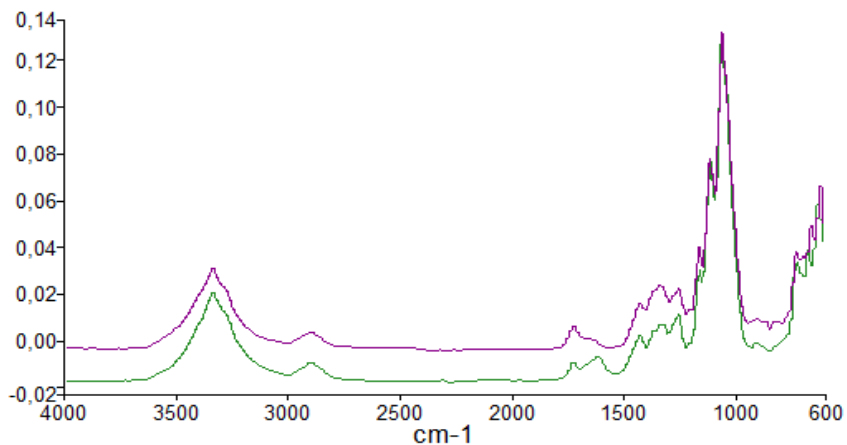
Figure 6. PET-CNCcoor (green) and corona treated PET-CNCcoor (violet)
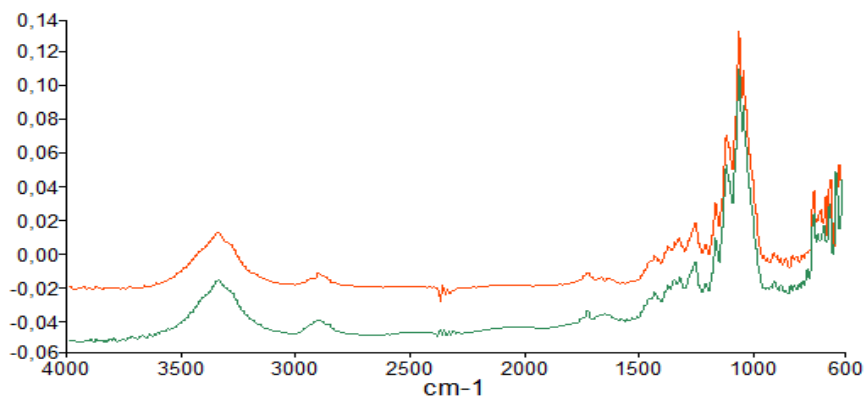
Figure7. PET-CNCso3h (green) and corona treated PET-CNCso3h (red)

Oxygen Permeability of coated polymers (P-CNC)

When comparing the oxygen permeability of coated polymers with the three types of cellulose nanocrystals, the difference is evident at both RH (50% and 80%). The improvements of the oxygen barrier properties are much higher on polymers coated CNCcoor, following by those coated with CNCcooh and CNCso3h. This elucidates the relevance of the esterification of cellulose nanocrystals which allowed to create structures less sensitive to water without modifying the crystallinity or compromising the integrity of the crystals. Although the oxygen barrier was enhanced in the three cases, the oxygen permeability of the coated polymers showed a significant loss of barrier properties at high relative humidity (80%), due to strong affinity between CNCs coatings and water.

P- CNCso3h	RH 50%	RH 80%
PET- CNCso3h	55,06±1,5	96,73±2,5
PLA- CNCso3h	158,71±1,5	484,18±2,5
OPP- CNCso3h	127,91±1,5	756,06±1,5
PP- CNCso3h	113,09±1,5	652,68±2,5
PE- CNCso3h	71,38±1,5	1388,29±1,5
P-CNCcooh	**RH 50%**	**RH 80%**
PET- CNCcooh	36,23±3,5	108,94±3,5
PLA- CNCcooh	107,17±3,5	409,91±3,5
OPP- CNCcooh	46,27±3,5	367,02±3,5
PP- CNCcooh	53,36±3,5	657,65±3,5
PE- CNCcooh	89,91±3,5	1035,71±3,5
P-CNCcoor	**RH 50%**	**RH 80%**
PET- CNCcoor	12,16 ±3,5	90,7±3,5
PLA- CNCcoor	43,99±3,5	339,82±3,5
OPP- CNCcoor	46,74±3,5	626,32±3,5
PP- CNCcoor	32,41±3,5	665,66±3,5
PE- CNCcoor	47,59±3,5	999,12±3,5

Table 3. Oxygen permeability of poymers coated with the three types of CNCs (50-80% RH)
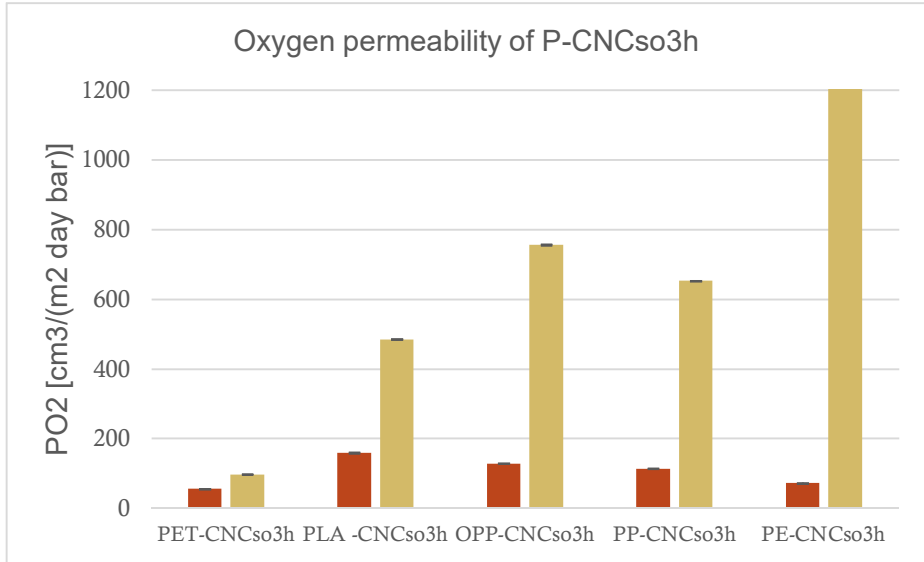
Figure 8. Oxygen permeability of coated polymers with CNCso3h at 50% (red) and 80% RH (brown)
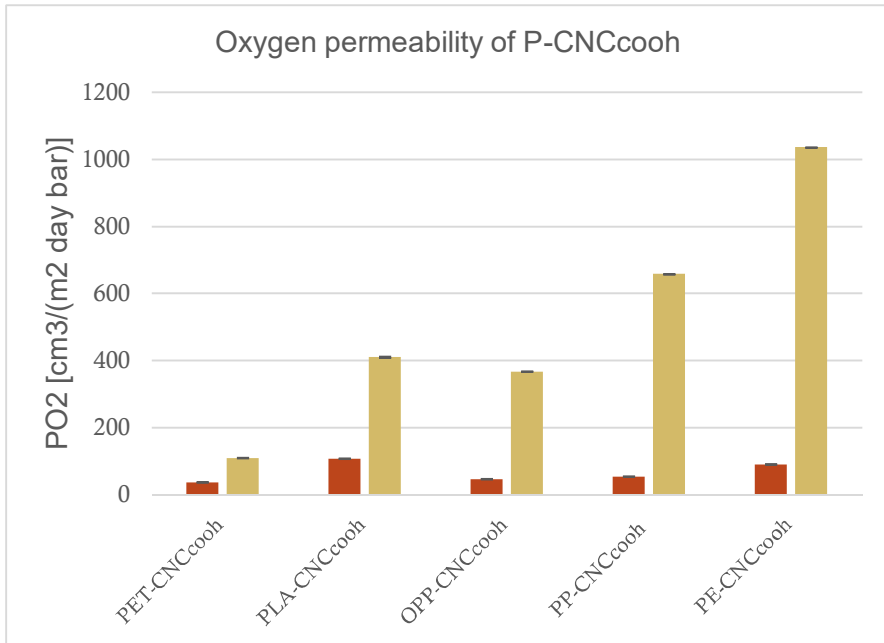
Figure 9. Oxygen permeability of coated polymers with CNCcooh at 50% (red) and 80% RH (brown)
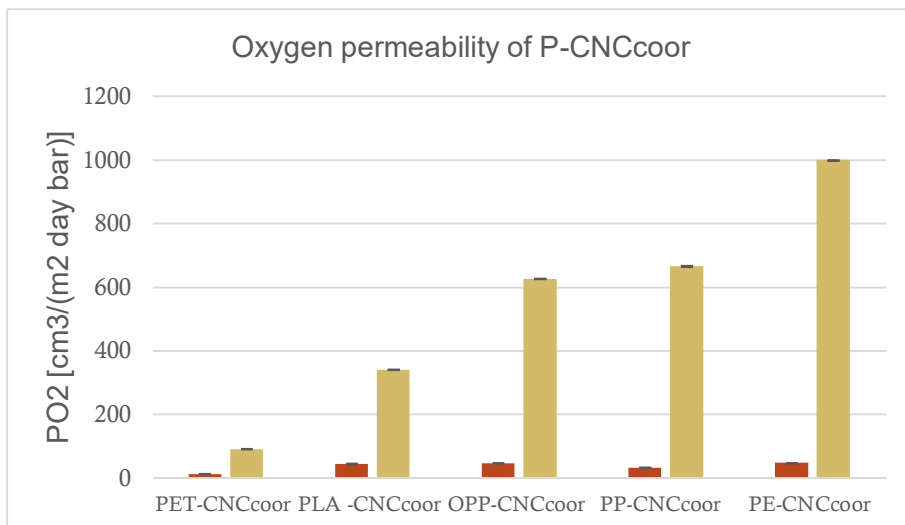
Figure 10. Oxygen permeability of coated polymers with CNCcoor at 50% (red) and 80% RH (brown)

Haze and transparency of coated and uncoated polymers

Uncoated and CNCs-coated polymers (P-CNC) showed similar values of haze and transparency. It proved that the coating of polymers with the three types of polymers has not affected the optical properties the standard polymers.
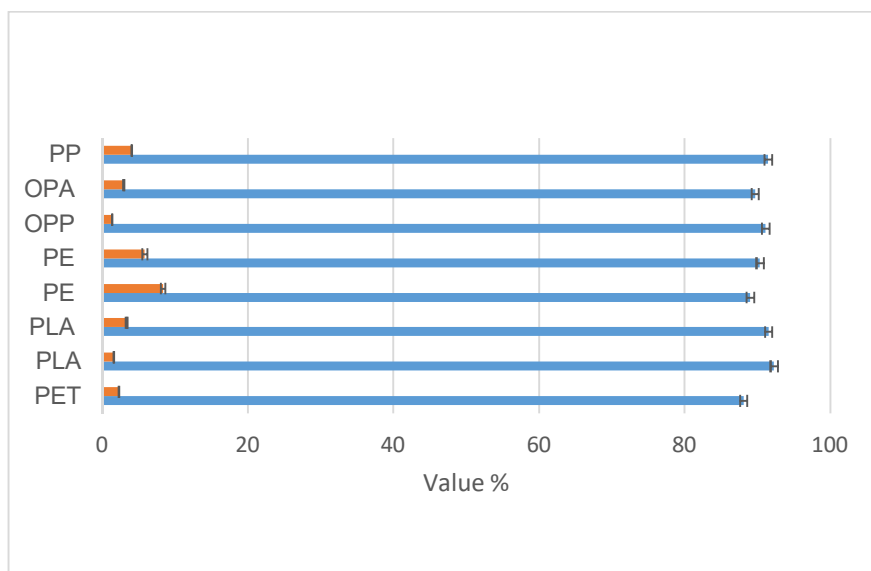
Figure 11. Haze (red) and transparency (blu) of uncoated polymers
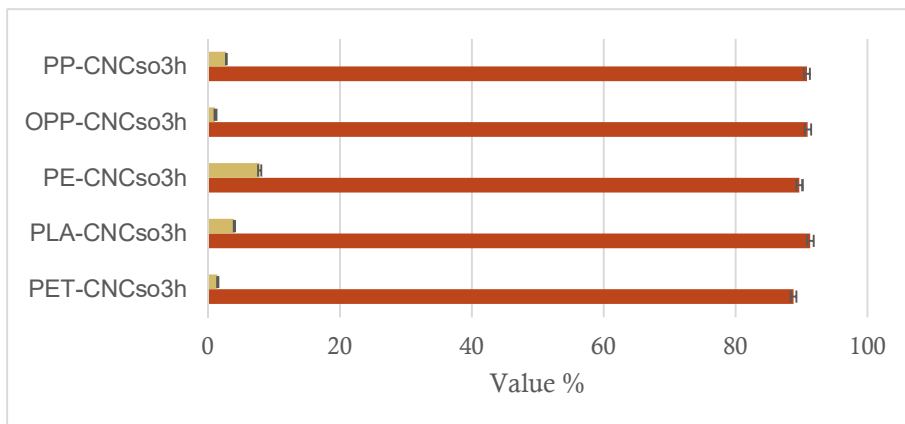
Figure 12. Haze (brown) and transparency (red) of polymers coated CNCso3h
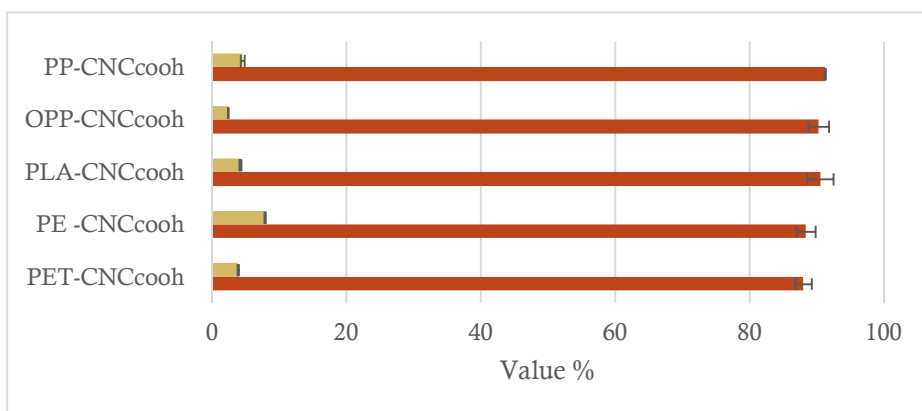
Figure 13. Haze (brown) and transparency (red) of polymers coated CNCcooh
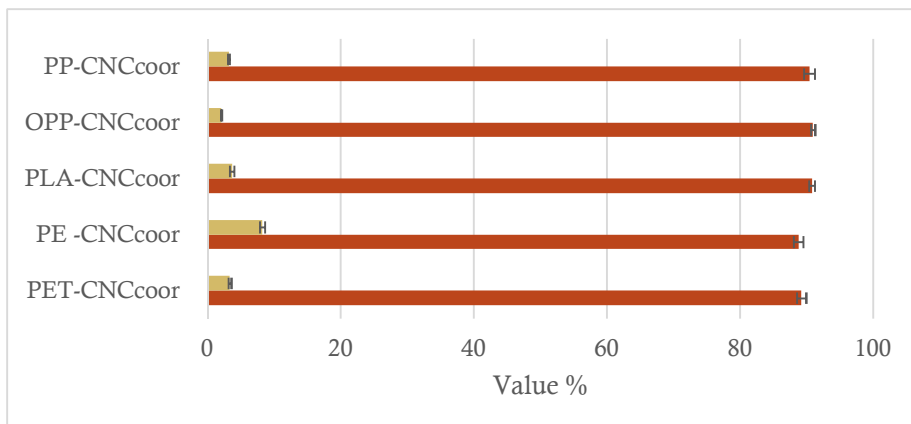
Figure 14. Haze (brown) and transparency (red) of polymers coated CNCcoor

3.3. Laminated CNCs-coated PET films (P-CNC-P)

Delamination Test

In light of the data of peeling test of laminated polymers collected according to ATM-D882-09, Stiffness and Elastic modulus were all acceptable. It has to be pointed out that the laminated based on esterified cellulose nanocrystas displayed the best performance in terms of mechanical properties. In addition, it can be confirmed that the corona-treatment of coated polymers before the lamination has definetly contributed to reinforce the adhesion between the cellulose nanocrystals and the adhesive.

P-CNCso3h-P	OPP-CNCso3h/OPP	PET-CNCso3h/OPP	PET-CNCso3h/PP	PE-CNCso3h/PE-
Maximum Load (N)	1,15	0,22	0,23	0,72
Breaking elongation (mm)	83,18	0,10	84,40	61,78
Elastic Modulus (N/m)	35462,34	9639,17	5209,85	2218,13
Percentage deformation at break (%)	109,27	0,13	110,91	76,74
Breaking Load (N)	0,09	0,31	0,02	0,10
Breaking Strength (N/m)	6,24	20,70	1,25	6,49
Yield strength (N)	1,04		0,19	0,50
Stiffness (N/m)	6986,45	1883,24	987,41	631,01

Table 4. Delamination test of CNCso3h-coated and laminated poymers

P-CNCcooh-P	PP-CNCcooh/PET	OPP-CNCcooh/PE-CNCcooh	PE-CNCcooh/PE	OPP-CNCcooh/PLA-CNCcooh
Maximum load (N)	3,07	1,38	1,34	0,34
Breaking elongation (mm)	17,35	49,22	77,13	0,10
Elastic Modulus (N/m)	25789,16	14257,53	-42863,36	18131,40
Percentage deformation at break (%)	22,82	64,72	101,36	0,13
Breaking Load (N)	0,19	0,09	0,86	0,47
Breaking Strength (N/m)	12,90	6,07	57,24	31,46
Yield strength (N)	3,40	1,27		
Stiffness (N/m)	5084,44	2811,08	-8454,85	3577,63

Table 5. Delamination test of CNCcooh-coated and laminated poymers

P-CNCcoor-P	Maximum load (N)	Breaking elongation (mm)	Elastic Modulus (N/M)	Percentage deformation at break (%)	Breaking Load (N)	Breaking Strength (N/m)	Yield strength (N)	Stiffness (N/m)
PET-CNCcoor/PP-CNCcoor	0,88	1,02	21107,12	1,34	1,09	73,07	0,94	4162,94
PET-CNCcoor/PE	0,32	0,16	17679,35	0,21	0,32	21,84		3488,29
PE-CNCcoor/PE	4,11	36,13	22792,91	47,49	0,81	54,408	2,80	4494,47
OPP-CNCcoor/PLA-	0,46	0,29	27934,36	0,38	0,46	31,18		-8261,17

Table 6. Delamination test of CNCcoor-coated and laminated polymers**.**

Oxygen Permeability of laminated polymers (P-CNC-P)

The lamination of coated polymers furtherly improved the gas barrier and that for all the three types of cellulose nanocrystals. This technique that implies protection of cellulose nanocrystals coatings against the surrounding

environment was very effective in blocking water to disrupt or modify the crystallinity network. The combination of both ways of controllong the swelling of the coatings through the chemical modification of cellulose nanocrystals surface and subsequent lamination was by far the most effective way to strongly enhance the gas barrier properties even at higher relative humidities.

P-CNCso3h	50% RH	80% RH
OPP- CNCso3h /OPP	4,56±3,5	9,78±3,5
PET- CNCso3h /OPP	<0,06	0,29±3,5
PET- CNCso3h /PP	<0,06	<0,06
PET- CNCso3h /PE	0,25±015	1,107±1,5
PE- CNCso3h /PE- CNCco3h	2,29±3,5	5,49±1,5
P-CNCcooh	**50% RH**	**80% RH**
PP- CNCcooh /PET	9,66±0,5	9,23±1,5
OPP- CNCcooh /PE- CNCcooh	<0,06	4,69±0,5
PE- CNCcooh /PE	4,29±0,5	13,45±3,5
OPP- CNCcooh /PLA- CNCcooh	12,41±3,5	201,11±3,5
P-CNCcoor	**50% RH**	**80% RH**
PP- CNCcoor /PET- CNCcoor	7,06	6,88±1,5
OPP- CNCcoor /PE- CNCcoor	<0,06	<0,06
PE-CNCcoor /PE	<0,06	<0,06
PET- CNCcoor /PE	<0,06	<0,06
OPP- CNCcoor /PLA- CNCcoor	3,78±3,5	103,55±3,5

Table 7. Oxygen permeability of coated and laminated poymers at RH 50-80%, the Standard dev. are calcolated from the mean (n=3)
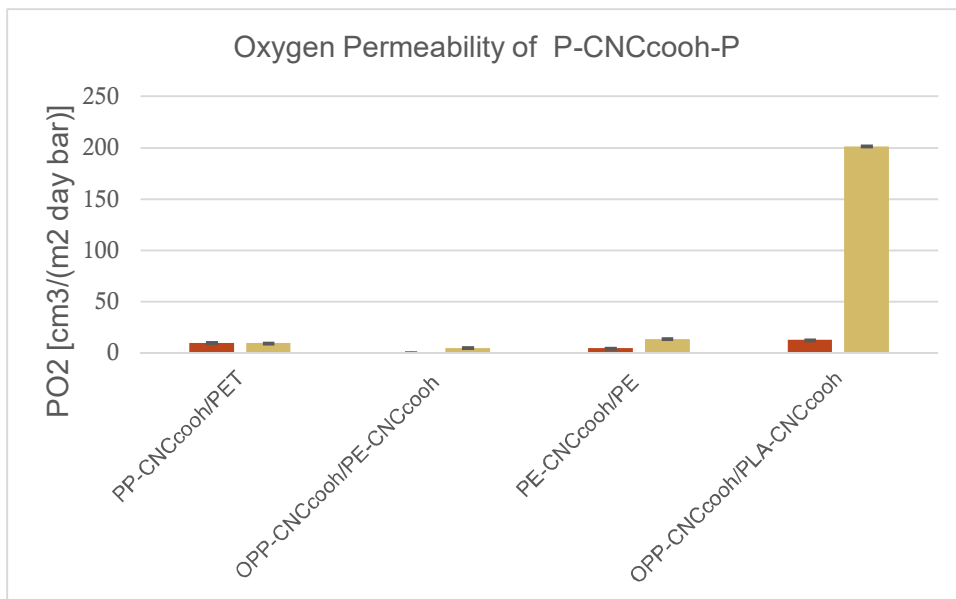
Figure 15. Oxygen permeability of laminated polymers with CNCcooh at 50% (bred) and 80% RH (brown)
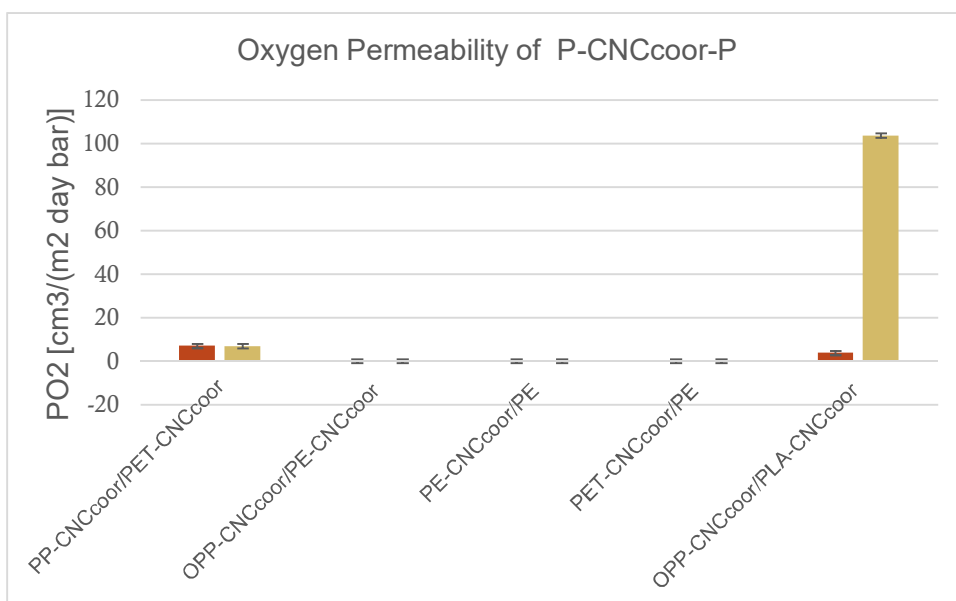
Figure 16. Oxygen permeability of laminated polymers with CNCcoor at 50% (red) and 80% RH (brown)
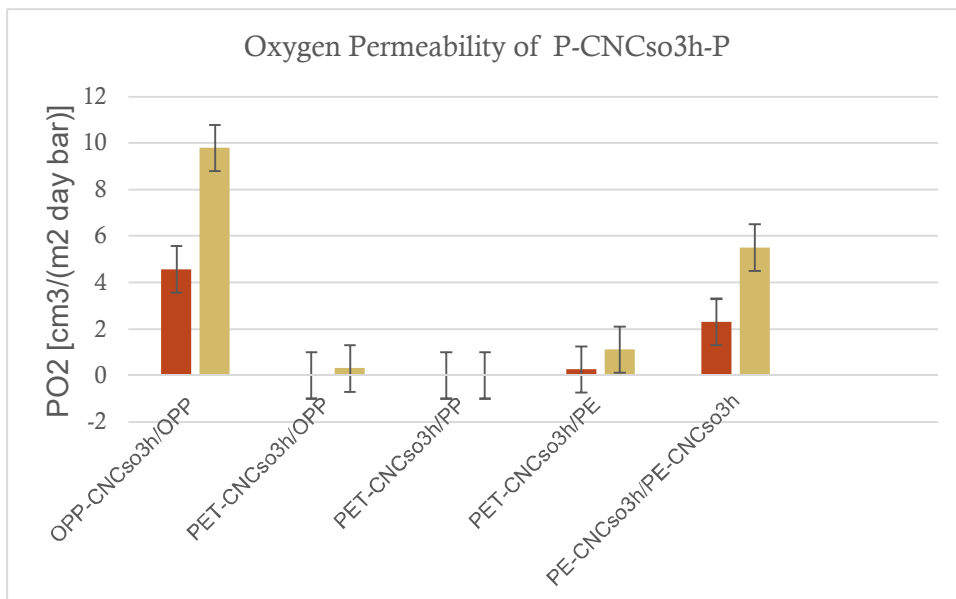
Figure 17. Oxygen permeability of laminated polymers with CNCso3h at 50% (red) and 80% RH
(brown)

4. Conclusions

The main problem to be sorted out was the sensibility of the cellulose nanocrystals to moisture that hampered their incorporation into food packaging. It was mentioning that the barrier gas properties of cellulose nanocrystals are effective in absence of humidity but are compromised in humid environment. The chemical modification of cellulose nanocrystals has improved the gas barrier compared to the unmodified ones. Oxygen permeability of laminated polymers showed very low values even in high relative humidity, which is the confirmation that the lamination has definitely isolated the CNCs coatings from the moisture and can be used for food shelf-life extension. From the results of the delamination test, it can be observed that the stiffness, elastic modulus and elongation at the end are relevant for any delamination test of polymers. It is very important to point out that the lamination of polymers coated with esterified cellulose nanocrystals were the best in terms of reducing the gas permeability even in higher relative humidity. This opens up a new gate for effective development of advanced materials

suitable for food shelf-life extension, taking care of environmental protection and circular economy principles

5. References

Araki, J., Wada, M. and Kuga, S., 2001. Steric stabilization of a cellulose microcrystal suspension by poly (ethylene glycol) grafting. *Langmuir*, *17*(1), pp.21-27.

Arrieta, M.P., Fortunati, E., Dominici, F., Rayón, E., López, J. and Kenny, J.M., 2014. PLA-PHB/cellulose based films: Mechanical, barrier and disintegration properties. *Polymer Degradation and Stability, 107*, pp.139-149.

Beck-Candanedo, S., Roman, M. and Gray, D.G., 2005. Effect of reaction conditions on the properties and behavior of wood cellulose nanocrystal suspensions. *Biomacromolecules*, *6*(2), pp.1048-1054.

Bendahou, A., Hajlane, A., Dufresne, A., Boufi, S. and Kaddami, H., 2015. Esterification and amidation for grafting long aliphatic chains on to cellulose nanocrystals: a comparative study. *Research on Chemical Intermediates*, *41*(7), pp.4293-4310.

Cheng, D., Wen, Y., Wang, L., An, X., Zhu, X. and Ni, Y., 2015. Adsorption of polyethylene glycol (PEG) onto cellulose nano-crystals to improve its dispersity. *Carbohydrate polymers*, *123*, pp.157-163.

Cherhal, F., Cousin, F. and Capron, I., 2015. Influence of charge density and ionic strength on the aggregation process of cellulose nanocrystals in aqueous suspension, as revealed by small-angle neutron scattering. *Langmuir*, *31*(20), pp.5596-5602.

Eyley, S. and Thielemans, W., 2014. Surface modification of cellulose nanocrystals. *Nanoscale*, *6*(14), pp.7764-7779.

Ferrer, A., Pal, L. and Hubbe, M., 2017. Nanocellulose in packaging: Advances in barrier layer technologies. *Industrial Crops and Products*, *95*, pp.574-582.

Fortunati, E., Peltzer, M., Armentano, I., Torre, L., Jiménez, A. and Kenny, J.M., 2012. Effects of modified cellulose nanocrystals on the barrier and migration properties of PLA nano-biocomposites. *Carbohydrate polymers*, *90*(2), pp.948-956.

Fotie, G., Rampazzo, R., Ortenzi, M., Checchia, S., Fessas, D. and Piergiovanni, L., 2017. The effect of moisture on cellulose nanocrystals intended as a high gas barrier coating on flexible packaging materials. *Polymers*, *9*(9), p.415.

George, J. and Sabapathi, S.N., 2015. Cellulose nanocrystals: synthesis, functional properties, and applications. *Nanotechnology, science and applications*, *8*, p.45.

Habibi, Y., Chanzy, H. and Vignon, M.R., 2006. TEMPO-mediated surface oxidation of cellulose whiskers. *Cellulose*, *13*(6), pp.679-687.

Lam, E., Male, K.B., Chong, J.H., Leung, A.C. and Luong, J.H., 2012. Applications of functionalized and nanoparticle-modified nanocrystalline cellulose. *Trends in biotechnology*, *30*(5), pp.283-290.

Leung, A.C., Hrapovic, S., Lam, E., Liu, Y., Male, K.B., Mahmoud, K.A. and Luong, J.H., 2011. Characteristics and properties of carboxylated cellulose nanocrystals prepared from a novel one-step procedure. *Small*, *7*(3), pp.302-305.

Li, F., Mascheroni, E. and Piergiovanni, L., 2015. The potential of nanocellulose in the packaging field: A review. *Packaging Technology and Science*, *28*(6), pp.475-508.

Mascheroni, E., Rampazzo, R., Ortenzi, M.A., Piva, G., Bonetti, S. and Piergiovanni, L., 2016. Comparison of cellulose nanocrystals obtained by sulfuric acid hydrolysis and ammonium persulfate, to be used as coating on flexible food-packaging materials. *Cellulose*, *23*(1), pp.779-793.

Rampazzo, R., Alkan, D., Gazzotti, S., Ortenzi, M.A., Piva, G. and Piergiovanni, L., 2017. Cellulose nanocrystals from lignocellulosic raw materials, for oxygen barrier coatings on food packaging films. *Packaging Technology and Science*, *30*(10), pp.645-661.

Reid, M.S., Villalobos, M. and Cranston, E.D., 2016. Benchmarking cellulose nanocrystals: from the laboratory to industrial production. *Langmuir*, *33*(7), pp.1583-1598.

Reid, M.S., Villalobos, M. and Cranston, E.D., 2016. Cellulose nanocrystal interactions probed by thin film swelling to predict dispersibility. *Nanoscale*, *8*(24), pp.12247-12257.

Shah, G.P., WR Grace and Co-Conn, 1991. *Oxygen barrier biaxially oriented film*. U.S. Patent 5,004,647.

Shimizu, M., Saito, T. and Isogai, A., 2014. Bulky quaternary alkylammonium counterions enhance the nanodispersibility of 2, 2, 6, 6-tetramethylpiperidine-1-oxyl-oxidized cellulose in diverse solvents. *Biomacromolecules*, *15*(5), pp.1904-1909.

Zhang, Z., Britt, I.J. and Tung, M.A., 2001. Permeation of oxygen and water vapor through EVOH films as influenced by relative humidity. *Journal of Applied Polymer Science*, *82*(8), pp.1866-1872.

6. Figure captions   page

7. Table captions   page

VI. Food shelf-life extension by use of the laminates based on cellulose nanocrystals in comparison with oil-based laminates

VI. Food shelf-life extension by use of the laminates based on cellulose nanocrystals in comparison with oil-based laminates

Abstract

The scope of this paper was to use the cellulose nanocrystals (CNCs) coatings with extraordinary gas barrier properties to implement fully compostable laminates (LAM_{CNC}), structured of "Cellophane (19µm)/Aluminum metallization (<1 µm)/Tie (2µm)/CNCs (1µm)/Tie (3µm)/PLA (55µm)" in replacement of synthetic laminates (LAM_{EVOH}) "PET (28µm)/Tie (1.2µm)/EVOH (3.3µm)/Tie (1.2µm) PET (25µm)/Tie (1.2µm)/PE (12.25µm)" currently used for oxidation-sensitive food products. And subsequently, a comparative two-month food shelf-life assessment was designed by using the two types of laminates to fabricate identical-sized pouches and filled with ground coffee and grated cheese then, sealed under 100% N_2 to be finally stored at 23°C/30°C/40°C and 5°C/23°C respectively. From the findings, Laminates-based CNCs were the better ones in the shelf-life extension of food products.

Keywords: cellulose nanocrystals (CNCs), food oxidation, food shelf-life, fully compostable and synthetic laminates.

1. Introduction

In recent years, oxidation has been one of the major challenges for the scientific and manufacturing community in terms of food quality decay, economic losses and environmental concerns. All foods containing lipids can undergo oxidation compromising their quality with adverse physicochemical changes (Labuza and Dugan, 1971). Although the level of oxidation depends on the chemical composition of the food and the storage environment, the packaging plays an essential role in protecting the foods. Nowadays, to prevent food spoilage from oxidation, vacuum, modified atmosphere

packaging (MAP) and oxygen-barrier synthetic laminates containing EVOH copolymer (Ethylene vinyl alcohol), Nylon 6,6 or PVDC (Polyvinylidene chloride) are employed (Barlow and Morgan, 2013). However, with the growing awareness of the environmental impact of these non-renewable oil-based materials, the search for more sustainable alternatives has recently been scientists' focus (Li et al., 2015). Bio-polymers such as PLA (Polylactic acid) and PHAs (Polyhydroxyalkanoates) might be a valid option; however, they lack gas barrier properties (Farah et al., 2016). Nowadays, nanotechnology has become a very captivating field because it allows materials to be manipulated on a nanometric scale by providing new properties useful for the development of more advanced materials (Rashidi et al., 2011). As a matter of fact, cellulose nanocrystals (CNCs) which are synthesized either by acidic or oxidative hydrolysis of cellulosic sources actually exhibit extraordinary gas barrier properties (Mascheroni et al., 2016). Cellulose is the most abundant natural polymer that consists of millions of glucoses linked by glicosidic bonds forming a hierarchical organization containing amorphous and crystalline (yang et al., 2007). As stated in several articles, CNCs have been isolated from cellulosic matrices such as wood pulp and cotton linters by sulfuric acid and ammonium persulfate (Mascheroni et al., 2016). By obtaining an oxygen permeability of 0.06 $cm^3*24h^{-1}*m^{-2}*bar^{-1}$ at 0% RH of PET (Polyethylene terephthalate) films coated with less than 1 µm thick CNCs, Li et al. confirmed the better improvement in gas barrier properties of the materials coated with CNCs in comparison with 3-4µm thick EVOH (Mokwena and Tang, 2012). Generally, gas diffusion through any materials broadly depends on direct factors such as crystallinity index, permeant solubility and concentration gradient. Other extrinsic factors such as temperature and relative humidity may also have a significant influence on the permeation of the gas (Piringer et al., 2008). Henceforth, CNCs being very hydrophilic by nature due to the presence of many hydrogen bonds and polar groups on their surface tend to swell in high relative humidity (from 40% to

100%), which then causes a gradual disentanglement of the crystalline lattice and causes a dramatic permeation of gases through the coated materials (Fotie et al., 2017; Fotie et al., 2018). In this paper, it was demonstrated that one of the best solutions to alleviate the water sensitivity of the CNCs, was to concur to the insulation of CNCs coatings through their lamination between two layers such as a water-repellent structure like the metalized cellophane and a sealable polymer like PLA to set up fully compostable laminates.

2. Materials and Methods

Materials

Fully compostable laminates implementation, 55µm PLA and 19 µm metalized cellophane films and 72 µm synthetic laminates (LAM_{EVOH}) constituted of PET (28µm)/Tie (1.2µm)/EVOH (3.3µm)/Tie (1.2µm) PET (25µm)/Tie (1.2µm)/PE (12.25µm) were provided by Goglio spa, Italy. Solvent-based adhesive was procured from Sapici spa, Italy and the cellulose nanocrystals obtained by acid hydrolysis (sulfuric acid) from wood pulp (Sacui et al., 2014) were bought from CelluForce, Canada. For food shelf-life assessment, grated cheese with 28% fat content of which 68% saturated and ground coffee with 46% of linolenic acid content, Sodium Thiosulfate, n-hexane, ethanol, starch, 1-decanol, NaOH 0.1M bought from SIGMA.

Methods

CNCs morphology assessment

Apparent dynanamic diameter of water-dispersed CNCs 1wt% at pH 5.5 was measured by using the PALS technology (mod. Litesizer 500, Anton Paar, Graz, Austria). Measures read at 90° detection angle by dynamic light scattering (DLS) (90° and 25.0 ± 0.1 °C, by means of a 35 mW diode laser (λ= 658 nm) were replicated 5 times. The actual dimensions of the CNCs were evaluated via Transmission Electron Microscopy (TEM).

Evaluation of CNCs charges density

Z potential of water-dispersed CNCs 1wt% at pH 5.5 was measured at 15° detection angle by electrophorectic light(ELS) by using the PALS technology (mod. Litesizer 500, Anton Paar, Graz, Austria) replicated 5 times, at 25.0 ± 0.1 °C, by means of a 35 mW diode laser (λ = 658 nm). Strong acid ($-OSO_3H$) and weak acid (-OH) concentrations were calculated through the conductometric titration.

PLA coating with CNCs and fully composites lamination

PLA films were coated with water-dispersed CNCs 4wt% through rotating roll then dried in tunnel at 70°C. Subsequently, coated PLA films (1st web unwind) were coupled with metalized cellophane (2nd web unwind) through the laminating process by rotating roll filled of solvent-based polyurethanic liquid adhesives. The lamination was set up at room temperature and the fully compostable laminated (LAM_{CNC}) were stored at the drying oven to allow the solvent to evaporate.

Thickness assessment of CNCs and adhesive layers

For the evaluation of the CNCs layer's thickness, the gravimetric method was adopted. Four samples of coated PLA (10 × 10 cm^2) were weighed (m_1, g), then the coating was removed by washing out the coating hot water (~70 °C) and the uncoated film obtained was dried and weighed (m_2, g). The coating thickness (L, cm) was estimated by Equation: $L = (m_1 - m_2)/100\rho$, where ρ = 1.58 g cm^{-3} is assumed as the density of the CNCs. The thickness of the adhesive in $LAM_{CNC}$was calculated by the difference between the total thickness of the laminated and the thickness of other constituents.

Gas permeability measurements of LAM_{CNC} and LAM_{EVOH}

All the carbon dioxide, oxygen and water vapor permeability measures were performed by an isostatic permeabilimeter (mod. Multiperm, PERMTECH S.r.l., Pieve Fosciana, Italy) according to ASTM standard methods (D-3985

and F-1249 respectively). Oxygen (PO2) and carbon dioxide (PCO2) permeability of both laminates measured at 23 °C under 35% RH as for the water vapor transmission rate (WVTR) which was measured at 38°C and 80% RH.

Pouches fabrication, storage and sampling

Pouches (20.5 x 12 cm) were fabricated with the two different laminates, filled with 80 g of ground coffee and 60 g of grated cheese and sealed under 100% of N2. Subsequently, both types of pouches were stored in dark conditions, at 23, 30 and 40 °C for ground coffee and at 5 and 23 °C for grated cheese at 35% RH. The pouches withdrawal in triplicate was at time 0 and then 14, 39, 53 and 67 days to perform headspace gas composition, chemical (color, conjugated dienes and trienes…), microbiological (total mesophilic bacterial counts) and sensory changes.

3. Results and Discussion

CNCs dimensions and charges density

Apparent hydrodynamic diameter of CNCs was confirmed by TEM and the CNCs length was found to be 115±4 nm moreover, the Z potential measured was -40 ±1 mV and the concentration of strong and weak acids were 0.28 mmol/kg and 0.35 mmol/kg respectively. The size obtained confirms the nanometric scale of the CNCs and the high z potential demonstrates the stability of the water-dispersed CNCs and strong charges residues derive from the sulfuric acid reaction with the cellulose.

Oxygen, carbon dioxide and water permeability

Laminates	T (°C)	GTR at 35% RH ($cm^3 d^{-1} bar^{-1} m^{-2}$)		CO_2TR/OTR Gas Selectivity	WVTR at 80% ΔRH ($g\ m^{-2}\ d^{-1}$)
		OTR	CO_2TR		
Compostable (CNCs)	23	0.47	1.33	2.83	-
	30	0.60	1.92	3.20	-
	38	-	-	-	6.31
	40	0.77	2.21	2.90	-
	23	0.67	1.38	2.00	-
	30	1.50	3.15	2.16	-
	38	-	-	-	3.84
	40	3.70	9.55	2.58	-

Table 1. Permeability values measured on the two laminates used in the Shelf Life tests

It is clearly evident that at 23°C the oxygen and carbon dioxide permeability

of the two materials are quite similar. This behavior suggested to assess the activation energy of the diffusional phenomena in the two different laminates. The Ea (activation energy, kJ/ml) estimated were 21.6 and 24.24 respectively, for O2 and CO2 for the fully compostable laminate, while they were 77.0 and 87.5 respectively for O2 and CO2, in the standard laminate, which confirmed that compostable laminates are less sensitive to the temperature.

Headspace gas composition

Gas composition was evaluated by GC-TCD and the selectivity (CO_2/O_2) was then calculated in the pouches containing the ground coffee (figure2).
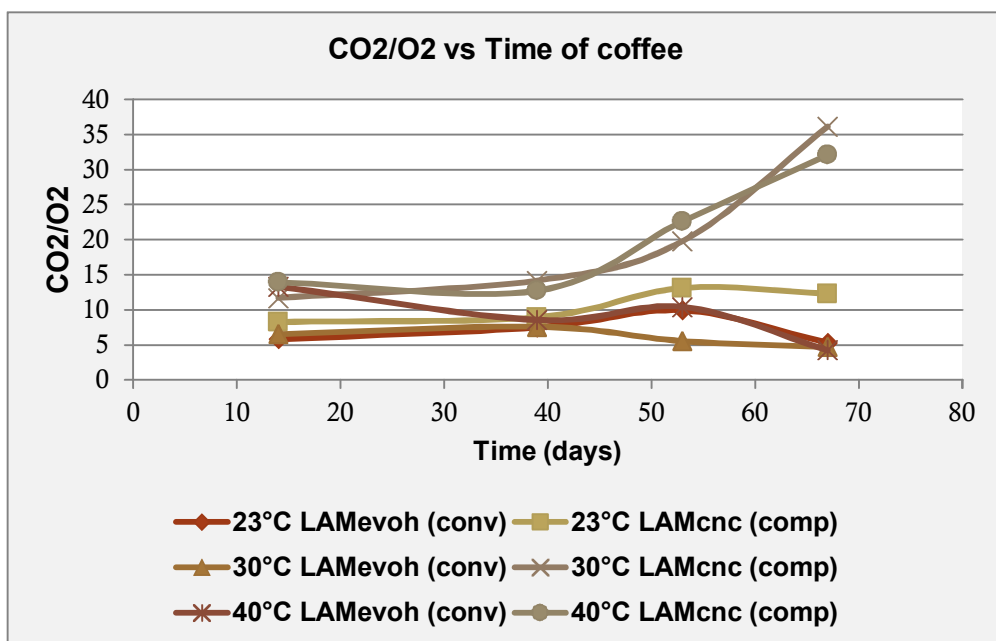
Figure 1. Gas evolution in the pouches containing ground coffee

Moreover, the two laminates tested did not show relevant discrepancies in gas permeability, at least at 23°C and partially at 30°C, a bigger difference however, was observed at 40 °C, with a better barrier offered by the compostable laminate. Less than 1% of O_2 was found in the pouches with grated cheese during the entire shelf-life.

Food Colour Changes

Colour difference was estimated according to CIE-LAB 1976 by the equation $dE = [(L_2-L_1)^2 - (a_2-a_1)^2 - (b_2-b_1)^2]^{1/2}$, where 'L' is the Lightness, 'a' the Redness and 'b' the Yellowness of the product colour. A colour difference detectable by human eye is generally considered when dE is higher than 1.8 but this value was never reached in our experiments as Figure 2a and 2b clearly indicate.
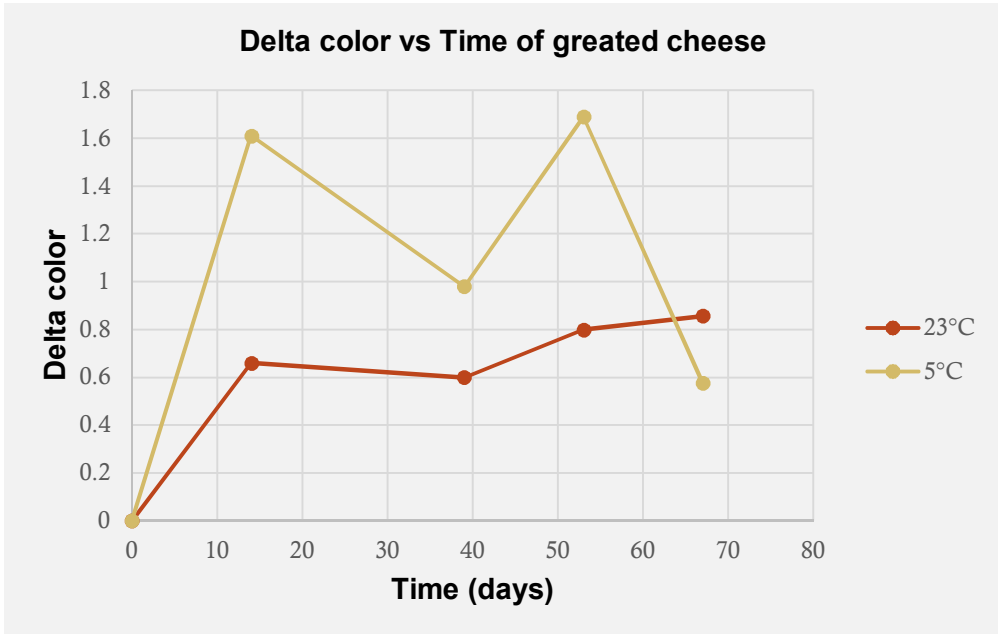
Figure 2a. Color difference of grated cheese over time
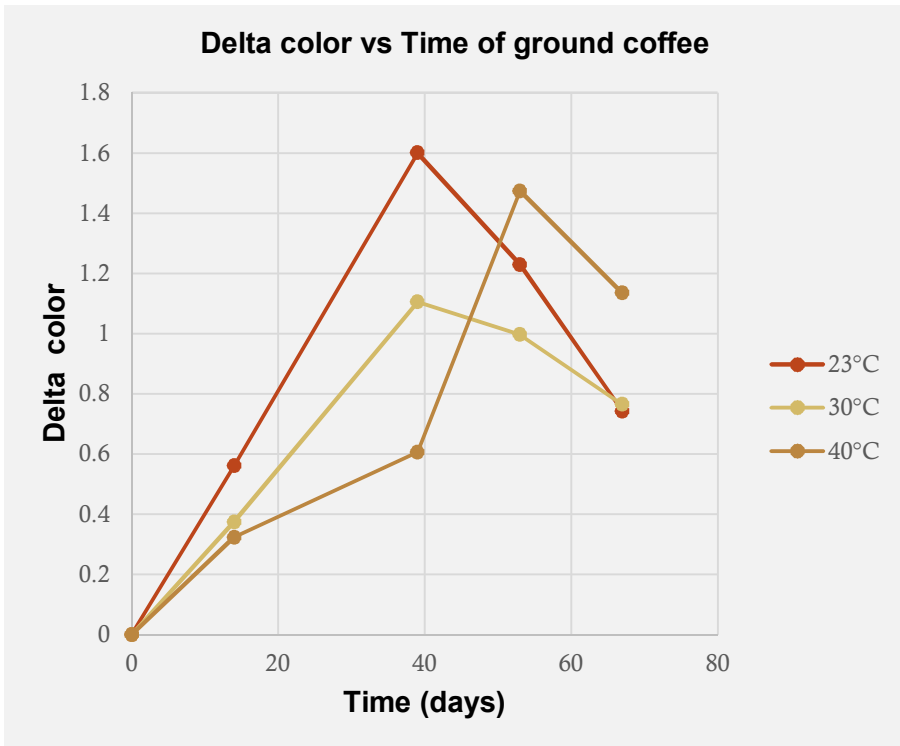
Figure 2b. Color difference of ground coffe over time

Microbiological analysis

Themicrobiological control was carried out, obviously, only on grated cheese.
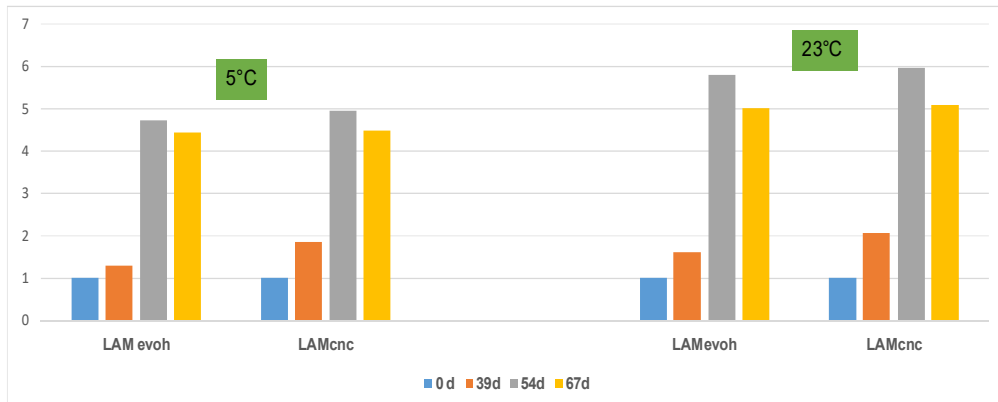
Figure 3. Mesophilic total bacterial count of grated cheese at two different temperatures and in the two different laminates (standard) with EVOH and compostable with CNCs

Sensory analysis

A panel of 20 tasters evaluated five different attributes of sensory quality of the ground coffee: overall odour intensity, overall acceptability, greasiness, rancid odour, odour persistence.
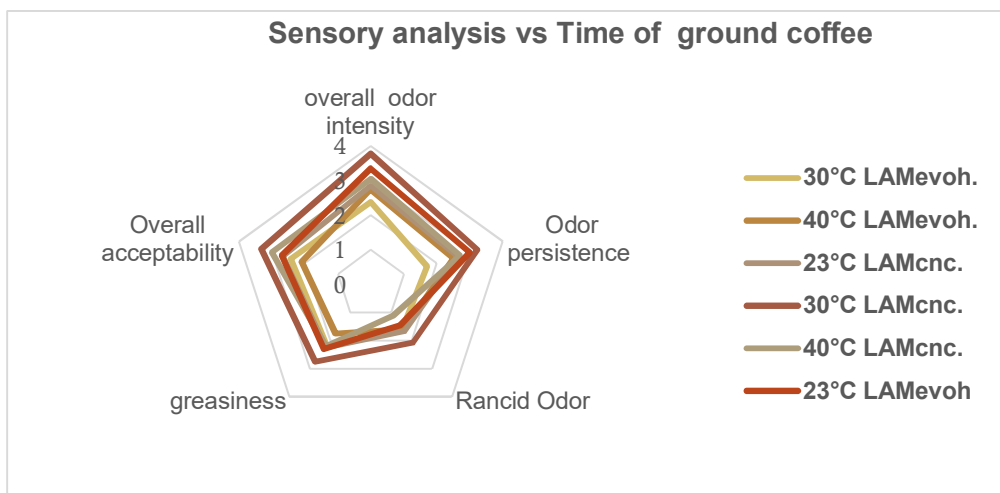
Figure 4. Sensory analysis of ground coffee in the two different pouches at three different temperatures.

11 different sensory attributes were evaluated by the same panel for the grated cheese in the two types of laminates and at two different temperatures, as shown in Figure 8. In no case, it was possible to observe a significant difference between the two different pouches.
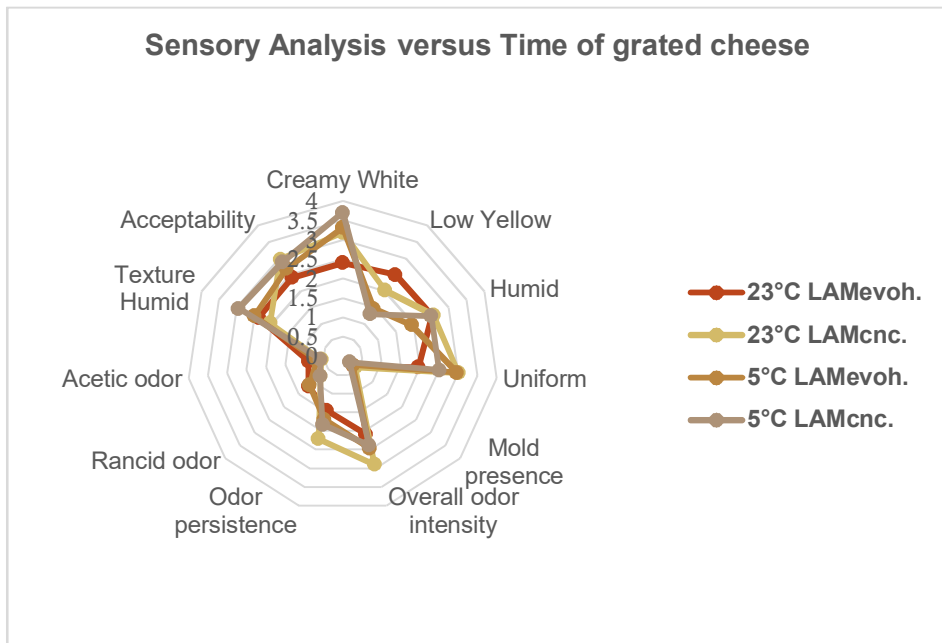
Figure 5. Sensory analysis of grated cheese in the two different pouches at two different temperatures.

4. Conclusions

The Shelf Life test was carried out taking into account also other quality attributes not described in this report. In particular, parameters of detecting oxidation phenomena or microbiological decay due to the possible oxygen inlet and loss of modified atmosphere have been measured during the test. No significant difference was found between samples packed in different pouches after more than two months at different temperatures.

5. References

Ashley, R.J., Cochran, M.A., Allen, K.W., 1995. Adhesives in packaging. International journal of adhesion and adhesives. Apr 1;15(2):101-8.

Barlow, C.Y., Morgan, D.C., 2013. Polymer film packaging for food: An environmental assessment. Resources, Conservation and Recycling. Sep 1; 78:74-80.

Farah, S., Anderson, D.G., Langer, R., 2016. Physical and mechanical properties of PLA, and their functions in widespread applications - A comprehensive review. Advanced drug delivery reviews. Dec 15; 107:367-92.

Fotie, G., Amoroso, L., Muratore, G., Piergiovanni, L., 2018. Carbon dioxide diffusion at different relative humidity through coating of cellulose nanocrystals for food packaging applications. Food Packaging and Shelf Life. Dec 1; 18:62-70.

Fotie, G., Rampazzo, R., Ortenzi, M., Checchia, S., Fessas, D., Piergiovanni, L., 2017. The effect of moisture on cellulose nanocrystals intended as a high gas barrier coating on flexible packaging materials. Polymers. Sep 5;9(9):415.

Labuza, T.P., Dugan, Jr, L.R., 1971. Kinetics of lipid oxidation in foods. Critical Reviews in Food Science & Nutrition. Oct 1;2(3):355-405.

Li, F., Mascheroni, E., Piergiovanni, L., 2015. The potential of nanocellulose in the packaging field: A review. Packaging Technology and Science. Jun; 28(6):475-508.

Mascheroni, E., Rampazzo, R., Ortenzi, M.A., Piva, G., Bonetti, S., Piergiovanni, L., 2016. Comparison of cellulose nanocrystals obtained by sulfuric acid hydrolysis and ammonium persulfate, to be used as coating on flexible food-packaging materials. Cellulose. Feb 1;23(1):779-93.

Mokwena, K.K.,, Tang J., 2012. Ethylene vinyl alcohol: a review of barrier properties for packaging shelf stable foods. Critical reviews in food science and nutrition. Jul 1;52(7):640-50.

Montanari, S., Roumani, M., Heux, L., Vignon, M.R., 2005. Topochemistry of carboxylated cellulose nanocrystals resulting from TEMPO-mediated oxidation. Macromolecules. Mar 8;38(5):1665-71.

Piringer, O.G., Baner, A.L., 2008. *Plastic packaging materials for food: barrier function, mass transport, quality assurance, and legislation*. John Wiley Sons.

Rashidi, L., Khosravi-Darani, K.,2011. The applications of nanotechnology in food industry. Critical reviews in food science and nutrition. Sep 1;51(8):723-30.

Sacui, I.A., Nieuwendaal, R.C., Burnett, D.J., Stranick, S.J., Jorfi, M., Weder, C., Foster, E.J., Olsson, R.T., Gilman, J.W., 2014. Comparison of the properties of cellulose nanocrystals and cellulose nanofibrils isolated from bacteria, tunicate, and wood processed using acid, enzymatic, mechanical, and oxidative methods. ACS applied materials & interfaces. Apr 18;6(9):6127-38.

Yang, H., Yan, R., Chen, H., Lee, D.H., Zheng, C., 2007. Characteristics of hemicellulose, cellulose and lignin pyrolysis. Fuel. Aug 1;86(12-13):1781-8.

Acknowledgements

6. Figures captions page

7. Table captions   page

Chapter 4.

General conclusions, implications and future perspectives

Chapter 4. General conclusions, implications and future perspectives

My research doctorate whose main goal was to create innovative food packaging using cellulose nanocrystals has been completely achieved. The cellulose nanocrystals (CNCs) that are chemically extracted from cellulosic sources such as biomass and by-products exhibit excellent gas and mechanical barrier properties required in food packaging for extending the shelf life of foodstuffs sensitive to oxidation. Today synthetic polymers such as EVOH (ethylene vinyl alcohol) and PVDC (polyvinylidene chloride) are used in laminates to mitigate the degradation of foods derived from oxidation. However, synthetic polymers are not biodegradable-friendly for the environment and are not absolutely safe for living beings. With increasing awareness and concern for the environment, scientists have been involved in the search for more sustainable applications. The cellulose nanocrystals are biodegradable and ecological materials can be positioned as a solid and valid alternative to oil-based materials. However, a serious pitfall has to be faced to make the integration of CNCs into packaging possible. Like most biodegradable materials, CNCs are very sensitive to water and this is detrimental to the oxygen barrier properties. In fact, in the absence of water, the CNCs coatings have almost no oxygen permeation, however, there is a sharp increase in oxygen diffusion when the relative humidity increases. The PhD project helped to discover tangible and successful solutions. Accurate strategies for alleviating the water sensitivity of cellulose nanocrystals were either by making the CNCs more hydrophobic through functionalization or by laminating the CNCs coatings to protect them from the wet environment. The best strategy that certainly worked was the blending

of functionalized (esterified) CNCs in multi-layer laminates, therefore, the combination of both techniques functionalization and lamination showed a significant improvement in the oxygen barrier properties even in conditions of higher relative humidity to such an extent that their applications in food packaging could be scaled-up immediately. In fact, the BIOCOMPLACK project financed by European Union (EU), which consisted of creating a fully compostable food package using cellulose nanocrystals was successfully achieved and used for food shelf-life assessement. Laminated polymers, including cellulose nanocrystals, were created and used with respect to EVOH-based laminates to extend the shelf life of foods with high content of polyunsaturated fatty acids such as grated cheese and ground coffee. Subsequently, the products were packaged in small bags manufactured and kept in the same storage conditions and time. The results of food shelf-life evaluation showed that the packages based on cellulose nanocrystals were the best laminates in the extension of food products compared to the existing ones based on the EVOH copolymer. Prior to implementing and commercializing a food packaging based on cellulose nanocrystals in Europe and in particular in Italy, the approval of EFSA (European Food Safety and Authority) of such nanoparticles as Food Contact Materials (FCM) is needed. Although many scientists proved through their findings the non-toxicity and non-harzardousness of CNCs, consumers still show strong scepticism and negative judgment about such tiny particles that they fear for their health. My PhD project has shown (chapter III) that there is nothing to worry about cellulose nanocrystals since, they are not used in direct contact with foods. Based on the facts, my work has proved that a minor quantity of cellulose nanocrystals is already present in the microcrystalline

cellulose (MCC), a food additive long approved by EFSA and granted the number E460(i) and has long been used as texturizer, anti-caking agent, emulsifier and coatings in food and pharmaceutical applications. In addition, scientists have already shown that particles of such dimensions cannot migrate through polymers and papers. In light of all these findings, the approval process has been implemented, and the expectations are such that, the exceptional advantages of the CNCs must be fully exploited for creating more advanced and sustainable food packaging with natural resources and cellulosic by-products. Finally, the approval of cellulose nanocrystals will encourage Italian and foreign companies to invest in a large production of cellulose nanocrystals to be marketed and used in other sectors in Italy.

Chapter 5

Appendices

Chapter 5. Appendices

Scientific publications

Fotie, G., Rampazzo, R., Ortenzi, M., Checchia, S., Fessas, D., Piergiovanni, L., 2017. The effect of moisture on cellulose nanocrystals intended as a high gas barrier coating on flexible packaging materials. *Polymers*, *9*(9), p.415.

Fotie, G., Amoroso, L., Muratore, G., Piergiovanni, L., 2018. Carbon dioxide diffusion at different relative humidity through coating of cellulose nanocrystals for food packaging applications. *Food Packaging and Shelf Life*, *18*, pp.62-70.

Piergiovanni, L., **Fotie, G.,** Amoroso, L., Akgun, B., Limbo, S., 2019. Are cellulose nanocrystals "alien particles" to human experience?. *Packaging Technology and Science*.

Oral communications

Ghislain Fotie, Luana Amoroso, Begum Akgun, Giuseppe Muratore, Sara Limbo, 2019. Shelf life extension provided by compostable laminates containing cellulose nanocrystals for oxygen sensitive foods, 9° Shelf life International meeting (SLIM) June 17-20th 2019, Naples, Italy.

Ghislain Fotie, Luciano Piergiovanni, 2019. Effective replacement in food packaging laminates of the conventional oil based oxygen-barrier polymers with bio-composite laminates containing Cellulose Nanocrystals (CNCs) extracted from waste and biomasses.XXIV Workshop 11-13 September 2019, Florence, Italy.

Ghislain Fotie, Luciano Piergiovanni, Julien Bras, 2018. Incorporation of Cellulose Nanocrystals (CNCs) extracted from waste and biomasses into Food Packaging. Nanocellulose, International meeting, Grenoble, France.

Poster communications

Ghislain Fotie, Sara Limbo and Luciano Piergiovanni, 2017. Effectiveness of cellulose nanocrystals application as bio-based oxygen barrier for shelled walnuts shelf-life extension. The 8th Shelf-life International Meeting (SLIM), 1-3 November 2017, Bangkok, Thailand.

Ghislain Fotie, Luca Zanetti, Claus Berend, Lidia Garcia, Guillaume Lebouteillerand and Luciano Piergiovanni, 2018. Biocomplack, the Fast-Track EU project for the implementation of a cellulose nanocrystals Barrier in Fully Compostable Novel Laminates. The 8th Shelf-life International Meeting (SLIM), 1-3 November 2017, Bangkok, Thailand.

Luciano piergiovanni, **Ghislain Fotie**, 2017. Studi e ricerche sulla «nanocellulosa» per un packaging piu' sostenibile. Open day, Milano, Italy.

Food Packaging & Shelf Life: New challenges, Nanocellulose. Luciano Piergiovanni, **Ghislain Fotie**, Luana Amoroso, Sara Limbo, Open day 2018, Milano, Italy.

New sustainable nano-materials for food packaging applications. Luciano Piergiovanni, **Ghislain Fotie**, Luana Amoroso, Begüm Akgün, Sara Limbo; Open day 2019, Milano, Italy.

Doctoral trainings

Coating and/or lamination of cellulose nanocrystals modified with chitosan and/or alginate to produce active packaging useful for prolonging the shelf-life of food. University of Grenoble, Laboratoire Génie des proceeds Papetiers (LGP2). 7 months, 2018.

Life cycle assessment (LCA) e sviluppo delle figure professionali: esperienze aziendali a confronto, sala convegni CNR presso area della ricerca Milano 1 - via Alfonso corti 12 Milano, 8 hours, 1° marzo 2019.

Poster Awards

Ghislain Fotie, Sara Limbo and Luciano Piergiovanni, 2017. Effectiveness of cellulose nanocrystals application as bio-based oxygen barrier for shelled walnuts shelf-life extension. The 8th Shelf-life International Meeting (SLIM), 1-3 November 2017, Bangkok, Thailand.

Acknowledgements

I would like to thank all my family's members especially my beloved parents Pa' *Simon* and Ma' *Jacqueline* for their selfless love and support they have shown during my entire life.

  Last but not the least, I do appreciate the support of all my friends *Chris, Glody, Charly, Ale, Luca, Fede, Ste*, to be always there for me, I am so grateful to have met you.